

Deep Learning Techniques for Hand Vein Biometrics: A Comprehensive Review

Mustapha Hemis^{a,*}, Hamza Kheddar^b, Sami Bourouis^c and Nasir Saleem^d

^aLCPTS Laboratory, University of Sciences and Technology Houari Boumediene (USTHB), P.O. Box 32, El-Alia, Bab-Ezzouar, Algiers 16111, Algeria.

^bLSEA Laboratory, Department of Electrical Engineering, University of Medea, 26000, Algeria

^cDepartment of Information Technology, College of Computers and Information Technology, Taif University, Taif 21944, Saudi Arabia

^dDepartment of Electrical Engineering, Faculty of Engineering and Technology, Gomal University, Dera Ismail Khan, Pakistan

ARTICLE INFO

Keywords:

Biometrics
Finger vein recognition
Palm vein recognition
Dorsal hand vein
Deep learning
Transfer learning

ABSTRACT

Biometric authentication has garnered significant attention as a secure and efficient method of identity verification. Among the various modalities, hand vein biometrics, including finger vein, palm vein, and dorsal hand vein recognition, offer unique advantages due to their high accuracy, low susceptibility to forgery, and non-intrusiveness. The vein patterns within the hand are highly complex and distinct for each individual, making them an ideal biometric identifier. Additionally, hand vein recognition is contactless, enhancing user convenience and hygiene compared to other modalities such as fingerprint or iris recognition. Furthermore, the veins are internally located, rendering them less susceptible to damage or alteration, thus enhancing the security and reliability of the biometric system. The combination of these factors makes hand vein biometrics a highly effective and secure method for identity verification.

This review paper delves into the latest advancements in deep learning techniques applied to finger vein, palm vein, and dorsal hand vein recognition. It encompasses all essential fundamentals of hand vein biometrics, summarizes publicly available datasets, and discusses state-of-the-art metrics used for evaluating the three modes. Moreover, it provides a comprehensive overview of suggested approaches for finger, palm, dorsal, and multimodal vein techniques, offering insights into the best performance achieved, data augmentation techniques, and effective transfer learning methods, along with associated pretrained deep learning models. Additionally, the review addresses research challenges faced and outlines future directions and perspectives, encouraging researchers to enhance existing methods and propose innovative techniques.

1. Introduction

Biometric authentication techniques have become integral in ensuring secure access and identity verification in various domains. These techniques are typically classified into two classes—behavioral and physiological. Behavioral biometrics encompass characteristics based on an individual's behavior, such as signature, keystroke dynamics [1], gait analysis [2], voice recognition [3, 4], and more. On the other hand, physiological biometrics include physical and static characteristics, which are classified also into two categories: extrinsic and intrinsic. Extrinsic biometrics include features that are external to the body, such as fingerprint, palm print, face, and iris patterns. Intrinsic biometrics, on the other hand, involve features that are inherent to the body, such as vein patterns and retinal scans.

From the hand, numerous physiological properties can be extracted for biometric purposes, as illustrated in Figure 1. Among these, hand veins-based biometric method has attracted widespread attention because of several distinct advantages. These biometrics are inherently more secure and difficult to forge, as they are internal to the body and not easily accessible. Finger vein (FV) biometrics, for instance, have been shown to exhibit a level of diversity similar to that of iris patterns, ensuring high security and suitability for biometric authentication [5]. Moreover, capturing vein patterns is only effective in a living body, making it impossible to steal vein patterns from deceased individuals [6, 7]. Additionally, vein patterns are permanent and do not change in adulthood [8]. Furthermore, vein images are typically captured by contactless sensors, ensuring hygiene and convenience [9]. Research has also shown that vein recognition is robust against various distortions such as motion blur, defocus, sensor aging, and compression [10]. Despite its advantages, hand vein-based biometrics face challenges. Factors like capture device configuration, ambient light, dust, humidity, and finger misplacement can affect performance [5, 11]. However, research has shown that these issues can be mitigated with optimized settings and processing strategies. Various methods have been developed to overcome those issues.

Since the vein-based biometric system was investigated, many significant achievements have been made in this area as new systems have been continuously designed and deployed over the years. deep learning (DL) has emerged as powerful tools in enhancing the accuracy and efficiency of vein-based biometric systems. DL significantly enhances hand vein recognition by automating feature extraction and improving accuracy. Traditional methods, such as principal component analysis (PCA), linear discriminant analysis (LDA), and Wavelet Transform, often rely on manual feature extraction and are sensitive to variations in lighting and hand positioning. In contrast, DL models like convolutional neural networks (CNNs) can identify complex patterns and variations in vein structures with minimal human intervention, leading to higher recognition rates and robust performance.

* The first is the corresponding author.

✉ mhemis@usthb.dz (M. Hemis); kheddar.hamza@univ-medea.dz (H. Kheddar); s.bourouis@tu.edu.sa (S. Bourouis);

nasirsaleem@gu.edu.pk (N. Saleem)

ORCID(s):

Acronyms and Abbreviations

AHE	adaptive HE	ELM	extreme learning machine	LSTM	long short-term memory
Acc	accuracy	F1	F1-score	LTGAN	local transformer-based GAN
ACER	average classification error rate	FAR	false acceptance rate	ML	machine learning
AE	autoencoder	FGSM	fast gradient sign method	MLP	multi-layer perceptron
APCER	attack presentation classification error rate	FPGA	field programmable gate array	ML-ELM	multilayer extreme learning machine
AUC	area under curve	FDR	false discovery rate-correction	MBCS	multi-biometric cancellable system
BERT	bidirectional encoder representations from Transformers	FID	Frechet inception distance	MTL	multitask learning
BIM	basic iterative method	FMR	false match rate	NIR	near-infrared
BPCER	bona fide presentation classification error rate	FNMR	false non-match rate	non-IID	non-independent and identically distributed
BSIF	binarized statistical image features	FL	Federated learning	NPCER	normal presentation classification error rate
BTP	biometric template protection	FRR	false rejection rate	PAD	presentation attack detection
CAE	convolutional autoencoder	FV	Finger vein	PCNN	pulse coupled neural network
CBAM	convolutional block Attention module	FVI	finger vein image	PCA	principal component analysis
CCA	canonical correlation analysis	FFN	feature fusion network	PLBP	partition local binary patterns
CCD	charge-coupled device	GAN	generative adversarial network	Pre	precision
CLHE	contrast-limited HE	GCNLE	graph convolutional network-based label enhancement	PSNR	peak signal-to-noise ratio
CLAHE	contrast-limited adaptive histogram equalization	GAR	genuine acceptance rate	PV	palm vein
CMH	cross-modality hashing	GNN	graph neural networks	Rec	recall
CNN	convolutional neural network	GPT	generative pre-trained Transformer	RAB	residual attention block
CIR	correct identification rate	GRU	gated recurrent unit	RBM	restricted Boltzmann machines
DA	domain adaptation	GPU	graphics processing unit	RNN	recurrent neural network
DBN	deep belief network	HE	histogram equalization	ROI	region of interest
DCNN	deep convolution neural network	HOG	histograms of oriented gradients	SIFT	scale-invariant feature transform
DHN	deep hashing network	HSJA	hop-skip-jump-attack	SPP	spatial pyramid pooling
DHV	dorsal hand vein	HTER	half total error rate	SVM	support vector machine
DL	deep learning	IoT	internet-of-things	SSIM	structural similarity index measure
DNN	deep neural network	IKP	inner knuckle print	SOTA	state-of-the-art
DRL	deep reinforcement learning	IRI	infrared image	TProt	template protection
DTL	deep transfer learning	KNN	k-nearest neighbors	T2T	tokens-to-token
DWT	discrete wavelet transform	LBP	local binary patterns	TL	transfer learning
ECG	electrocardiogram	LDA	linear discriminant analysis	ViT	vision Transformer
EER	equal error rate	LED	light emitting diode	WD	Wasserstein distance
		LLM	large language model	WV	wrist vein
		LPQ	local phase quantization		

Additionally, DL's ability to learn from large datasets enables continuous improvement and adaptation, offering superior security and reliability for biometric authentication.

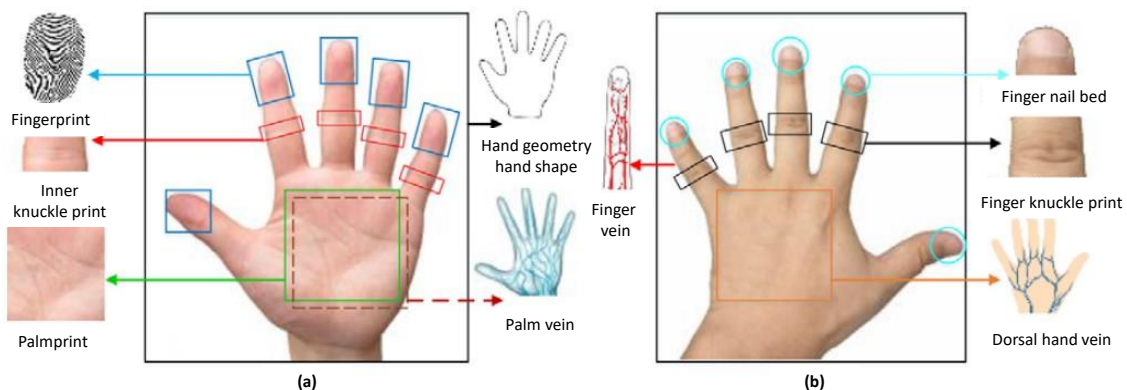


Figure 1: Biometrics of hands [12]. (a) Palm hand features. (b) Dorsal hand features. These characteristics serve as unique biometric identifiers for accurate and reliable personal identification and authentication.

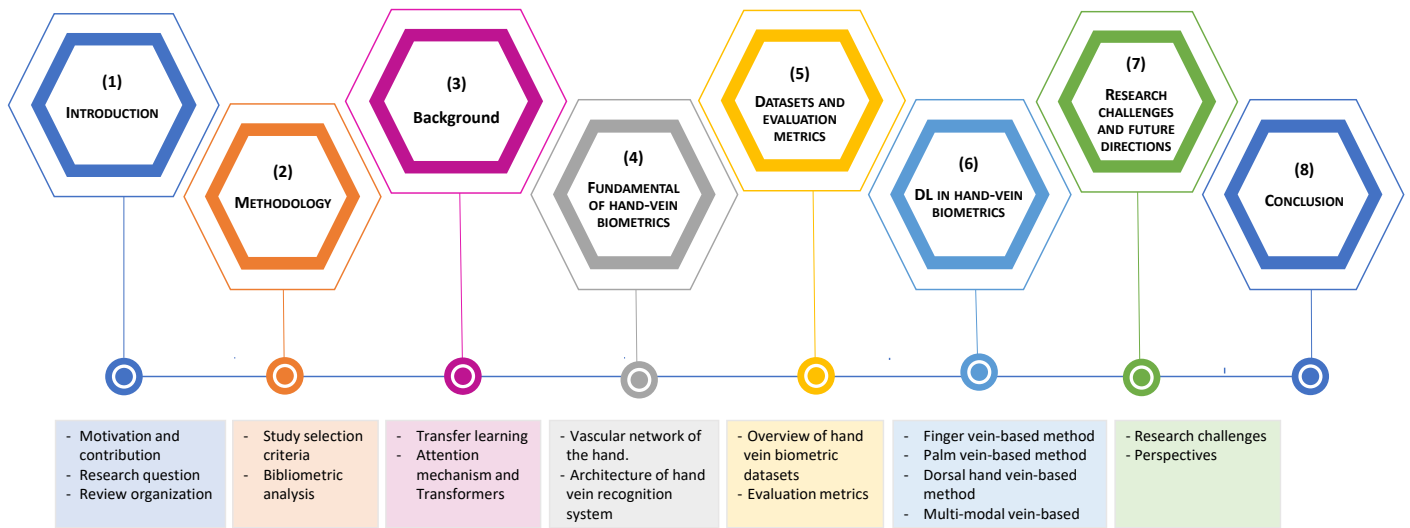


Figure 2: Roadmap of the review, showing main sections of the manuscript.

1.1. Motivation and contribution

The motivation behind this comprehensive review stems from the increasing significance of DL in the field of vein biometrics. As the demand for robust and secure authentication methods grows, understanding the advancements in DL for FV, palm vein (PV), and dorsal hand vein (DHV) recognition becomes pivotal. This review aims to provide a thorough examination of the current state-of-the-art (SOTA) in these areas, spanning the period from 2015 to 2024, highlighting key contributions, breakthroughs, and challenges encountered in the application of DL techniques. To the best of the authors' knowledge, there has been no prior research paper that has explored and critically evaluated contributions in FV, PV and DHV using DL until now.

In recent years, a multitude of survey papers have been published, evaluating various facets of vein biometric models, as summarized in Table 1. Most of these reviews focus on specific hand vein types such as FV [5, 13–16], PV [17, 18] or DHV [19], while others include several physiological biometrics [20, 21]. Some of these reviews focus on specific topics such as presentation attack detection (PAD) in biometric systems [21], feature extraction [15], or the generation of synthetic vein images [18]. These reviews primarily cover traditional approaches, with partial inclusion of DL approaches or an exclusive focus on DL. Also, many of these reviews partially address or miss critical areas such as datasets and metrics reviews, challenges, and future directions.

Unlike previous reviews, our work addresses all three hand vein types—FV, PV, and DHV—as well as multimodal vein recognition, focusing solely on DL approaches. Additionally, our review provides an extensive analysis of existing datasets and evaluation metrics. It also examines data augmentation and deep transfer learning (DTL) techniques, which are crucial for limited hand vein data. Finally, the review outlines current challenges in the field and future directions for research. The contribution of the manuscript is summarized as follows:

- This paper reviews recent methods for hand vein-based biometrics using DL, including preprocessing, feature extraction, and classification. It also covers PAD and template protection (TProt), primarily for FV recognition.
- The review analyzes DTL and data augmentation techniques across all reviewed DL-based approaches. It also covers evaluation metrics and main datasets exploited in hand vein biometrics.
- The review spans literature from 2017 to 2024, with insights presented through tables and figures to aid understanding DL-based hand vein SOTA methods.
- The paper aims to motivate further research in vein-based biometrics by highlighting research gaps, challenges, and proposing future directions.

This research suggest paths for further investigation in hand vein biometrics, focusing on various technologies, methodologies, and datasets. By analyzing infrared images (IRIs), researchers can accurately identify vein patterns in fingers, hands, and palms. The subsequent section provides a concise overview of these contributions. Table 1 compares the proposed contribution with other hand vein biometric surveys. It is evident that our survey is the most comprehensive.

1.2. Research questions

To streamline this systematic mapping review, we outlined ten research questions in Table 2. Following the study's roadmap, the reader will gain the main insights and understand the study's objectives. The table presents a structured overview of the research questions (RQ) along with their corresponding motivating features. Each row of the table is dedicated to a specific research question, providing a clear understanding of the objectives driving the research in the domain of hand vein identification using automated technologies.

Table 1

Comparison of the proposed contribution against other hand vein biometric surveys. The symbols ●, ◐, and ○ indicate that the specific field has been addressed, partially addressed, and missed, respectively.

Ref.	Year	Description of the survey/review	DL-FV	DL-PV	DL-DHV	DL-MMV	DTL	DAT	Dataset review	Metrics review	Current challenges	Future directions
[13]	2018	A systematic review of FV recognition methods	◐	○	○	○	○	○	●	○	○	◐
[14]	2020	A review of FV biometric verification systems based software and hardware components	◐	○	○	○	○	○	◐	○	●	●
[19]	2021	A survey of DHV biometrics	○	○	◐	●	○	○	●	○	●	◐
[17]	2019	A review of PV recognition methods	○	○	○	○	○	○	●	○	●	●
[15]	2021	A review of feature extraction methods applied for FV recognition	◐	○	○	◐	○	○	●	○	○	○
[5]	2022	A review of finger vein recognition methods	●	○	○	○	○	○	◐	◐	●	●
[16]	2022	A survey of DL, PAD and Multimodal based finger vein recognition systems	●	○	○	●	○	○	○	◐	●	◐
[18]	2023	A review of methods for generating synthetic images of PV patterns	○	●	○	○	○	○	◐	◐	●	●
[20]	2024	A systematic review of physiological-based biometric recognition systems	●	◐	○	◐	○	○	◐	●	●	○
[21]	2024	A systematic review of DL-based PAD systems	◐	○	○	○	○	○	○	◐	◐	○
Our	2024	A review of DL-based hand vein recognition systems including FV, PV and DHV	●	●	●	●	●	●	●	●	●	●

Abbreviations: DL-based Finger vein (DL-FV), DL-based Palm vein (DL-PV), DL-based dorsal hand vein (DL-DHV), DL-based multimodal vein (DL-MMV), Data augmentation techniques (DAT).

1.3. Review organization

To achieve a structured and insightful exploration, this review is organized into several key sections. The methodology in Section 2 outlines the criteria used for selecting studies and employs bibliometric statistics to present an overview of the research landscape. Following this, Section 4 delves into the fundamentals of hand vein biometrics, covering the vascular network of the hand, its characteristics, and the architecture of hand vein recognition systems. Section 3 offers background knowledge essential for understanding the proposed ML/DL-based hand vein identification approaches, including DTL, attention mechanisms, and Transformers. Moving forward, Section 5 provides an overview of available datasets and discusses evaluation metrics relevant to DL models in the hand vein biometrics domain. Subsequently, the DL in hand vein biometrics, Section 6, explores most suggested SOTA DL-based vein techniques, including FV-based, PV-based, DHV-based, and multi-modal vein-based. As the review progresses, research challenges and future directions, thoroughly detailed in Section 7, highlight the existing hurdles in the field, offering perspectives on potential solutions and paving the way for future advancements. The conclusion in Section 8 summarizes the key findings, emphasizing the importance of DL in advancing the reliability and security of vein-based biometric systems. Figure 2 illustrates the roadmap and detailed organization of the paper.

2. Methodology

The research methodology is crucial for conducting any type of research or survey. This section covers the research approach we utilized to conduct a thorough survey. It outlines our criteria for selecting studies and provides bibliometric statistics to offer an overview of the research landscape.

2.1. Study selection criteria

To identify and review existing studies on DL-based hand vein biometrics, a comprehensive search was conducted across several leading publication databases renowned for their high-quality scientific research written in English. The primary search was carried out in Scopus, which systematically includes databases such as Web of Science, Elsevier, IEEE, among others. Articles published in the last ten years were prioritized. However, older publications were also considered when necessary to provide fundamentals, datasets, metrics, etc. Additionally, high-quality pre-prints from arXiv, SSRN, among others, were selected. Figure 3 summarizes the most frequently used keywords by authors. Keywords with larger font sizes indicate higher usage, while smaller font sizes indicate less frequent usage.

Table 2
Research Questions and Motivating Features

RQ	Research Questions	Motivating Features
Q1	Which technologies and approaches are mostly used for automated vein detection in IRIs?	Objective: To understand the latest innovative methods and the difficulties faced in this endeavor.
Q2	How have conventional machine learning (ML) methods been used in hand vein identification systems?	Objective: To investigate techniques that use carefully selected attributes/features and established criteria for hand vein identification.
Q3	How have DL methods been used for hand vein identification systems?	Objective: To explore techniques and architectures that use advanced neural networks to learn features and classifiers from IRIs data.
Q4	Which databases are being employed to assess the effectiveness of hand vein identification and categorization methodologies?	Objective: To conduct a comprehensive analysis of the quality and availability of current datasets, and to determine shortcomings and the need for additional data sources.
Q5	How is the challenge of limited datasets addressed in hand vein biometrics ?	Objective: To investigate the strategies and techniques used to overcome the limitations of small datasets in hand vein biometric research, including data augmentation, synthetic data generation, and transfer learning.
Q6	Which measures have been used to evaluate the performance of hand vein identification techniques?	Objective: To better understand the requirements and benchmarks used in assessing the precision and effectiveness of various methodologies.
Q7	Which DL model is most commonly utilized in hand vein recognition ?	Objective: To identify the predominant DL architectures used in hand vein biometrics and to analyze their effectiveness and popularity among researchers.
Q8	Which types of hand vein biometrics are most extensively studied by researchers ?	Objective: To explore the focus areas within hand vein biometrics research, identifying whether FV, PV, or DHV receive the most attention from the scientific community.
Q9	How can DL enhance the security of hand vein recognition systems to mitigate presentation attacks and protect biometric templates ?	Objective: To explore DL techniques that can detect and prevent presentation attacks, and to develop methods for securing biometric templates against potential threats.
Q10	What are the research challenges and future directions in hand vein biometrics ?	Objective: To identify the current limitations and obstacles in the field, to highlight areas requiring further research, and to propose potential future research directions to advance hand vein biometrics.

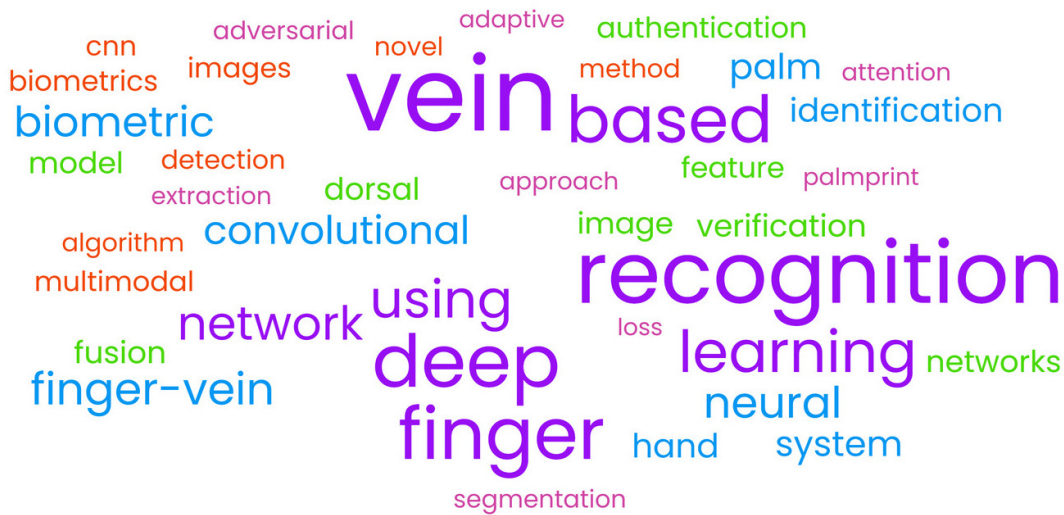


Figure 3: Word cloud of the most essential terms in the field of hand vein biometrics.

2.2. Bibliometric analysis

A total of 174 papers published between 2015 and 2024 were involved in the main sections discussing fundamentals and DL-based hand vein biometrics. Figure 4(a) illustrates the distribution of these papers over the years. Additionally, 145 out of the 174 papers discussed in Section 6 belong to one of the following domains: FV, PV, DHV, and multi-modal. Figure 4(b) illustrates the distribution of these papers across these vein biometrics domains. The remaining papers in this review, some of which fall outside the 2015-2024 range, include review papers used for comparison, reviews and studies related to DL techniques, DTL, Transformers, preprocessing, metrics, datasets, and more. Additionally, other papers were included to provide a comprehensive foundation for the introduction, address the challenges faced, and offer insights into future directions.

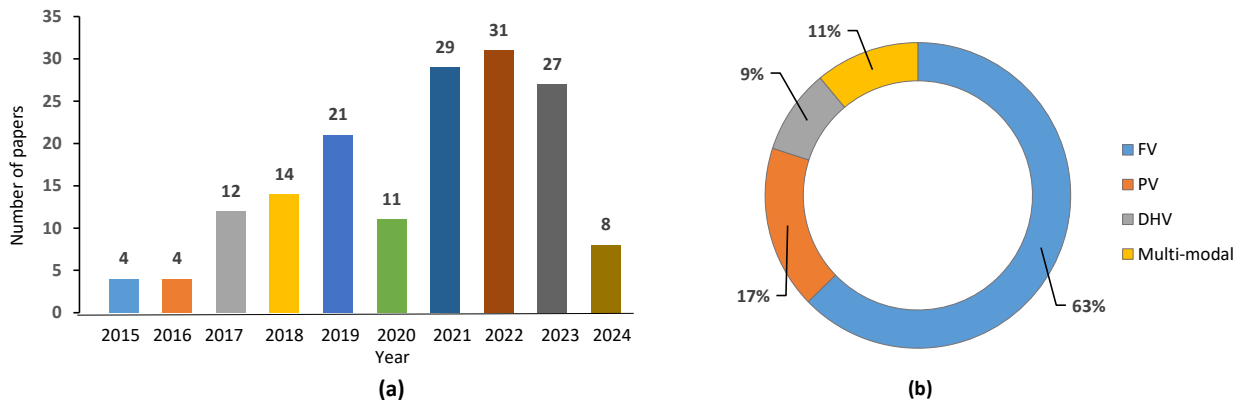


Figure 4: Improved caption: Bibliography Statistics: (a) Annual publications on DL-based hand vein research; (b) Percentage distribution of publications across different domains: FV, PV, DHV, and multi-modal. The data clearly indicates a predominant research focus on DL-based FV.

3. Background

According to the reviewed SOTA work, some background knowledge is necessary to deeply understand the proposed ML/DL-based hand vein identification approaches. For a comprehensive understanding of various ML and DL techniques, researchers are encouraged to consult our previous work in [22]. This publication covers a broad spectrum of methodologies, including deep belief network (DBN), graph neural networks (GNN), deep neural network (DNN), recurrent neural network (RNN), long short-term memory (LSTM) networks, autoencoders (AEs), restricted Boltzmann machines (RBM), and CNN. These techniques are valid and adaptable across multiple fields of research. In contrast, the background section of this review is specifically focused on advanced DL techniques employed in hand vein recognition research. For instance, DTL, particularly fine-tuning and domain adaptation (DA), is widely adopted. Additionally, attention layers and Transformers, which are advanced versions of attention mechanisms, are also extensively used. By concentrating on these newer and more complex concepts, this review aims to equip readers with the necessary foundation to comprehend current trends and innovations in the field. While fundamental concepts like CNNs are crucial to many approaches, they are well-established in the literature and thus are not detailed in this section.

3.1. Deep transfer learning

DTL is a ML technique where a pre-trained model, which was initially trained on a large dataset for a specific task, is reused or fine-tuned for a different but related task. Instead of training a model from scratch, DTL leverages the patterns and knowledge learned by the pre-trained model to improve performance on the new task, often with less training data [23].

(a) Fine-tuning all layers in a model: When researcher fine-tune all layers of a pre-trained model, he adjust the weights of the entire network on your new dataset (Figure 5 (a)). This approach is beneficial when the new task is similar but has some significant differences from the original task [3].

(b) Fine-tuning some layers in a model: In this approach, the researcher only fine-tune certain layers of the pre-trained model while keeping others frozen, i.e. their weights remain unchanged (Figure 5 (b)). This is useful when the new task is very similar to the original task [3].

(c) DA: Is a subfield of DTL where the goal is to adapt a model trained on a source domain to perform well on a target domain, despite the differences between the domains (Figure 5 (c)). This involves adjusting the model, by feature adaptation or fusion, to bridge the gap between the source and target domains, which may have different distributions or feature spaces [23].

For example, in the context of FV biometric recognition, fine-tuning all layers in a model might involve starting with a CNN pre-trained on ImageNet and then training it entirely on a FV dataset to capture the unique patterns of veins across different individuals. Fine-tuning some layers could involve freezing the initial layers of the same pre-trained CNN, which capture general features, and only training the later layers on the FV dataset to adapt to vein-specific details. For DA, a model pre-trained on a similar biometric dataset, such as PV images, could be adapted to FV images by using techniques like adversarial training to align the feature distributions between the two domains, ensuring robust performance despite the differences in image characteristics. Thus, DTL and DA can be extremely useful due to the limited availability of hand-vein image datasets.

3.2. Attention mechanism and Transformers

In recent years, the fields of DL and ML have been revolutionized by the concepts of Attention mechanisms and Transformers. These innovations have significantly improved the performance of models in tasks such as language translation, text generation, and image processing.

(a) Attention mechanism: The attention mechanism is a concept that enables models to focus on specific parts of the input data when making predictions. It was introduced to address the limitations of traditional sequence models, such as RNNs and LSTMs, which often struggle with long-range dependencies and information retention over long sequences. Attention works by assigning different weights to different parts of the input sequence. This allows the model to prioritize important information and ignore irrelevant details. The key components of the attention mechanism include [4]:

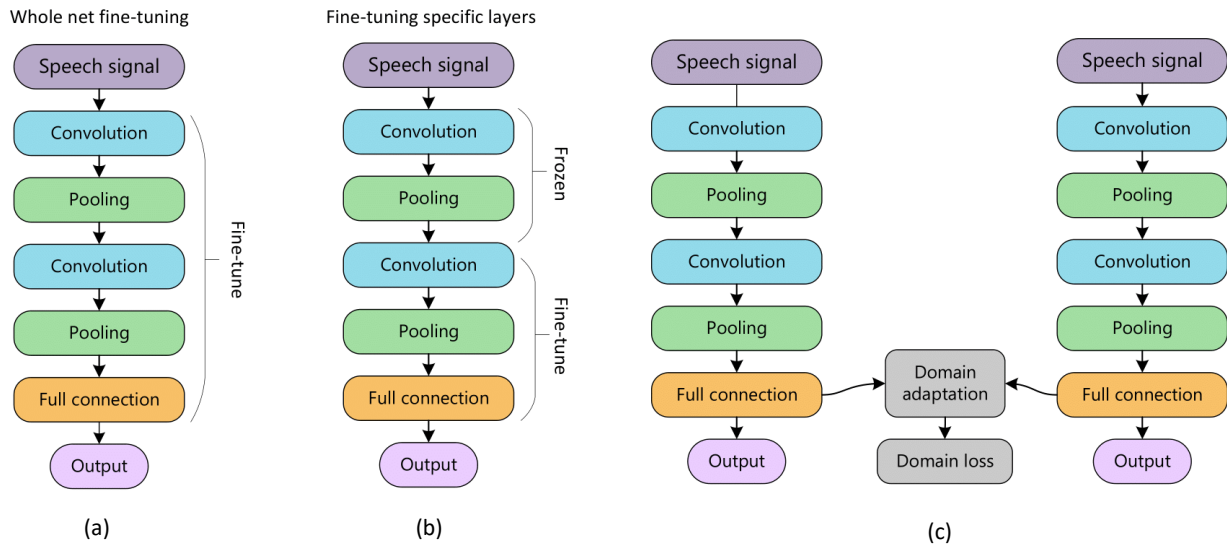


Figure 5: DTL principles. (a) Full fine-tuning; (b) Partial fine-tuning; (c) DA.

- **Query (Q):** Represents the current state or the part of the sequence that is being processed.
- **Key (K):** Represents all parts of the input sequence.
- **Value (V):** Also represents all parts of the input sequence, but these are the actual values being processed.

The attention score is calculated as a similarity measure between the query and the keys, and this score is used to weigh the values. This weighted sum then forms the attention output.

(b) Transformer model: The Transformer model, introduced by Vaswani et al. in [24], is built entirely on attention mechanisms, eschewing the use of recurrence altogether. Transformers have become the foundation for SOTA models in NLP, such as bidirectional encoder representations from Transformers (BERT), generative pre-trained Transformer (GPT), among others [25]. Key components of the Transformer model include:

- **Multi-head self-Attention:** Allows the model to focus on different parts of the input sequence simultaneously by employing multiple attention mechanisms (heads). Each head captures different aspects of the input.
- **Positional encoding:** Since transformers do not process sequences in a sequential manner, positional encoding is added to the input embeddings to give the model information about the position of each word in the sequence.
- **Feed-forward neural Networks:** Applied to the attention outputs, adding non-linearity and improving the model's expressive power.
- **Layer normalization and residual connections:** Help in stabilizing and improving the training of deep models by normalizing the inputs and adding skip connections.

Transformers consist of an encoder and a decoder. The encoder processes the input sequence and generates a set of attention-based representations. The decoder takes these representations and generates the output sequence, often using a similar attention mechanism to focus on different parts of the input.

4. Fundamentals of hand vein biometrics

4.1. Vascular network of the hand

Hand vein biometrics utilize the vascular patterns present in various parts of the hand, including the fingers, palms, and the dorsal hand (Figure 6). The hand's vascular network consists of veins and arteries. Veins carry deoxygenated hemoglobin (Hb), while arteries transport oxygenated hemoglobin (HbO₂) [18]. The hand's vascular structure displays intricate patterns that facilitate unobstructed blood flow during hand movements. These specific patterns enable the vascular network to serve as a biometric identifier, with superficial networks being primarily utilized due to the optical limitations of acquisition systems [26]. Each individual's vein pattern is unique, akin to fingerprints, due to the random development of vascular structures influenced by genetic and environmental factors. The following are the types and characteristics of hand veins:

- **FVs:** The vascular network in the fingers is composed of several small veins running parallel to the bones and joints. These veins are typically arranged in a branching pattern that varies significantly from person to person. These patterns offer high resolution due to the smaller captured area, revealing rich details. However, the smaller area limits the amount of data captured compared to PVs.

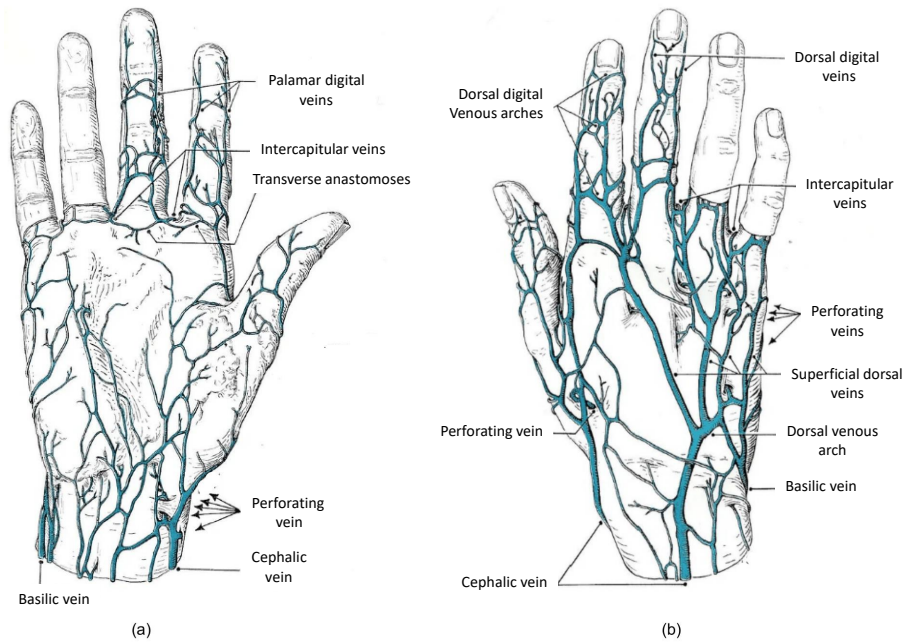


Figure 6: Illustration of the hand's vascular network [27]. (a) Palmar view; (b) Dorsal view.

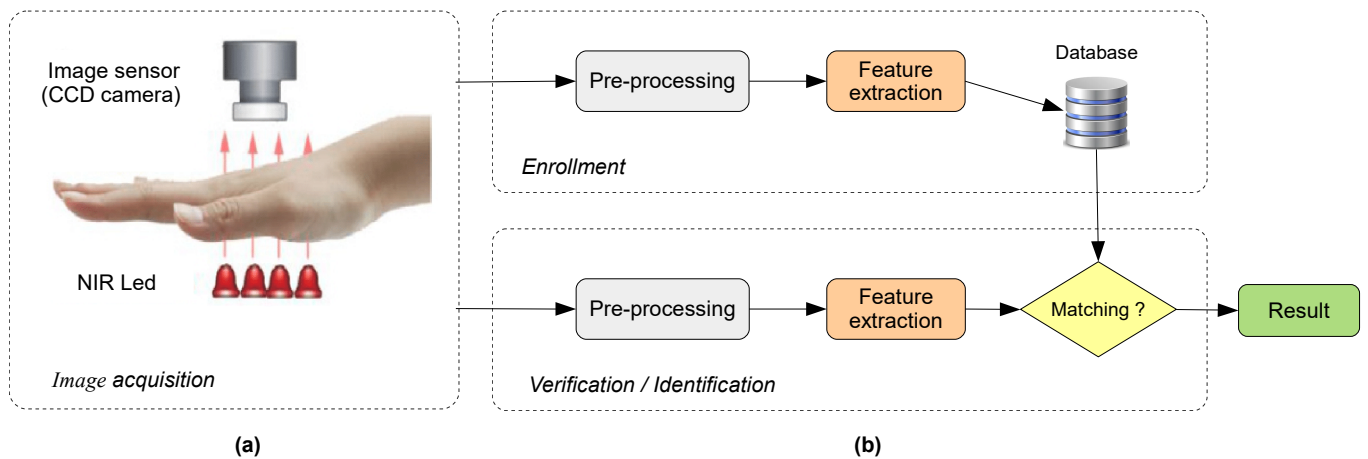


Figure 7: Framework of hand vein verification system. (a) hand vein image acquisition, specifically the PV using transmission mode; (b) Enrollment and identification phases.

- **PVs:** The palm's vein structure includes a more complex and denser network of veins, owing to the larger surface area. The palm's veins are situated beneath the skin and muscle, providing a unique and stable pattern for each individual. Because the palm has no hair, it is easier to photograph its vascular pattern. The palm also has no significant variations in skin color compared with fingers or the dorsal hand, where the color can darken in certain areas. The larger surface area offers more data for recognition, but recognition accuracy might be affected by wrinkles or scars present on the palm.
- **DHVs:** The veins on the back of the hand are more superficial and visible compared to those in the palm. They form distinctive patterns that can be easily captured with appropriate imaging techniques. They are more convenient for non-intrusive capture (easier to position the hand).

4.2. Architecture of hand vein recognition system

A hand vein recognition system operates through a three-step process: acquisition, enrollment, and verification (or identification), as illustrated in Figure 7. During the enrollment phase, individual images are collected and undergo preprocessing to remove noise. Feature extraction algorithms then identify unique characteristics of the vein network. These features are compiled into a secure digital template specific to the user and stored in a database. In the identification phase, the user's image is captured, and the system repeats the preprocessing and feature extraction steps. The extracted features are then compared with the database templates to either determine the user's identity in identification mode or verify the user's identity in verification mode [28].

4.2.1. Image acquisition

The acquisition of hand vein images is carried out usually using near-infrared (NIR) devices that interact with oxidized hemoglobin (HbO₂) and deoxidized hemoglobin (Hb) in the vascular network [17, 29]. When the light wavelength is between 720 nm and 760 nm, the radiation is strongly absorbed by Hb, producing a shadow corresponding to the vein pattern. At 790 nm, there is an intersection point where Hb and HbO₂ present the same absorption, which allows the visualization of veins and arteries. Meanwhile, for higher spectral ranges of the optical window HbO₂ presents a slight increase compared to Hb. Thus, the vascular pattern inside the hand can be rendered visible with the help of an NIR light source in combination with an NIR-sensitive image sensor. Several studies highlighted that wavelength range of 875nm-890nm is the best choice for hand vein recognition [30–32].

In NIR-based hand vein image acquisition (Figure 7 (a)), the device initially uses an light emitting diode (LED) array to emit NIR light onto the hand. A charge-coupled device (CCD) camera, which is sensitive to NIR light, then captures the detailed hand vein image. Several acquisition modes can be found:

- Based on NIR imaging technique, hand vein image acquisition can be categorized into transmission mode and reflection mode [33]. In transmission mode, NIR light passes through the hand, and an NIR-sensitive camera captures the light on the opposite side, creating a clear vein pattern due to the absorption properties of hemoglobin. In reflection mode, NIR light is emitted onto the hand's surface, and the reflected light is captured by an NIR-sensitive camera placed on the same side as the light source. This mode is more practical for various applications due to its ease of use and less restrictive positioning.
- Based on contact with the capture device, the acquisition modes can be divided into two categories: touch-based acquisition [34, 35] and touchless-based acquisition [36]. In the first mode, the hand is in contact with the device, ensuring stable positioning and consistent imaging conditions. The second mode does not require physical contact, enhancing hygiene and user comfort. It is particularly suitable for public or high-traffic environments but may require more advanced image processing to handle variations in hand positioning.
- Based on the illumination type, it can be divided into four categories: top-light illumination [37], side-light illumination [38], bottom-light illumination [39], and both-light (side and top) illumination [40]. In top-light illumination, NIR light is directed from above the hand, which highlights vein patterns with minimal interference from ambient light. In side-light illumination, NIR light is directed from the side, providing contrast that can enhance the visibility of veins through light reflection. In bottom-light illumination, NIR light is directed from below the hand, which can be effective in transmission mode setups. Both-light illumination combines side and top lighting, utilizing both reflection and transmission for comprehensive lighting and improved image quality.
- Based on hand pose for dorsal hand imaging, the acquisition modes can be classified into two categories: open hand mode [41], where the hand is positioned open and flat, making it easier to capture the dorsal vein patterns, and clenched hand mode [42], where the hand is clenched, which might be used to highlight different aspects of the dorsal vein network.

These various acquisition modes can be selected based on the specific needs and constraints of the hand vein recognition system, optimizing for factors such as image quality, user convenience, and application environment.

4.2.2. Image preprocessing

Image preprocessing plays a crucial role in hand vein recognition systems by ensuring that captured images are suitable for feature extraction and of high quality. Various factors, such as ambient light, sensor cleanliness, humidity, temperature, illumination, and user behavior, can affect the acquisition of hand vein images. Neglecting these factors can lead to low-quality images and decreased recognition accuracy. To address these issues, preprocessing involves several steps to improve vein pattern visibility and eliminate artifacts or noise that might hinder recognition. These steps include image quality assessment, image restoration and enhancement, and region of interest (ROI) extraction.

- **Image quality assessment:** Image quality assessment is a crucial initial step in the preprocessing of hand vein images. This process involves evaluating the overall quality of the captured images to determine if they meet the required standards for further processing. Factors such as focus, contrast, brightness, and overall clarity are assessed to ensure that the vein patterns are clearly visible and suitable for feature extraction. Images that do not meet the desired quality criteria may be discarded or undergo further enhancement to improve their suitability for subsequent processing steps.

Based on the human visual system's sensitivity and prior knowledge, numerous handcrafted descriptor-based methods have been developed for image quality assessment [43–45]. However, these handcrafted descriptor-based methods face several challenges. Firstly, some features directly derived from human visual system characteristics and prior knowledge may not adequately represent the quality of hand vein images. Secondly, single-feature methods are insufficient for comprehensive evaluation, while multi-feature methods are complex and time-consuming [5]. Integrating DL into image quality processes can significantly enhance the performance and efficiency of hand vein recognition systems. Unlike traditional handcrafted descriptor-based methods, DL models can automatically learn and extract relevant features from images without the need for explicit human knowledge or sensitivity to the visual system. DL models are capable of handling the complex and diverse characteristics of hand vein images, making them more effective at evaluating image quality. By utilizing large amounts of training data, DL models can establish an accurate mapping between image features and quality, enabling them to effectively assess the quality of new images. Several approaches have been developed, primarily focusing on FV recognition. An overview of these DL-based approaches is presented in section 6.1.1.

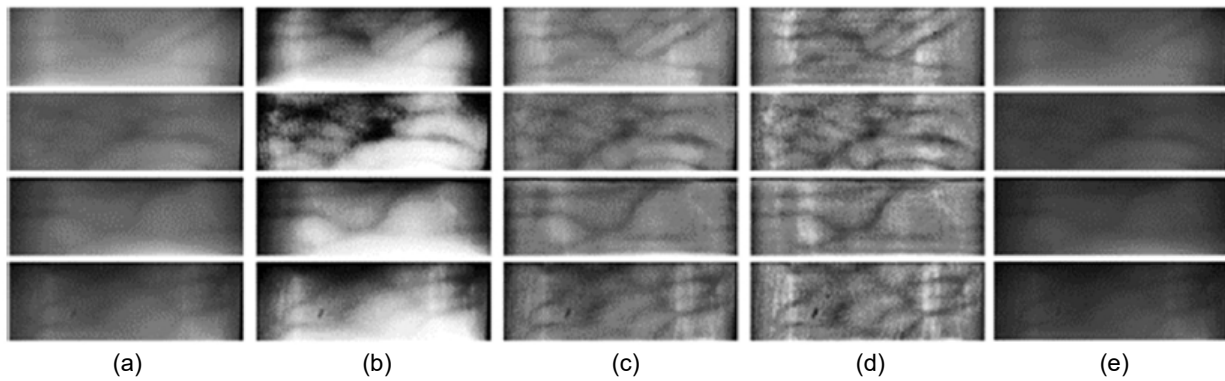


Figure 8: Examples of image enhancement methods applied to FV images (adopted from [5]). (a) Original images, (b) HE enhanced images, (c) AHE enhanced images, (d) CLAHE enhanced images, (e) Gabor enhanced images.

- Image restoration and enhancement:** Image restoration and enhancement processes are designed to improve the quality and clarity of captured images, making them more suitable for feature extraction and subsequent analysis. Image restoration focuses on recovering the original vein pattern from degraded images caused by factors such as sensor noise, motion blur, and compression artifacts. Several traditional image restoration techniques, primarily focusing on removing scattering in FV images, include the point spread function (PSF) [46, 47] and the biological optical model (BOM) [48, 49].

On the other hand, image enhancement techniques are principally used for denoising and contrast enhancement to further improve the visibility of vein patterns. These techniques are crucial for ensuring the accuracy and reliability of hand vein recognition systems by providing high-quality input images for subsequent processing stages. Common denoising methods include median filters, Gaussian smoothing filters, Wiener filters, and wavelet transforms. For contrast enhancement, widely used techniques include histogram equalization (HE), contrast-limited HE (CLHE), adaptive HE (AHE), contrast-limited adaptive histogram equalization (CLAHE) and Gabor filter. An example of image enhancement applied to FV images using these methods is illustrated in Figure 8. These tools are primarily integrated with handcrafted feature extraction approaches but are also widely combined with DL methods.

Both traditional and DL-based image restoration and enhancement techniques have their strengths and limitations. On one hand, traditional methods often rely on predefined mathematical models or filters, such as Gaussian filters for noise reduction, Gabor filters for edge detection to enhance vein patterns, and HE for contrast enhancement. These techniques have well-established mathematical foundations, making them computationally efficient and easy to implement without the need for training data. However, they may struggle to capture the full complexity of hand vein images across varied imaging conditions, such as changes in lighting, skin texture, or vein visibility. On the other hand, DL approaches, while potentially more powerful in learning complex image features, indeed rely on the predefined network architecture and training data. This reliance can limit their generalizability to different imaging conditions or noise types not represented in the training set. Therefore, successful DL models often require training data encompassing a wide range of image conditions and noise types to ensure robust performance and transferability. When properly trained on diverse datasets, they can often outperform traditional methods in specific tasks, particularly in handling complex, non-linear image degradations that are difficult to model mathematically.

- Image ROI extraction:** The ROI extraction process is crucial for isolating the specific regions of the hand that contain vein patterns, enhancing the accuracy of feature extraction, and reducing computational load by focusing only on relevant portions of the image. This process typically includes steps such as boundary selection and ROI localization. Image alignment techniques are also primarily applied to FV images during the ROI extraction process to reduce the effects of finger movement and rotation. This ensures that the extracted region is consistent and accurately represents the vein patterns, despite any variations in finger positioning during image capture [5]. ROI localization relies principally on detecting key points in the hand or finger. Due to the differences in vein pattern positions among the finger, palm, and dorsal hand, this process varies for each type. For FVs, the process often involves identifying the phalangeal joints, which are typically used to locate the region in the middle of the phalanx of a finger, ensuring that the central vein patterns are accurately captured [5]. For the palm and dorsal hand, the key points include the contours and reference (generally, the mid-point of the wrist) points, helping to define a consistent and precise ROI that encompasses the dense vein patterns [17, 19]. Several approaches have been explored for this step, each tailored to the specific characteristics of the vein patterns and the anatomical structure of the finger, palm, or dorsal hand. Figures 9 and 10 illustrate the ROI localization process for the finger [50] and dorsal hand [29]. The process for PV ROI localization is quite similar to that of the dorsal hand.

4.2.3. Feature extraction

After preprocessing, Feature extraction is a crucial step in hand vein recognition systems, as it involves identifying and quantifying the unique patterns in vein images that can be used for accurate identification and authentication. This process translates

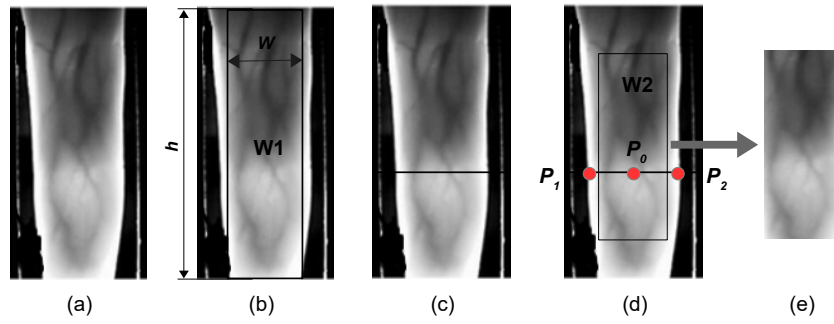


Figure 9: FV ROI extraction process [50]. (a) FV image; (b) A candidate region $W1$ centered in the $w \times h$; (c) Inter-phalangeal joint position; (d) A ROI region denoted by $W2$ extracted after locating three key points P_0 , P_1 and P_2 points; (e) A FV ROI image.

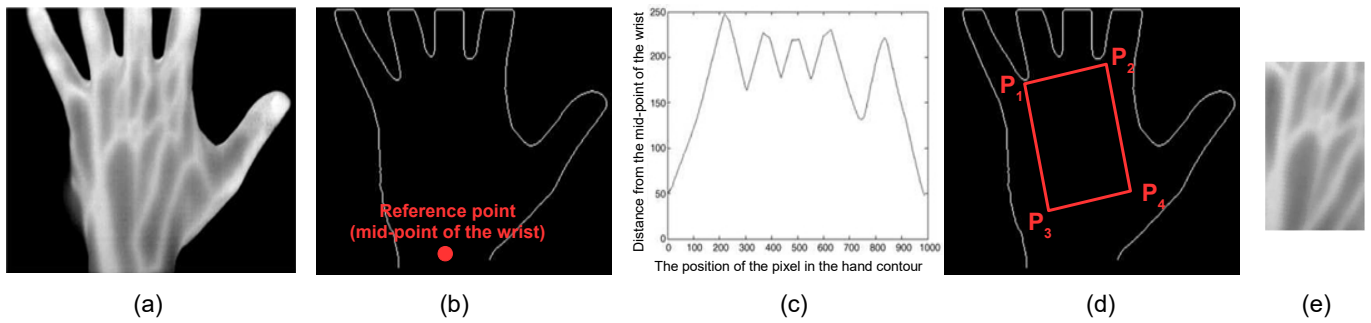


Figure 10: DHV ROI extraction process [29]. (a) DHV image, (b) the boundary of the hand, (c) the distance profile between the reference point and the contour points, (d) ROI localization after locating P_1 , P_2 , P_3 and P_4 . (e) A DHV ROI image.

the raw, preprocessed images into a set of numerical features that represent the essential characteristics of the vein patterns, facilitating the subsequent matching and classification stages. Traditional methods for feature extraction from vein images often rely on handcrafted techniques that utilize domain-specific knowledge. While traditional methods have been successful to some extent, they often require careful tuning and may not generalize well across different imaging conditions and populations. Handcrafted features are sensitive to noise and do not perform well on low-quality images. Additionally, setting standard parameters for these methods can be challenging, requiring extensive experimentation to determine suitable parameters for different databases. The choice of matching strategy after feature extraction can also significantly affect recognition performance [5].

DL methods have revolutionized feature extraction in recent years, offering a more automated and robust approach compared to traditional methods. DL can learn hierarchical feature representations directly from raw images without the need for handcrafted descriptors. These methods can simultaneously extract features, reduce data dimensionality, and classify within a single network structure. Compared to traditional methods, a significant advantage of DL is its ability to maintain good and stable recognition performance regardless of image quality and hand/finger placement. DL methods also reduce the need for extensive parameter tuning and can handle the complex and varied characteristics of hand vein images more effectively. Most proposed DL approaches in hand vein recognition focus on feature extraction tasks, as reviewed in section 6.

4.2.4. Matching

After feature extraction, the final stage involves comparing the acquired vein image to a stored template. This comparison generates a matching score that indicates how similar the two images are. A high score suggests the input image belongs to the enrolled individual, while a low score implies a potential imposter. Two main methods are used in this phase: distance-based and classification-based [5, 51]. The distance-based method directly compares the extracted feature vectors using a distance metric. The smaller the distance, the more similar the images are. On the other hand, the classification-based method utilizes ML algorithms to classify the input image as either a match or a non-match based on the extracted features.

In the context of DL approaches, classification methods often integrate feature extraction and classification into a single model. This integration allows the model to learn the most relevant features for matching during the training process, leading to more accurate and efficient recognition performance.

5. Datasets and evaluation metrics

This section outlines the datasets utilized in this study, detailing their composition, diversity, and relevance to the task of FV, PV and DHV recognition. Additionally, the section discusses the evaluation metrics employed to rigorously measure the effectiveness of our proposed DL approaches. These metrics provide a comprehensive understanding of model accuracy, robustness, and real-world applicability.

5.1. Overview of hand vein biometric datasets

Vein biometric datasets are essential for the development, testing, and evaluation of hand vein recognition systems. These datasets provide the necessary data to train and validate algorithms, ensuring they perform accurately and reliably under various conditions. In this section, the paper reviews the most commonly used datasets in DL-based approaches, focusing on FV, PV, and DHV images, as summarized in Table 3. These datasets are developed by the research community and are generally collected using self-designed and low-cost devices and different collection protocols. Consequently, they encompass a range of image parameters, including illumination, contrast, and performance results. Most of these datasets are publicly available on the internet or can be obtained by requesting them from the principal investigator.

For FV, THUMVFV-3V and MultiView-FV are two datasets specifically designed for multi-view recognition problems, offering data from various angles to enhance recognition accuracy in rotation and translation in practical applications. Additionally, the SCUT-SFVD, ISPR, and VERA finger vein datasets are utilized for PAD. These datasets include fake images created by printing real FV images, making them valuable for developing and testing anti-spoofing techniques.

DL models developed for hand vein recognition face significant challenges related to the small number of samples, which limits the training data for vein recognition tasks and, consequently, reduces the generalization performance of the models, and hinders their effectiveness. To address these challenges, researchers have explored two main solutions: (i) the use of pre-trained models, which leverage knowledge from large, diverse datasets, improving performance even with limited hand vein data, and (ii) the application of data augmentation techniques, which artificially increase the dataset size by creating variations of the existing data, enhancing the model's ability to generalize. Given the importance of these techniques in DL, this paper systematically analyzed their usage across all the reviewed articles in our study, as indicated in the Tables 5, 6, 8, 9, 10, and 11.

Additionally, some researchers have adopted the generation of synthetic databases, such as S-PVDB and NS-PVDB for PV recognition [52, 53]. Synthetic images can be highly effective for evaluating the performance of image processing algorithms. However, their use in biometric applications remains controversial. Synthetic databases have the advantage of avoiding the time-consuming process of real data collection and can facilitate the validation of proposed approaches on large-scale databases. Despite these benefits, synthetic datasets cannot entirely replace validation with real images. Therefore, while they help in large-scale testing, real-world data remains crucial for final validation and ensuring the robustness and reliability of hand vein recognition systems. The research conducted by Salazar-Jurado et al. [18] provides an overview of cutting-edge methods in synthetic PV imaging for biometric purposes, examining their strengths and weaknesses.

5.2. Evaluation metrics

A variety of evaluation metrics have been employed in assessing biometric recognition systems focusing on finger, hand, palm, and multi-modal approaches. While some metrics, such as peak signal-to-noise ratio (PSNR), structural similarity index measure (SSIM), area under curve (AUC), accuracy (Acc), recall (Rec), precision (Pre), and F1-score (F1), are commonly used for general image assessment and DL tasks, their definitions can be found in [3, 22, 79]. Other specific metrics tailored to hand vein-based DL assessment are summarized in Table 4.

Table 4: An overview of the evaluation measures utilized for appraising DL techniques applied to hand vein recognition.

Metric	Formula	Description
False acceptance rate (FAR)	$\frac{FP}{FP+TN} \cdot 100$	This refers to instances where unauthorized individuals are mistakenly allowed access. Adjusting the system's threshold gradually shifts security levels from high to low, causing FAR to increase from 0 to 1. FAR is called also false match rate (FMR).
False rejection rate (FRR)	$\frac{FN}{TP+FN} \cdot 100$	It measures legitimate users denied access due to unrecognized vein patterns. Crucial for system reliability, it influences user experience and security by evaluating hand vein biometric authentication effectiveness. When FAR increase from 0 to 1, FRR decrease from 1 to 0. FRR also referred to as false non-match rate (FNMR).
Equal error rate (EER)	$\frac{FAR+FRR}{2} \cdot 100$	Acts as a measure of the equilibrium between security and convenience within a biometric authentication setup. It serves as the primary safety gauge for the verification system. It also quantifies the overall error rate when referred to as half total error rate (HTER).
Genuine acceptance rate (GAR)	$\frac{TP}{TP+FN} \cdot 100$	It represents the rate at which legitimate users are correctly granted access by the biometric authentication system. It could also be expressed as $GAR = 1 - FRR$. GAR also referred to as Correct identification rate (CIR).
False discovery rate-correction (FDR)	$\frac{FP}{FP+TP} \cdot 100$	Refers to the rate at which the system incorrectly identifies a non-matching vein pattern as a match.

Table 4 (continued)

Metric	Formula	Description
Attack presentation classification error rate (APCER)	$1 - \left(\frac{1}{I_{\text{fake}}}\right) \sum_{i=1}^{I_{\text{fake}}} \text{Res}_i$	The APCER denotes the rate of error in misclassifying a spoof attack image (a fake image) as a genuine one (a real image). I_{fake} is the number of fake images. Res_i are the responses from authentication system. Res_i equals 0 if fake image wrongly classified as real, 1 if correctly classified as fake for input fake image i .
Bona fide presentation classification error rate (BPCER)	$\left(\frac{1}{I_{\text{real}}}\right) \sum_{i=1}^{I_{\text{real}}} \text{Res}_i$	This refers to the error rate of misclassifying a genuine image as a fake one. Also known as normal presentation classification error rate (NPCER). Res_i becomes 1 if real image wrongly classified as fake, 0 if correctly classified as real. Average classification error rate (ACER) represents the mean of both APCER and BPCER.
Frechet inception distance (FID)	$\ \mu_X - \mu_Y\ ^2 + \text{Tr}\left(\Sigma_X + \Sigma_Y - 2(\Sigma_X \Sigma_Y)^{\frac{1}{2}}\right)$	Evaluate the extent of contrast between the GAN-generated image and the authentic real image. X and Y are the feature distribution of real and synthetic vein patterns, respectively, μ_X and μ_Y are the mean feature vectors of X and Y respectively, Σ_X and Σ_Y are the covariance matrices of X and Y respectively, Tr represents the trace operator, and $\ \cdot\ ^2$ denotes the squared Euclidean norm.
Wasserstein distance (WD)	$\left(\inf_{\pi \in \Pi(P;Q)} \int_{\mathbb{R}^d \times \mathbb{R}^d} X - Y ^p d\pi\right)^{\frac{1}{p}}$	In the context of biometric vein recognition, it can be used to quantify the dissimilarity between two sets of vein patterns. P and Q represent the probability distributions of vein patterns from two different individuals, and X and Y represent feature vectors extracted from vein patterns of individuals.
Similarity(\mathbf{x}, \mathbf{y})	$\cos(\theta) = \frac{\mathbf{x}^T \cdot \mathbf{y}}{\ \mathbf{x}\ \cdot \ \mathbf{y}\ }$	The cosine similarity score is crucial for calculating the matching score between feature vectors x and y , distinguished by angle θ . It facilitates hand vein pattern recognition by comparing feature vectors' angles [80].

6. DL in hand vein biometrics

This section reviews SOTA DL approaches in hand vein biometrics recognition, focusing on FV, PV, and DHV identification. It examines recent advancements and methodologies proposed for enhancing biometric accuracy and robustness. By exploring various neural network architectures and training techniques, this section aims to highlight significant contributions and breakthroughs in the field.

6.1. FV-based methods

FV recognition has gained significant attention through the use of DL. Several approaches have been proposed in this field, with a focus on applying DL in preprocessing steps to enhance the quality of input images or in feature extraction to automatically learn discriminative features. Additionally, DL methods have been employed to protect biometric template and to detect presentation attacks, such as spoofing with fake FVs.

6.1.1. Preprocessing-based methods

In the preprocessing step, DL models have been developed to automatically assess the quality of FV images, enabling the selection of the most reliable samples for feature extraction. Furthermore, image enhancement and restoration techniques based on DL have been proposed to improve the clarity and contrast of FV images, enhancing the overall recognition accuracy. Tables 5 and 6 summarize proposed schemes identified by their *objective* fields, including preprocessing techniques for image quality assessment, enhancement and restoration.

- 1) **Image quality assessment:** Qin and El-Yacoubi [81, 82] were the first to apply DL for FV quality assessment. They proposed training a CNN on binary images to predict vein quality, aiming to minimize verification errors. Low and high-quality images are automatically labeled, assuming low-quality images are false rejected FV images. Experimental outcomes show the proposed method's efficacy in achieving high performance in a public database. Zeng et al. [83] utilized a light-CNN approach for assessing image quality, specifically to determine if it contains well-defined and consistent vein patterns. They segmented the image into multiple blocks and calculated average results from these block images to assess overall quality. This light-CNN architecture reduces computation time while also extracting strong features to represent the quality of FV images. In [84], a CNN-based method for evaluating FV image quality was introduced to improve recognition performance and reduce false rejection of low-quality images. The method uses statistical analysis to compare different finger samples, automatically determining and classifying image quality. A lightweight CNN is then used to train images classified as high or low quality based on the evaluation criteria. By identifying common attributes among low-quality images, the system can efficiently assess image quality in practical

Table 3

Summary of publicly available hand vein datasets. The quantity of subjects and samples is denoted as subjects \times hands (or fingers) and samples \times acquisition sessions, respectively.

VM	Dataset	Total images	Subjects	Samples	Images sizes	SIs	Ref	
FV	FV-USM	5904	123 \times 4	6 \times 2	640 \times 480	>15 days	[54]	
	HKPU-FI	6264	156 \times 2	6 \times 2	513 \times 256	1 to 6 months	[37]	
	MMCBNU_6000	6000	100 \times 6	10 \times 1	480 \times 640	–	[55]	
	SDUMLA-HMT	3816	106 \times 6	6 \times 1	320 \times 240	–	[56]	
	UTFVP	1,440	60 \times 4	2 \times 2	672 \times 380	15 days	[38]	
	THU-FVDT1	1760	220 \times 1	4 \times 2	720 \times 576	12 sec	[57]	
	THU-FVFDT2	1220	610	1 \times 2	720 \times 576	3 to 7 days	[57]	
	THU-FVFDT3	9760	610	16 \times 2	720 \times 576	–	[57]	
	THUMV-FV-3V	23,760	180 \times 4	6 \times 2	–	30-106 days	[58]	
	MultiView-FV	6480	135 \times 4	12 \times 2	1280 \times 1024	30-106 days	[59]	
	NUPT-FPV*	16800	140 \times 6	10 \times 2	300 \times 400	–	[60]	
	PLUSVein-FV3	7200	60 \times 6	20 \times 1	1280 \times 1024	–	[61]	
	SCUT-FV	61344	568 \times 1	108 \times 1	640 \times 288	–	[62]	
	SCUT-SFVD	7200 ^a	14 \times 6	6 \times 1	158 \times 467	–	[63]	
	PV	ISPR	5820 ^b	33 \times 10	10 \times 1	640 \times 480	–	[64]
VERA FingerVein		880 ^c	110 \times 2	2 \times 1	250 \times 665	–	[65, 66]	
CASIA		7,200	100 \times 2	3 \times 2	768 \times 576	30 days	[67]	
VERA PalmVein		2,200	110 \times 2	5 \times 2	480 \times 680	5 minutes	[68]	
PUT		1,200	50 \times 2	4 \times 3	1,280 \times 960	7 days	[69]	
PolyU		6,000	250 \times 2	6 \times 2	352 \times 288	9 days	[70]	
Tonji		12,000	300 \times 2	10 \times 2	800 \times 600	61 days	[71]	
IITI		2,220	185 \times 2	6 \times 1	2,592 \times 1944	–	[72]	
FYO*		640	160 \times 2	1 \times 2	800 \times 600	10 minutes	[73]	
S-PVDB		12,000	10,000 \times 1	6 \times 1	128 \times 128	–	[52]	
NS-PVDB		12,000	2,000 \times 1	6 \times 1	128 \times 128	–	[53]	
DHV		NCUT	2040	102 \times 2	10 \times 1	640 \times 480	–	[74]
		Bosphorus	1575	100 \times 1	3 \times 4	300 \times 240	–	[75]
		Badawi's dataset	5000	500 \times 2	5 \times 1	320 \times 240	–	[76]
		JLU	3680	736 \times 1	5 \times 1	320 \times 240	–	[77]
	DHVI	1782	251 \times 2	4/3 \times 2	752 \times 560	2 months	[78]	

Abbreviation: Vein mode (VM), session intervals (SIs), (*): Means dataset used in many modes.

^a(3600 real, 3600 fake): Fake images are generated from each real image by printing them onto two aligned and stacked overhead projector films.

^b(3300 real, 2520 fake): Fake images are created by printing 56 real images using three printers, each set at three different z-distances.

^c(440 real, 440 fake): Fake images are generated by printing real images from 50 subjects using a laser printer.

settings. Experimental results demonstrate the method's excellent performance on three public datasets, showing its effectiveness in enhancing the original recognition system's performance.

- 2) **Image restoration and enhancement:** Guo et al. [85] proposed an image restoration approach to enhance the integrity of venous networks. The method involves an adaptive threshold method to detect the unknown incomplete regions in FV images. Subsequently, a convolutional autoencoder (CAE) network model is employed to restore the FV images. Experimental results demonstrate the effectiveness of the approach in improving vein network integrity in FV images. CAE was also used for FV image enhancement [86], where a residual CAE architecture is trained in a supervised manner to enhance vein patterns in near-IRIs. The method has been evaluated on several databases, showing promising results on the UTFVP database as a main outcome. In [87], authors proposed a method using a modified conditional generative adversarial network (GAN) to restore optically blurred FV images. The GAN includes a generator with an encoder and decoder, along with a discriminator. The restored images were then used for FV recognition using a deep CNN, leading to improved recognition performance. Similarly, a GAN-based restoration model was proposed in [88] to recover missed patterns in FV images. The results show that the proposed method restores missed vein patterns and reduces the EER of the FV verification system. Jiang et al. [89] proposed a finger vein restoration algorithm based on neighbor binary Wasserstein GAN (NB-WGAN). The method uses texture loss as part of the loss function of the generator to recover more vein texture details. In recent work [90], GANs were used to restore FV images by addressing multiple degradation factors like non-uniform illumination and noise. The approach classified the degradation factor using a task adaptor and adaptively restored the image based on this factor through task channel-wise attention. Gated fusion was employed to merge features from four points in the generator, simultaneously considering feature characteristics from low to high levels. Deep reinforcement learning (DRL) approach enables automatic decision-making by considering the environment's state, the desired actions, and the rewards obtained, is used with GAN for FV image restoration [91]. This model trains an agent to select restoration behaviors based on the image state, enabling continuous restoration. The tasks are divided into deblurring, defect restoration, and denoising/enhancement. For deblurring, a FV deblurring GAN based on DeblurGAN-v2 with an Inception-ResNet-v2 backbone is used. For defect restoration, a FV feature-guided restoration network is proposed with two stages: feature image restoration and original image restoration. Experimental results show reduced EER for single and multiple image restoration problems.

Lei et al. [92] proposed a model based on the pulse coupled neural network (PCNN) to enhance the quality of FV images. They developed a parameter setting scheme to automatically adjust the parameters in the PCNN model, eliminating the need for empirical correlations or training. The results demonstrate that the PCNN can produce enhanced FV images with higher quality, thereby improving the efficiency of FV image recognition. Du et al. [93] proposed FVSR-Net architecture, an end-to-end CNN designed for restoring FV scattering images. The network utilizes a multi-scale CNN for the task of FV scattering removal, aiming to extract clear vein backbone features. Experimental results demonstrate that the proposed method achieves better visual and recognition performance.

6.1.2. Features extraction-based methods

DL methods for feature extraction have demonstrated significant advancements in capturing discriminative features from FV images. These approaches utilize DL models to learn hierarchical representations of FV patterns, enhancing their potential for matching and identification tasks. Deep features extracted through these methods have exhibited superior performance compared to traditional handcrafted features, particularly in terms of recognition accuracy. The DL approaches discussed in this section focus either on feature extraction alone or on both feature extraction and matching processes.

Due to the robust feature learning capabilities of DL, a majority of the proposed approaches for FV analysis fall into this category, accounting for 67 articles in our case. To enhance organization and readability, these approaches are categorized based on the specific DL techniques employed. Tables 5 and 6 summarize proposed schemes for feature extraction, without and with use of DTL, respectively.

Table 5: Summary of proposed works in preprocessing, feature extraction and matching-based DL for FV recognition without DTL. Some studies have employed specific data augmentation techniques to achieve the reported results. In cases where multiple scenarios are examined, only the top-performing outcome is mentioned.

Ref.	Year	Obj.	DL approach	Data augmentation	Dataset	Results
[81]	2015		CNN+P-SVM	-	HKPU-FI, FV-USM	Acc=88.99%, 74.98%
[83]	2018	Image quality assessment	Lightweight CNN	-	MMCBNU_6000, SDUMLA-HMT	Acc=71.95%, 74.63%
[84]	2022		CNN	Low quality images generation by applying cropping and mirroring	SDUMLA-HMT, MMCBNU_6000, FV-USM	Acc=81.97%, 75.27%, 73.85%
[85]	2019		CAE	-	Self-built dataset	EER = 0.0016%
[86]	2021		CAE	Images random horizontal flip, rotation, translation and shear	UTFVP, SDUMLA-HMT	HTER=1.0%, 9.8%
[87]	2020		GAN+CNN	Images shifting by 1-3 pixel (up, down, left, right directions), applying Gaussian blur	SDUMLA-HMT, HKPU-FI	EER= 3.934%, 2.746%
[88]	2020	Image restoration and enhancement	GAN	-	MMCBNU_6000, FV-USM	EER = 5.66%, 2.37%
[89]	2022		NB-WGAN	-	Self-built dataset	PSNR= 52.085dB; FRR= 30.77% (when FAR= 0%)
[91]	2023		DeblurGAN-v2+DRL	-	MMCBNU_6000, SDUMLA-HMT, FV-USM, UTFVP	PSNR=41.18dB, 44.26dB, 53.49dB, 49.85dB; EER≈ 6.5%, 4.3%, 4.8%, 3.7%
[92]	2019		PCNN	-	Self-built (NJUST-FV) & SDUMLA-HMT, THU-FV, HKPU-FI	EER ≈ 4.7%, 5.1%, 0.2%, 5.9%
[93]	2021		CNN	-	Self-built dataset, SDUMLA-HMT	PSNR= 15.95dB, 13.59dB; EER= 0.11%, 8.39%
[94]	2017		CNN	-	HKPU-FI, FV-USM	EER = 2.70%, 1.42%
[95]	2018		CNN	-	HKPU-FI, FV-USM, SDUMLA-HMT, UTFVP	Acc=96.55%, 98.58%, 97.48%, 95.56%
[96]	2023		CNN + FL	-	MMCBNU_6000, HKPU-FI, PLUSVein-FV3, SDUMLA-HMT, THU-FVFD3, FV-USM, UTFVP, VERA FingerVein, SCUT-FV	EER=0.35%, 0.48%, 0.76%, 1.52%, 2.09%, 0.07%, 1.62%, 4.54%, 0.82%
[97]	2024		CNN + FL	-	FV-USM, HKPU-FI, NUPT-FPV, SDUMLA-HMT, UTFVP, VERA FingerVein	EER=0.68%, 0.97%, 1.10%, 3.73%, 1.62%, 9.09%
[98]	2019		Gabor CNN	-	MMCBNU_6000, FV-USM, SDUMLA-HMT	EER=0.11%, 0.57%, 1.09%
[99]	2023		Lightweight CNN	Images shifting and rotating	Self-built dataset, SDUMLA-HMT	Acc=95.82%; EER=4.17%; Inference time=0.356 s
[100]	2023		CNN	-	HKPU-FI, FV-USM	Acc=92.11%, 94.17%
[101]	2017		CNN	-	Self-built dataset, MMCBNU_6000, SDUMLA-HMT, FV-USM	EER= 2.04%, 0.17%, 0.87%, 0.50%
[102]	2021		CNN	-	SDUMLA-HMT, FV-USM, MMCBNU_6000	EER= 2.29%, 0.47%
[103]	2021		Merge CNN	-	FV_USM, SDUMLA-HMT, THU-FVFD2	Acc=96.15%, 99.48%, 99.56%
[104]	2018		Lightweight CNN	-	MMCBNU_6000, SDUMLA-HMT	EER=0.10%, 0.47%
[105]	2019		Lightweight CNN	-	HKPU-FI	EER=0.097%
[106]	2021		Lightweight CNN	-	SDUMLA-HMT, PKU-FVD	Acc= 99.3%, 99.6%; EER=1.13%, 0.67%
[107]	2020		Lightweight CNN	-	MMCBNU_6000, FV-USM	Acc=99.05%, 97.95%; EER= 0.503%, 1.070%
[108]	2023		Lightweight CNN (LModel)	-	HKPU-FI	Acc=99.13%
[109]	2023		Residual CNN	Gabor	Grayscale normalization and linear mixing of ROI fine FVIs image	Acc=99.67%, 100%, 97.22%, 98.98%, 100%; EER=0.08%, 0.00%, 0.55%, 0.31%, 0.0003%
[110]	2019		CNN	-	Self-built dataset, SDUMLA-HMT	Acc=100%, 98.78%; EER=0.21%, 2.82%

Table 5 (Continue)

Ref.	Year	Obj.	DL approach	Data augmentation	Dataset	Results
[111]	2019		CNN		SDUMLA-HMT	EER=0.30%
[112]	2018		CNN + RAB	-	FV-USM, MMCBNU_6000	Acc= 98.58%, 97.54%
[113]	2022		CNN+Attention	-	SDUMLA-HMT	Acc=100%
[114]	2022		CNN+Attention	-	SDUMLA-HMT, MMCBNU_6000, FV_USM, Self-built dataset	EER=0.35%, 0.08%, 0.34%, 0.49%
[115]	2022		Lightweight CNN+CBAM	-	FV_USM, HKPU-FI	Acc=100%, 100%
[116]	2023		CNN+Residual AM	Luminance transformation and gaussian noise	SDUMLA-HMT, FV_USM, MMCBNU_6000, UTFVP, HKPU-FI	EER=0.44%, 0.05%, 0.01%, 1.21%, 0.18%
[117]	2023	Feature extraction	CNN+Attention	-	SDUMLA-HMT, HKPU-FI, NUPT-FPV	Acc=94.50%, 97.86%, 98.92%; EER=0.53%, 0.32%, 0.14%
[118]	2023		CNN+Attention	Random color jitter, translation and perspective	FV_USM, MMCBNU_6000, THU-FVDT2, SDUMLA-HMT, HKPU-FI, PLUSVein-FV3, UTFVP, VERA FingerVein, SCUT-FV	EER=0.20%, 0.18%, 2.15%, 1.10%, 0.81%, 1.32%, 2.08%, 6.82%, 0.83%
[119]	2021		ViT	-	FV_USM, SDUMLA-HMT, MMCBNU_6000	Acc=93.50%, 91.75%, 91.84%
[120]	2022		ViT	-	FV_USM, MMCBNU_6000, SDUMLA-HMT, HKPU-FI	EER=0.44%, 0.92%, 1.50%, 2.37%
[121]	2022		ViT	Images cropping, rotation and dropout	FV_USM, SDUMLA-HMT	Acc=99.73%, 92.77%; EER= 0.042%, 1.033%
[122]	2022		T2T-ViT	-	FV_USM, SDUMLA-HMT	Acc=94.85%, 99.48%; EER= 2.46%, 0.94%
[58]	2022		ViT	-	Self-built dataset (THUMV-FV-3V)	Acc=99.79%
[123]	2016		DBN	-	Self-built dataset	Acc=96.9%
[124]	2020		CAE+SVM	Image flip, rotation, shift, shear, and zoom	FV-USM, SDUMLA-HMT	Acc=99.95%, 99.78%; EER=0.12%, 0.21%
[125]	2018		CAE	-	UTFVP, SDUMLA-HMT	Acc=99.95%, 99.78%; EER=2.17%, 2.87%
[126]	2018		CAE+CNN	-	FV-USM	Acc=99.49%; EER=0.16%
[127]	2019		SCNN+LSTM	-	HKPU-FI	EER=2.38%
[128]	2019		FCGAN+CNN	GAN	HKPU-FI	EER=0.87%
[129]	2019		GAN+CNN	GAN	Self-built dataset, FV_USM, SDUMLA-HMT, HKPU-FI	EER=0.06%, 0.03%, 0.05%, 0.15%
[130]	2022		ViT+CapsNet	-	MMCBNU_6000, SDUMLA-HMT, FV_USM, HKPU-FI	Acc=97.52%, 93.24%, 98.68%, 95.61%; EER=0.63%, 1.3%, 0.28%, 1.66%
[131]	2019		PCANet	-	FV_USM, SDUMLA-HMT, THU-FVDT2	Acc=99.49%, 98.19%, 100%
[132]	2018		CycleGAN	-	THU-FVDT2, SDUMLA-HMT	EER=1.12%, 0.94%
[133]	2022		SDBCCML	-	SDUMLA-HMT	Acc=94%; F-Score=96%; Time complexity=66ms
[134]	2022		TFHFT-DPFNN	-	SDUMLA-HMT	PSNR=58.58; Acc=98%; Time complexity=60ms
[135]	2023		FNN	Modified Mixup Method [136]	FV_USM, SDUMLA-HMT, MMCBNU_6000	EER=0.10%, 0.06%, 0.24; Time complexity=32.24ms
[137]	2022		Deep Forest	-	SDUMLA-HMT	Acc=98.40%; EER=2.8%
[138]	2024		GRU+attention +NAS	-	Self-built dataset, HKPU-FI, MMCBNU_6000	Acc=97.33%, 97.92%, 98.29%; EER=1.25%, 0.99%, 1.00%

Table 6: Summary of proposed works in preprocessing, feature extraction and matching-based DL for FV recognition with DTL. Some studies have employed specific data augmentation techniques to achieve the reported results. In cases where multiple scenarios are examined, only the top-performing outcome is mentioned.

Ref.	Year	Obj.	DL approach	DTL	Data augmentation	Dataset	Results
[82]	2018	Image quality assessment	CNN+P-SVM	Pretraining and fine-tuning between datasets	-	FV-USM & HKPU-FI & MMCBNU_6000 & SDUMLA-HMT	Acc=73.57%, 87.08%
[90]	2024	Image restoration and enhancement	GAN+CNN	Domains adaptation with DenseNet-161, and ConvNeXt-small	Images Cropping and 4-way translation	SDUMLA-HMT, HKPU-FI	FID= 15.09, 26.63; WD=2.89, 3.22; EER = 4.72%, 1.73%
[139]	2024		VGG-Net-16+ELM	DTL form source dataset to target dataset using ELM	Images cropping, scaling, brightness and contrast transformation, masking, and rotation	SDUMLA-HMT, THU-FVDT2, HKPU-FI	Acc= 99.21%, 99.51%, 98.62%, 99.88
[140]	2023		ResNet+Attention	Domains adaptation	FV_USM, SDUMLA-HMT, THU-FVDT3	Acc=99.90%, 100%, 100%	
[141]	2023		EfficientNetV2+Attention	Domains adaptation	-	FV_USM, SDUMLA-HMT	Acc=98.96%, 97.29%
[59]	2021		CAE+Siamese CNN	Pretrained weights from ImageNet dataset	-	MultiView-FV, SDUMLA-HMT and MMCBNU_6000	EER=1.69%, 0.47%, 0.1%
[62]	2019		Lightweight CNN	Knowledge distillation from pretrained-weights ResNet-50	Images gamma transformation, shear, translation, rotation, enlargement and channel color shifting	Self-built dataset (SCUT-FV), SDUMLA-HMT, FV-USM, HKPU-FI	Acc= 97.90%, 99.25%, 99.79%, 97.90%; EER= 3.97%, 1.53%, 0.25%, 1.30%
[142]	2019		DensNet	Fine-tuning pretrained DensNet-161	Images translation	SDUMLA-HMT, HKPU-FI	EER = 2.35%, 0.33%
[143]	2021		InceptionResNetV2	Pretrained weights from COCO dataset	-	SDUMLA-HMT, Self-built dataset	Acc=99.25%, 99.08%
[144]	2023		Densenet-161	Pretrained weights from ImageNet dataset	-	FV-USM, SDUMLA-HMT, THU-FVDT2	Acc=97.66%, 99.94%, 88.19%; EER=2.03%, 0.24%, 12.61%
[145]	2024		ResNet152V2 and MobileNetV3	Domains adaptation	-		Acc=99.6%, Precision=99.42%

Table 6 (Continue)

Ref.	Year	Obj.	DL approach	DTL	Data augmentation	Dataset	Results
[146]	2022		Lightweight CNN	Fine-tuning pre-trained MobileNetV2	–	HKPU-FI, FV-USM, SDUMLA-HMT	Acc=93.05%, 94.67%, 96.61%, EER=2.47%, 1.37%, 0.99%
[147]	2022		AlexNet	Domains adaptation	–	FV-USM, SDUMLA-HMT	Acc= 99.1%, 98.1%; EER = 0.002%, 0.003%
[148]	2021	Feature extraction	ECA-ResNet	Domains adaptation	Image flip, rotation, shift, shear, and zoom	SDUMLA-HMT, FV-USM, MMCBNU_6000	EER= 1.20%, 0.76%, 0.30%
[149]	2023		Lightweight CNN	Fine-tune first pretrained layers of MobileNetV2 on CIFAR dataset	–	HKPU-FI, FV-USM, SDUMLA-HMT, UTFVP	Acc=91.03%, 96.17%, 95.07%, 92.50%; EER=4.25%, 1.21%, 1.27%, 1.93%
[150]	2018		CNN	Fine tuning pretrained VGGFace-Net	Images projective transform, rotation and cropping	Self-built dataset, SDUMLA-HMT, FV-USM, HKPU-FI	Acc= 97.90%, 99.25%, 99.79%, 97.90%; EER= 3.97%, 1.53%, 0.25%, 1.30%
[151]	2020		Lightweight CNN (ShuffleNet V2)	Pretrained weights from ImageNet dataset	Images random brightness, cropping, rotating and erasing	SDUMLA-HMT, FV-USM, and MMCBNU_6000	EER= 0.37%, 0.31%, 0.05%
[152]	2021		ResNet	Pretrained weights from ImageNet dataset	Inter-class augmentation via vertical flip and intra-class augmentation via geometric and color transformations	FV_USM, MMCBNU_6000, HKPU-FI	EER=0.48%, 0.21%, 1.90%
[153]	2017		CNN	Fine tuning pretrained VGG Net-16	Image translation and cropping	2 self-built datasets, SDUMLA-HMT	EER = 0.804%, 2.967%, 6.115%
[154]	2019		CNN	Pre-trained convolutional filters from ImageNet dataset	–	MMCBNU_6000, SDUMLA-HMT	EER=0.74%, 2.37%
[155]	2022		CNN	Fine-tuning pre-trained Xception on ImageNet dataset	Image rotating, width shifting, zooming, horizontal flipping and shearing	SDUMLA-HMT, THU-FVFDT2, FV_USM,	Acc=98.5%, 90%
[156]	2022		Local attention Transformer	Fine-tuning several pre-trained models	–	Self-built dataset, FV_USM	Acc=98.44% (12 views, 0° rotation), 99.80%
[157]	2024		MobileViT	DA	Mixup method [136]	SDUMLA-HMT, FV_USM	Acc=99.53%, 100.00%; EER=0.47%, 0.02%; Time complexity=10m
[158]	2021		CAE+CNN	Fine-tuning pretrained U-Net and ResNet on ImageNet dataset	Images cropping	SDUMLA-HMT, THU-FVFDT2	Acc=99.53%, 98.64%

1) **CNN:** Qin and Yacoubi [94] introduced a segmentation model for FV verification based on DL. They utilized a CNN to predict the probability of pixels belonging to veins or background by learning deep feature representations. Additionally, they presented a method for recovering missing FV patterns using a fully convolutional network to enhance recognition performance. Das et al. [95] introduced a DL approach utilizing CNN to extract robust features, achieving high accuracy regardless of image quality. Experimental evaluations on four widely used databases validated the method's robustness in feature extraction and classification under varying image qualities. Song et al. [142] employed a deep densely connected CNN, DensNet, for FV recognition, utilizing composite images as input data. This approach exhibited robustness against noise and misalignment. Hsia et al. [147] introduced an enhanced edge detection method designed to adapt to the rotational and translational movements of detected fingers, as well as to mitigate interference from external light and other environmental factors. They proposed integrating this approach, which utilizes the CNN AlexNet, into computer systems. Tran et al. [144] introduced a FV recognition system designed for the virtual reality human-robot equipment in the Metaverse to prevent misappropriation. Their approach utilizes a CNN and anti-aliasing technique, yielding promising results across three public datasets. Recently, Federated learning (FL) technique is introduced in FV to solve the problem of small sample size and category diversity while protecting user privacy [96, 97].

To enhance the capacity for learning features, metric learning, which is proposed to measure the distance between sample features, is introduced in DL-based FV systems [62, 101, 102, 105–107, 148, 151, 152]. Huang et al. [101] applied contrastive loss in a deep CNN for FV identification. They paired intra-class and inter-class samples as input, aiming to maximize inter-class distance and minimize intra-class distance during training. Their method used metric learning to enhance the network's ability to distinguish between different FV patterns. Later, Tang et al. [62] further modified the contrastive loss to extract more discriminative features, pairing intra-class and inter-class samples to achieve the same goal of maximizing inter-class distance and minimizing intra-class distance. Hou and Yan [148] presented the Arc-vein method, which incorporates a novel arccosine center loss into a CNN to improve its ability to extract and recognize FV features. Figure 11 illustrates this Arc-vein method, providing a prominent example of metric learning applied to FV verification. The diagram effectively demonstrates the complete process, from Region of ROI extraction to feature extraction using the efficient channel attention residual network (ECA-ResNet), and finally, feature identification using the combined softmax and arccosine center loss. In [102], the authors proposed a shallow CNN with improved interval-based loss function for efficient real-time application in both closed-set and open-set architectures of FV recognition. Several approaches [105–107] have employed the triplet loss function, which has shown promising results. Figure 12 illustrates the general mechanism of this widely used metric learning approach. It clearly shows how the function learns effective embeddings for FV images, ensuring that images from the same individual are grouped closely together in the embedding space, while images from different individuals are separated.

The increasing depth of CNNs raises computation costs, posing challenges for deploying network architectures efficiently on various hardware platforms. Training a customized CNN model from scratch demands substantial computing resources in terms of time, energy, finances, and environmental impact. Research in DL aims to miniaturize neural networks, reducing model

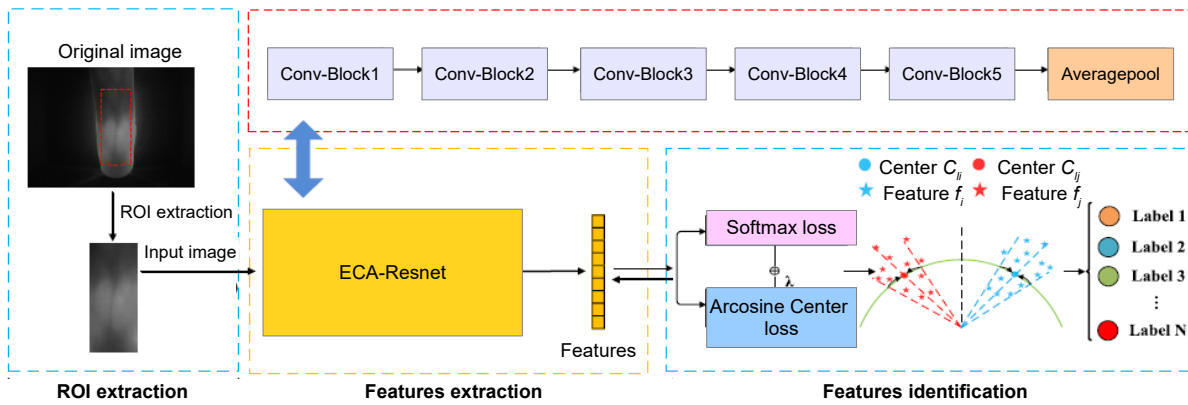


Figure 11: Arc-Vein FV image verification framework. This approach combines the softmax loss with the newly designed arccosine center loss during model training, with the goal of enhancing FV image verification performance. The Arc-vein framework, which includes ROI image extraction, feature extraction using efficient channel attention residual network (ECA-ResNet), and feature identification with arccosine loss and softmax loss [148].

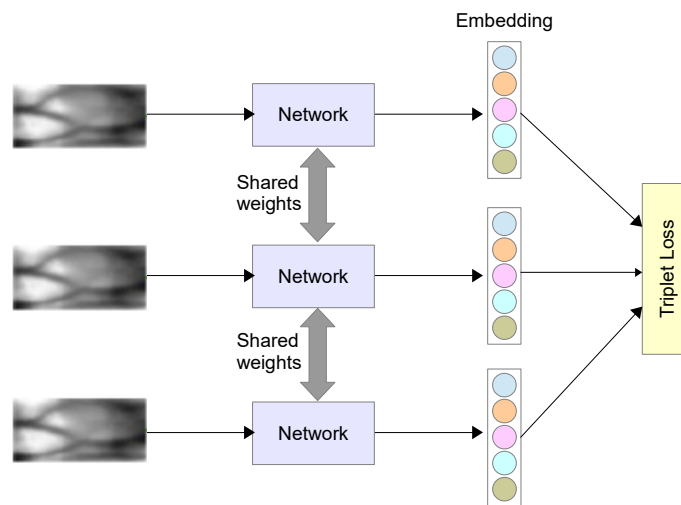


Figure 12: Mechanism of action of Triplet loss function. The triplet loss in FV recognition aims to learn effective embeddings for each FV image. In the embedding space, FV images from the same individual should be closely grouped together, forming distinct clusters. The objective of the triplet loss is to ensure that examples with the same label have their embeddings positioned closely together, while examples with different labels have their embeddings placed far apart.

depth and parameter count. Lightweight networks focus on minimizing the size of CNN-based FV recognition methods while maintaining satisfactory accuracy. Several work have been proposed in this context [62, 104–108, 115, 149, 151]. For instance, Fang et al. introduced a lightweight CNN framework for FV verification [104], which overcomes the high computational demands and training sample requirements of traditional CNNs. Their approach involves a two-stream model integrating the original image with a mini-ROI image, addressing displacement and data limitations. Leveraging features extracted from this two-stream network, they achieved SOTA results with reduced computational costs. Similarly, in their study, Xie et al. [105] introduced a light CNN framework to improve FV matching performance using enhanced images. Their experiments demonstrated that, when combined with a triplet similarity loss function (as illustrated in Figure 12) and incorporating supervised discrete hashing, superior accuracy was achieved while also reducing the template size. Moreover, Shen et al. [106] proposed algorithm using a lightweight CNN model in the backbone network and employs a triplet loss function to train the model. While the feature and pattern extraction is based on Min-ROI and Gaussian filter optimization, recognition and matching is based on lightweight CNN. On the other hand, Zhao et al. [107] proposed a lightweight linear CNN model similar to AlexNet. This model achieved exceptional performance in FV verification by implementing dynamic regularization and center loss. To illustrate the simplified structure of a lightweight CNN, the architecture adopted in [105] is depicted in Figure 13 as an example. This architecture, with its reduced depth and complexity compared to traditional models, effectively balances accuracy and efficiency.

Data augmentation technique have been introduced DL-based FV methods to improve the feature learning ability when the amount of FV database is limited [62, 99, 109, 116, 118, 139, 142, 148, 150–153, 155]. Hu et al. [150] introduced the FV Network (FV-Net), a CNN model to learn discriminative and robust features representative of FVs. They first applied sample augmentation strategies to expand the training set and transplanted a pre-trained model to prevent overfitting. Additionally, they designed a network structure to extract features with spatial information and proposed a matching strategy to address misalignment issues caused by translations and rotations in vein pattern recognition. Their approach demonstrated effectiveness on three publicly

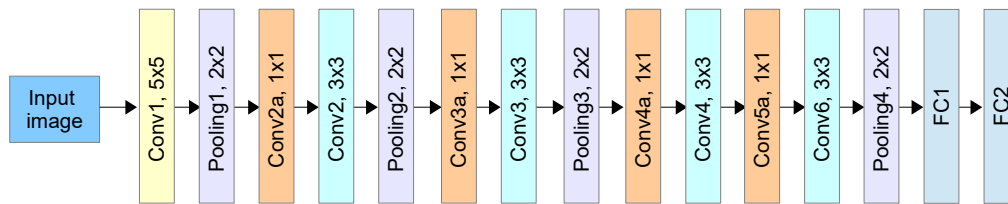


Figure 13: Example of lightweight CNN architecture used in [105].

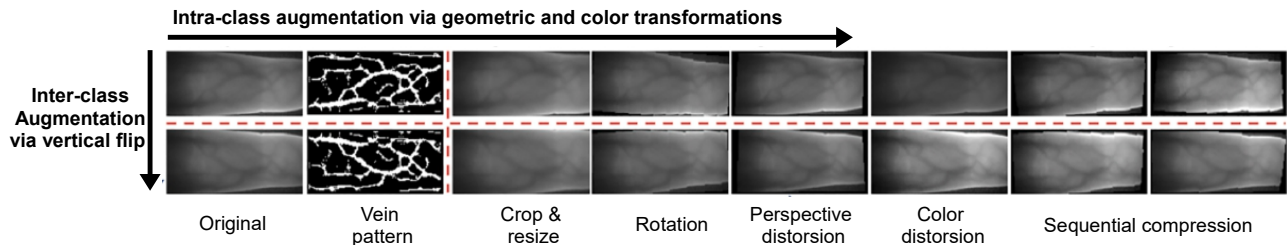


Figure 14: Demonstration of data augmentation using an actual FV example (top left), as depicted in [152]. Four types of intra-class transformations were empirically chosen and applied sequentially to the image: random crop and resize, rotation, perspective distortion, and color jittering. For inter-class, vertical flipping of FV images is utilized, significantly altering the vein pattern to create new identity semantics, thus defining a new label for such synthetic samples. It should be noted that all data augmentations in this approach are applied solely to the training set.

available databases. Zheng et al. [151] presented a lightweight ShuffleNet V2 CNN model for FV verification. They devised a data augmentation strategy to address the issue of insufficient training samples with brightness variations, partial cropping, or rotation. Additionally, they incorporated label smoothing and a joint loss function for enhancing the learning of discriminative features. Ou et al. [152] introduced a framework for FV recognition, integrating intensive data augmentation, robust loss function design, and network architecture selection. This approach integrates interclass data augmentation with traditional intra-class data augmentation, effectively addressing the data shortage challenge in FV recognition. Figure 14 provides a visual example of how this approach is applied to an actual FV sample. By showcasing the most widely used transformations, including cropping, rotation, perspective distortion, and color jittering, the figure offers a clear and intuitive understanding of how data augmentation artificially expands the training dataset and introduces variability. Wang et al. [109] presented a FV data augmentation strategy named FV-Mix, which involves grayscale normalization and linear mixing of fine FV ROI. They also introduced a residual Gabor convolutional network for FV recognition, enhancing scale and directional information using Gabor filters. Additionally, they proposed a dense semantic analysis module to assist in classifying and recognizing FV images.

To achieve better accuracy and reduce the training time complexity, transfer learning has been adopted in FV recognition [62, 110, 111, 139, 142–144, 146, 149–155]. For instance, Hong et al. [153] proposed a CNN-based approach for FV recognition, aiming to address misalignment and shading issues. They trained the CNN using three databases with varying characteristics from a vein recognition system's camera, to make it robust to environmental changes. The proposed method simplified the CNN structure by using one difference image as input, eliminating the need for complex structures and post-processing steps. Results showed that fine-tuning VGG Net-16 on difference images, as proposed in the research, achieved higher accuracy than existing methods and other CNN structures across all three databases. In [154], CNN competitive, a pre-trained CNN model from ImageNet is utilized for feature extraction. Specifically, CNN filters similar to Gabor filters, which capture line structures, are selected. A local descriptor leveraging these selected CNN filters is then proposed for FV recognition. This approach eliminates the need to develop a specific training strategy for CNN models using limited FV datasets. Shaheed et al. [155] introduced the Xception model, a pre-trained CNN based on depth-wise separable CNNs with residual connections, which is deemed to be a more efficient and less complex neural network for extracting robust features. Huang and Guo [139] proposed a cross-dataset FV recognition solution using a single-source dataset for training. Their approach includes an instance alignment transformation to reduce dataset gaps, a feature alignment and clustering learning algorithm based on VGG Net-16 for learning invariant features, and a modified ELM-based classifier for fast DTL. Experimental results on four public datasets show that their model transfers efficiently to target datasets, achieving recognition performance comparable to SOTA models trained end-to-end on the target data.

- 2) **Attention and Transformers:** This section explores two significant advancements in DL architectures for FV recognition, extending beyond traditional CNNs: (i) the integration of attention mechanisms—fundamental components of Transformers—into CNN-based models, and (ii) the advent of Transformer-based models, particularly vision Transformer (ViT). These developments are presented together as they epitomize a continuum in the evolution of attention-based techniques within image processing. The integration of attention mechanisms in CNN aims to selectively focus on the most pertinent parts of the input, thereby enhancing feature extraction and improving recognition performance.

- CNN-Attention-based approaches:** Attention mechanisms have been increasingly integrated into CNN architectures to enhance feature extraction and improve recognition performance in FV recognition [112–118, 140, 141, 148]. These mechanisms allow models to focus on specific parts of the input data that are most relevant to the task at hand, effectively reducing noise and improving the overall robustness of the system. For instance, Liu et al. [112] introduced a CNN model with a modified residual attention block (RAB) and incorporated the Inception structure to capture features across various scales. The results demonstrate the model's strong recognition performance with reduced parameters. Huang et al. [114] introduced an attention mechanism called the joint Attention, JA module, to extract discriminative features from low-contrast images. This module dynamically adjusts and aggregates information in the spatial and channel dimensions of feature maps, emphasizing fine-grained details and enhancing the contribution of vein patterns for identity feature extraction. Their approach achieved competitive results on various datasets. Zhang and Wang [115] proposed a lightweight CNN with a convolutional block Attention module (CBAM) for FV recognition, aiming to capture visual structures more accurately. In [140], the authors introduced a ResNet model enhanced with self-attention. By combining the global focusing ability of self-attention with the local feature extraction capability of CNN, this approach achieves higher accuracy in FV recognition. Huang et al. [117] introduce the axially enhanced local attention network, called ALA Net, to enhance the extraction of long-distance vessels and local textures in vein images. They propose a feasible variable ALA to improve identity discrimination of multi-scale features, inferring attention using a given vascular topological distribution. Additionally, feature amplification via low-cost grouped convolution generates convolutional feature mappings directly, reducing the parameter size for miniaturized device deployment. Experimental results demonstrate ALA Net's significant accuracy improvement over baseline networks without attention blocks. Huang et al. [118] developed FVFSNet model for FV authentication, processing spatial and frequency domains. The frequency domain module uses transformation and convolution layers, the spatial module employs efficient convolution layers, and the coupling module combines features with channel and spatial attention mechanisms. Experimental results demonstrate FVFSNet's effectiveness, particularly the frequency domain network, in FV authentication. The majority of DL-based FV approaches have traditionally relied on manually designed architectures, which can be time-consuming and prone to errors. Recently, Qin et al. [138] introduced AG-NAS, a neural architecture search method based on attention-gated recurrent units. AG-NAS automatically discovers the optimal network architecture, leading to improved recognition performance. By integrating self-attention and gated recurrent units in an attention gated recurrent unit (GRU) module, AG-NAS acts as a controller to generate architectural hyperparameters. Additionally, a parameter-sharing supernet policy is used to reduce the search space and computational costs. Experimental results on multiple datasets demonstrate that AG-NAS outperforms existing methods, achieving SOTA accuracy.

- ViT:** The Transformer architecture, particularly the ViT, represents a significant shift from traditional CNNs. Unlike traditional CNNs, or CNNs-attention-based models, ViT divides an image into patches and processes them using a Transformer encoder with multi-head attention mechanisms. This approach captures long-range dependencies and contextual information across the image more effectively. A comparative analysis of traditional CNN, CNN-Attention, and ViT-based models, highlighting their characteristics, advantages, and disadvantages, is provided in Table 7.

The general architecture of the ViT, which serves as a foundation for various approaches in FV recognition [119–122], is illustrated in Figure 15. For example, Lu et al. [119] proposed a FV recognition method using the ViT. They split FV images into patches, linearly embed each patch, and feed the sequence into the Transformer encoder. The model employs multi-head attention mechanisms to capture long-range contextual information without explicitly considering spatial distances, showing advantages over other CNNs, particularly with smaller data categories. Huang et al. [120] proposed using ViT for FV authentication. Their model utilizes a pyramid structure to improve multiscale feature extraction and introduces conditional position embedding to aggregate local information. They also proposed an efficient multi-layer perceptron (MLP) module and adopted the local feature fusion network (FFN) to improve the local information extraction. Experimental results on benchmark datasets show competitive performance with SOTA methods. Later, Li and Zhang [121] enhance the recognition capability of the ViT in FV recognition. Their approach, FV-ViT, achieves remarkable performance by applying rigorous regularization only to the MLPs head without altering the ViT backbone architecture, surpassing other SOTA methods. Moving on, in their work [122], the authors propose a FV feature extraction model based on the tokens-to-token (T2T) ViT (T2T-ViT). The T2T module is utilized for its ability to integrate local information from vein patterns.

FV-LT, introduced in [156], addresses limitations in multi-view FV recognition by employing a local Attention Transformer for robust 3D vein vessel feature representation, reducing sensitivity to finger positional variations from roll movements, and mitigating costs and space constraints associated with multiple cameras. The approach involves designing a contactless, low-cost image capturing device using a single camera for acquiring full-view FV images. Additionally, a local attention transformer-based identification method is proposed, considering tokens in adjacent nodes for dependency feature learning. Experimental results on public databases demonstrate that FV-LT outperforms existing 2D/multi-view vein recognition approaches, particularly in overcoming variations caused by finger roll, achieving superior performance for full-view FV recognition. Similarly, Zhao et al. [58] proposed a ViT-based model, VPCFormer, for multi-view FV feature extraction, effectively capturing global intra- and inter-view correlations with the constraint of vein patterns. VPCFormer achieves excellent performance in multi-view FV recognition. Recently, Li et al. [157] proposed a MobileViT model for FV recognition, addressing high parameter counts and limited training samples. The model includes the Mul-MV2 block, for multi-scale convolutions and the enhanced MobileViT block, for separable self-attention, reducing parameter counts

Table 7
Comparison of CNN-only, CNN-Attention, and ViT models for hand vein recognition.

Model Type	Characteristics	Advantages	Disadvantages
CNN-only	<ul style="list-style-type: none"> - Utilizes multiple convolutional layers to extract features from hand vein images, focusing primarily on local spatial relationships. - Does not incorporate attention mechanisms, relying solely on stacked convolutions for feature hierarchy. 	<ul style="list-style-type: none"> - Highly efficient with moderate to small-sized datasets due to efficient parameter usage and fewer computational requirements. - Simpler architectural design facilitates easier optimization and faster training times. 	<ul style="list-style-type: none"> - Limited in capturing long-range dependencies between vein structures without the help of attention mechanisms. - May not perform as well with very complex vein patterns or large-scale datasets compared to models incorporating attention.
CNN-Atten.	<ul style="list-style-type: none"> - Combines CNN to capture local vein patterns with Transformer layers to model long-range dependencies between vein structures. - Leverages CNN's spatial hierarchies and the Transformer's attention mechanism for a more holistic understanding of vein networks. 	<ul style="list-style-type: none"> - Effective at capturing both local vein details and global vein structures. - Performs well on tasks involving complex vein patterns, even with moderate datasets. - More efficient on smaller hand vein datasets compared to ViT, due to CNN's feature extraction capabilities. 	<ul style="list-style-type: none"> - Higher architectural complexity, requiring careful tuning of CNN-Transformer balance. - Potentially more computationally intensive than pure CNN models, depending on the depth of Transformer layers.
ViT	<ul style="list-style-type: none"> - Divides hand vein images into patches and processes them as sequences, similar to language tokens, using multi-head attention mechanisms to extract features. - No convolution layers are used, purely attention-based for global context understanding. 	<ul style="list-style-type: none"> - Capable of capturing long-range dependencies and structural relationships between distant vein patterns. - Highly scalable and can generalize well with large hand vein datasets. 	<ul style="list-style-type: none"> - Requires large amounts of labeled hand vein data for optimal performance and pre-training. - Struggles with small hand vein datasets without extensive pre-training. - Computationally expensive, demanding high graphics processing unit (GPU)/memory resources.

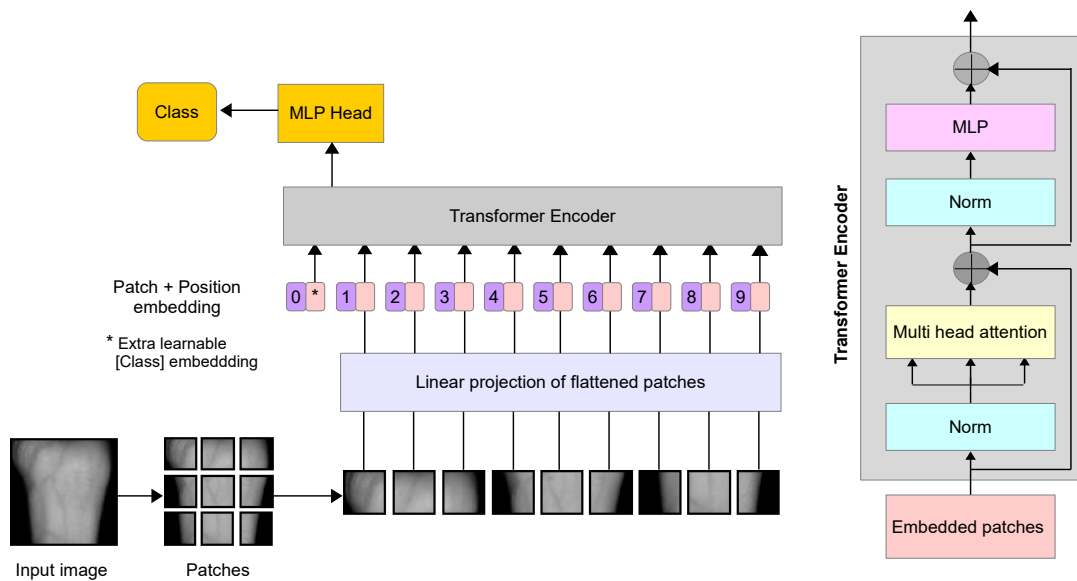


Figure 15: ViT architecture for FV image. The ViT applies transformer models, originally designed for NLP, to image processing by treating image patches as sequence tokens with positional embeddings, enabling efficient handling of visual data. MLP head performing classification or regression tasks based on the learned features.

and feature extraction times. They also introduced a soft target center cross-entropy loss function. Experimental results show high accuracy and low computational time.

- AE:** AEs are neural networks designed to learn efficient data representations, primarily for dimensionality reduction or feature learning. They consist of an encoder that compresses the input data and a decoder that reconstructs it. In FV recognition, AEs are used to extract meaningful features from vein images for improved accuracy in verification tasks [124, 125]. As an example, Hou et al. [124] proposed a DL method that combines a CAE with a support vector machine (SVM) for FV verification. The CAE learns features from FV images, with an encoder extracting high-level features and a decoder reconstructing images. The

SVM classifies the feature codes. Results show that this approach outperforms traditional methods, indicating its potential in FV verification. One more example, Jalilian et al. in their study [125] assessed the effectiveness of three classical CAE architectures—U-net, RefineNet, and SegNet—in extracting FV patterns. Their experiments revealed that the RefineNet AE architecture, when paired with automatically generated labels, exhibited the best performance and remained consistent regardless of the quantity of training labels.

- 4) **Hybrid:** Hybrid approaches in FV recognition represent a cutting-edge strategy that leverages the strengths of different DL techniques to achieve superior performance. These approaches are designed to address the challenges inherent in FV recognition, such as robustness to varying lighting conditions, accurate feature extraction, and efficient classification. Several approaches in the literature have explored this concept [59, 123, 126–128, 128–130, 158].

For example, Chen et al. [123] combined feature block fusion and DBN for FV recognition to address issues of template matching and whole feature recognition methods, which are prone to low robustness due to light instability in acquisition equipment. FBF-DBN utilizes the DNN's nonlinear learning ability to recognize FV features. The algorithm improves the deep network's input by using a feature points set in vein images, reducing learning and detection time. Experimental results show that FBF-DBN achieves good recognition performance and faster speed. In [126], the author employed a combination of CAE and CNN to verify vein patterns in images. The CAE was utilized to learn the extracted features, while the CNN was applied to classify FV images based on the extracted feature code. The results demonstrated an enhancement in FV verification performance. Qin et al. [127] proposed a DL model that combines the stacked CNN and LSTM models to extract vein features. The SCNN-LSTM model outputs represent the vein patterns, and a P-SVM is used to predict pixel probabilities for vein networks. The CNN learns robust features of FV images, while the LSTM captures complex spatial relationships of vein patterns. Experimental results on a public FV database show significant improvement in verification accuracy. In [128], a combination of GAN and CNN is proposed for FV data augmentation and recognition. They introduce FCGAN, a fully convolutional GAN-based architecture, to generate high-quality and diverse FV images. Subsequently, a CNN is employed for feature extraction and classification. Experimental results demonstrate that the generated FV images improves classification performance compared to classic sample augmentation methods. Similarly, Hou et al. [129] utilized a combination of GAN and CNN in their work. In contrast to traditional GAN methods, their triplet-classifier GAN utilizes generated "fake" data to enhance the learning capability of the triplet loss-based CNN classifier. This approach expands the training data and improves the CNN's discriminative ability. Experimental results demonstrate the superior performance of the proposed triplet-classifier GAN in FV verification. Huang and Guo [158] introduced a CNN-based method for FV recognition that incorporates bias field correction and a spatial attention mechanism. The bias field correction aims to eliminate unbalanced bias fields from original images using a two-dimensional polynomial fitting algorithm, while the spatial attention module employs a U-Net to extract robust vein patterns. Classification is performed using a ResNet CNN model. Experimental results demonstrate the effectiveness of the approach on two public databases. Liu et al. [59] designed an end-to-end deep CNN for robust FV recognition, incorporating an intrinsic feature learning module with a CAE network and an extrinsic feature learning module using a Siamese CNN. The intrinsic module estimates intra-class FV features under different offsets and rotations, while the extrinsic module learns inter-class feature representations. The experimental results demonstrated that the proposed method achieved comparable EER with existing methods on public datasets. Li et al. [130] introduced a FV recognition model that combines a CapsNet with a ViT. This approach leverages CapsNet's strength in processing visual hierarchies and ViT's ability to handle relationships between visual elements and objects. By addressing CapsNet's limitation in encoding long-range dependencies and selectively focusing on important features, the proposed model achieved improved classification accuracy for FV recognition.

- 5) **Other models:** In [131], the authors proposed a method that utilizes PCANet to efficiently extract features from FV images. PCANet combines cascaded PCA, binary hashing, and block-wise histogram techniques. The method focuses on the vein line feature as an essential part of the filter to extract optimal vein features for classification. The approach uses the original grayscale image in combination with the vein line image using the canonical correlation analysis (CCA) method to generate the filters. This method achieved high accuracy in three public datasets. To resolve the issue of low-level ground-truth pattern maps for training CNNs due to outlier and vessel break problems, Yang et al. [132] developed a model based on cycle-consistent (CycleGAN). Their approach aimed to extract FV patterns and outperformed previous CNN models in performance. Muthusamy et al. [133] proposed the steepest deep bipolar cascade correlative ML, called SDBCCML technique [133], and trilateral filterative hermitian feature transformation based deep perceptive fuzzy neural network, named TFHFT-DPFNN technique [134], to efficiently perform the FV verification with minimum time.

To enhance FV recognition accuracy and reduce verification time while addressing limited training data, Wan et al. [137] introduce a deep forest approach. This method utilizes the deep forest algorithm to identify feature points and the oriented FAST and rotated BRIEF algorithm, called also ORB, to match these features, extracting angular information from matched pairs. Identity determination is based on the sparse distribution of angles. Compared to traditional ML models, this approach maximizes the feature representation capacity of deep forest, particularly in scenarios with limited samples.

6.1.3. PAD-based methods

Even though FV recognition system offers advantages and attractive characteristics, it also presents a vulnerability to presentation attacks where fake FV images are used to deceive a recognition system, posing a serious threat to its reliability. Figure 16 shows examples of real and presentation attack FV images taken from the VERA database. Therefore, incorporating PAD mechanisms into these systems is essential to maintain their reliability and security. The integration of a PAD system with a

recognition system is presented in Figure 17. The PAD system is used initially to classify whether an input image is real or fake. If fake, an alarm is triggered; if real, the recognition system proceeds.

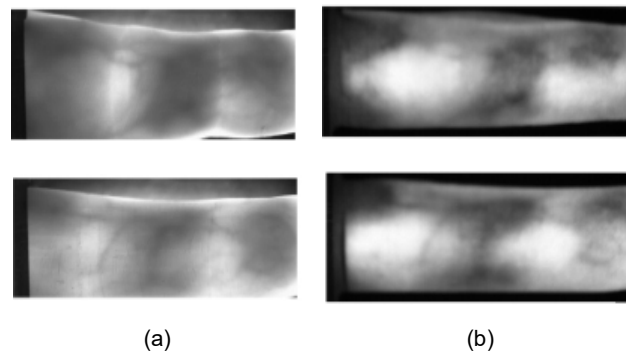


Figure 16: Example of real and presentation attack FV images in VERA FingerVein database. (a) Real images; (b) Presentation attack (fake) images.

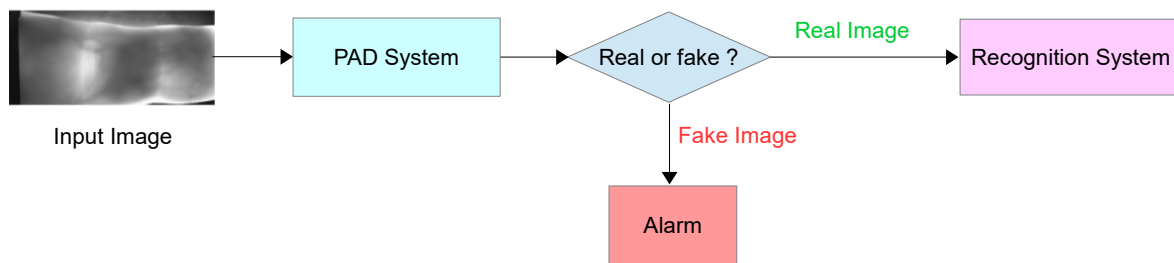


Figure 17: Integration of PAD System with FV Recognition System.

Despite the increasing popularity of FV recognition technology, research on PAD for FV images remains limited. Traditional PAD methods have been proposed but are limited by their feature extraction methods. These methods typically use handcrafted feature extractors designed to distinguish between real and presentation attack FV images based on observations of differences in spatial and/or frequency domains. This approach results in limited detection accuracy. Recently, DL-based methods have shown promise in improving the detection accuracy of PAD systems. While most proposed DL methods focus solely on designing and testing PAD systems independently of the recognition system [159–164], there is a gap in exploiting DL in overall systems that combine PAD with recognition [165].

One of the first DL-based PAD methods for FV was proposed by Nguyen et al. [159]. They introduced a CNN approach with DTL to combat overfitting issues caused by limited training data or complex CNN architectures. DTL was applied using pre-trained models like AlexNet and VGGNet-16 from the ImageNet database. To further improve detection, post-processing steps involving PCA for feature space dimensionality reduction and SVM for classification were employed. Experimental results demonstrated the effectiveness of DTL in addressing overfitting and highlighted the suitability of CNN-based methods for FV PAD. Qiu et al. [160] developed FPNNet, a shallow CNN, for FV PAD. FPNNet was trained without pre-trained models using patches extracted from vein images for dataset augmentation. Mixing training patches from two databases improved model generalizability and robustness, achieving 100% accuracy on both test datasets, surpassing SOTA PAD methods. DTL was also applied for FV PAD system in [161]. The authors augmented the pre-trained AlexNet architecture with seven additional layers and fine-tuned the modified CNN using a FV artefact database. This approach aimed to adapt the pre-trained and modified network to the specific application of FV PAD. Experiments were conducted using two different FV presentation attack databases, with two different FV artefact species generated using two different kinds of printers such as Laser print artefact and Inkjet print artefact. Shaheed et al. [163] developed a FV PAD method by combining residual connections and a depth-wise separable CNN with a linear SVM technique. It aims to address challenges like limited datasets, high computational complexity, and the lack of efficient feature descriptors. The depth-wise separable CNN automatically extracts features from spoof and genuine FV images, which are then classified by the linear SVM. Experimental results demonstrate that this method outperforms existing DL models in both performance and computational cost efficiency.

Previous PAD studies have primarily concentrated on methods for identifying presentation attacks that involve the use of printed or replayed fake FV images. Kim et al. [162] introduced a novel PAD method focusing on fake FV images generated through a GAN. They utilized CycleGAN to create presentation FV images aimed at compromising traditional FV recognition systems. Their proposed PAD method utilizes a score fusion technique that leverages ensemble networks. These networks are based on SVM and optimized using both Adam optimization and a sharpness-aware minimization optimizer, known as SAM. Experimental evaluations conducted on public datasets demonstrate the efficacy of this method in detecting GAN-based fake FV images.

Table 8

Summary of proposed works in PAD and TProt-based DL for FV recognition. In cases where multiple scenarios are examined, only the top-performing outcome for each dataset used in the test is mentioned.

Ref.	Year	Obj.	DL approach	DTL	Data augmentation	Dataset	Results
[159]	2017		AlexNet, VGGNet-16	Pretrained weights from ImageNet dataset	Images shifting and cropping	ISPR, VERA FingerVein	APCER=0%; BPCER=0%; ACER=0%, 0.0311%
[160]	2017		Shallow CNN	–	Patches extraction with stride s	VERA FingerVein, SCUT-SFVD	ACER=0.00%
[161]	2017		AlexNet	Fine-tuning	–	Two self-built datasets	APCER=0%,0.4%; BPCER=0%,0% (Laserjet printed artefact species)
[165]	2020	PAD	Lighweight CNN	Fine-tuning between datasets	Images rotating, cropping and blurring	PAD (VERA FingerVein, SCUT-SFVD), Recognition (FV USM, SDUMLA-HMT, MMCBNU_6000, Idiap, Self-built dataset)	PAD (HTER=0.00%, 0.00%); Recognition (EER=0.95%, 1.71%, 1.11%, 3.25%, 2.02%)
[162]	2022		GAN, DensNet-161, DensNet-169, and SVM	Fine-tuning DensNet-161 and DensNet-169 on ImageNet dataset	–	ISPR, VERA FingerVein	FID=20.57, 28.85; WD=5.95, 8.30; APCER=0.64%, 0.45%; BPCER=0.00%, 0.00%; ACER= 0.32%, 0.23%
[163]	2022		Xception+LSVM	Fine-tuning Xception on ImageNet dataset	Image rotating, shifting, zooming, horizontal flipping and shearing	VERA FingerVein, SCUT-SFVD	APCER, BPCER, and ACER all at 0.00%, and Acc. of 100%
[164]	2024		MobileNetV2 and MobileViT with FV	Fine-tuning	–	VERA FingerVein, SCUT-SFVD, Self-built dataset	ACER= 0.00%; EER=0.00%; BPCER=0.00%
[166]	2018	TProt	ML-ELM	–	–	SDUMLA-HMT, MMCBNU_6000, UTFVP	EER= 7.04%; CIR=93.09%, 98.70%, 98.61%
[167]	2018		DBN	–	–	Self-built dataset	GAR= 91.2%; FAR=0.3%
[168]	2021		CAE	–	Images rotating, shifting and zooming	UTFVP	FMR= 0%; FMNR=0%; HTER= 0%

Recently, Mu et al. [164] proposed the use of FL for FV PAD across various clients. This approach addresses the challenges faced by terminal clients and enhances model generalization for institutional clients. The framework accounts for differences in data volume and computational power among clients, categorizing FL clients into two groups: institutional and terminal. For institutional clients, an enhanced triplet training mode combined with FL is suggested to boost the generalization of the FV PAD model. For terminal clients, an unsupervised learning module is designed to enhance performance in terminal devices.

While the aforementioned methods concentrate exclusively on developing standalone PAD systems, Yang et al. [165] developed a comprehensive FV recognition system that integrates both recognition and PAD tasks using a unified CNN model, leveraging a multitask learning (MTL) approach. Additionally, they adopted a multi-intensity illumination strategy to improve the captured image quality, obtaining vein images with the best quality. Experimental results demonstrate that the proposed system achieves outstanding performance in both recognition and PAD tasks on public datasets, as well as a Self-built dataset containing images depicting axial rotation.

6.1.4. Template protection-based methods

Biometric systems face a critical issue regarding privacy, as once a biometric template is compromised, it cannot be changed or revoked. To tackle this challenge, various biometric template protection (BTP) schemes have been developed. However, while these schemes enhance privacy, they can also impact recognition performance. Several DL approaches have been proposed to mitigate this issue. Yang et al. [166] devised a novel BTP algorithm using binary decision diagrams for DL-based FV biometric systems. This algorithm creates a noninvertible version of the original FV template, which is then combined with an artificial neural network, specifically the multilayer extreme learning machine (ML-ELM), to form a privacy-preserving FV recognition system, called BDD-ML-ELM. This approach provides an advantage over existing ML/DL biometric systems, as the raw biometric templates are protected from inversion attacks on the artificial neural network. Liu et al. [167] introduced a secure FV recognition method, FVR-DLRP, using DBN and random projections. The DBN, comprising two RBMs, generates the biometric template. Experimental results show that the proposed approach maintains identification accuracy and enhances security for FV authentication. In [168], a CAE-based method for secure FV recognition is proposed. The approach utilizes a CAE neural network with a multi-term loss function, incorporating both AE and triplet loss functions for embedding features. Biohashing is then applied to these deep features to generate protected templates.

6.2. PV-based methods

Moving from FV to PV recognition for biometric identification offers several advantages. PV recognition captures a larger and more intricate vascular pattern than FV (Figure 1 (a)), providing higher accuracy and security. The palm's wider surface area allows for more data points, improving matching reliability and reducing false acceptance/rejection rates. Additionally, PV scanning is

less invasive and more user-friendly, as it doesn't require precise finger placement. This technology is also less affected by external factors like skin conditions, cuts, or dryness, enhancing its robustness. Furthermore, the contactless nature of PV scanning promotes hygiene, an important consideration in public or shared environments. Overall, PV recognition's enhanced security, reliability, user experience, and hygiene make it a superior choice for efficient biometric identification. Numerous ML/DL-based PV recognition methods have been proposed in the literature. These methods are discussed and classified below. Table 9 summarizes the proposed schemes for PV recognition.

6.2.1. DL-based methods

PV characteristics, including high recognition rates, stable features, easy localization, and superior image quality, have garnered significant attention from researchers. This feature makes it suitable for individual identification. For example, the contactless PV recognition system proposed in [169] was developed based on prior research and CNN technology. It comprises two main components: training and testing. Initially, the ROI method was employed to identify the relevant area, followed by convolution calculations using the ROI image and Gabor filter to extract features. During the deep network training phase, input fusion was executed between the original ROI image and Gabor features. Subsequently, in each subsequent deep network training batch, triplet loss and cross-entropy were computed to optimize the network weights via backpropagation, thus ensuring the capture of sufficient PV data. In the same manner, Obayya et al. [80], the CNN operates as a feature extraction algorithm, and accomplished through the utilization of a Bayesian optimization algorithm, aimed at reaching the optimal network structure and training parameters within the search space of potential solutions. When the ROI underwent processing through a Jerman vessel enhancement filter, the process notably reduced the EER. The authors in [170] introduce a CNN based method for PV authentication, so-called FCPVN, integrating label information into self-supervised contrastive learning. They propose a focal contrastive loss to prioritize hard examples, enhancing model focus. FCPVN demonstrates competitive performance across five PV databases, compared to existing SOTA methods.

Recent advances in hand vein identification via DNNs rely on extensive training data, hindering robust feature extraction from single images. Addressing this, Qin et al. in [171] propose single-sample-per-person PV identification. The proposed method, combines multi-scale and multi-direction GANs for data augmentation with a CNN. The scheme generates diverse samples, improving CNN stability in PV recognition, as demonstrated on public databases, CASIA and PolyU. The authors later introduced an enhanced multi-scale PV identification method based on Transformer in [172]. The method employs convolutional and self-attention blocks to capture local and scale information. It enhances vein classification via a graph convolutional network-based label enhancement (GCNLE) approach, which leverages label correlations to improve feature representation in a multiscale vein Transformer. Horng et al. [173] introduces a cost-effective PV recognition system for smartphones, utilizing RGB images. It enhances vein patterns using the saturation channel, instead of red channel, and introduces a novel method for ROI extraction based on convex hulls and key vectors. Additionally, a lightweight DL model, called MPSNet, optimized for smartphones is proposed, incorporating convolutional layers, depthwise separable convolution, inverted residual bottleneck, and spatial pyramid pooling (SPP) modules, enhancing accuracy through fusion strategy. Moving forward, in their work [174], Thapar et al. introduced a CNN architecture, called Siamese framework (The same principle is illustrated in Figure 18, a widely used architecture in image recognition, face verification, and few-shot learning due to its unique twin networks that compare pairs of inputs to determine similarity), coupled with a triplet loss function. This latter is derived from the disparities among (i) anchor, (ii) positive, and (iii) hard-negative embeddings. Initially, an encoder-decoder network is employed to capture domain-specific traits, followed by the assembly of the inception layers to produce PV characteristics. Augmentation techniques are utilized to address the scarcity of positive samples for a specific subject and to boost learning, and a smaller batch size is chosen to expedite convergence, while dropouts are incorporated to prevent overfitting. Another method, [175], presents an iterative DBN specifically designed for hand vein verification. It initially extracts vein features from labeled data and then iteratively refines them during training. The DBN is a probabilistic generative model formed by stacking DBNs using a layer-wise pre-training approach. This study trains the DBN to estimate the likelihood of a pixel belonging to a vein pattern. To accomplish this, it utilizes established handcrafted image segmentation techniques for vein extraction, creates a training dataset based on labeled pixels, and employs the DBN for training. This approach effectively addresses the challenges of vein segmentation and leads to improved verification performance.

Regrettably, recent studies [3, 176] have revealed the vulnerability of DL algorithms to attacks involving the addition of carefully crafted adversarial perturbations to authentic samples as input. These perturbations are often subtle and imperceptible to human eyes, yet they can result in significant misclassification of genuine samples during inference. In this context, adversarial attacks pose a threat to the security of DL-based biometric models. Currently, numerous attacking techniques have been devised to manipulate network classifiers into altering their predictions. For instance, Goodfellow et al. suggested the fast gradient sign method (FGSM), which introduces adversarial perturbations to create adversarial examples [176], among others. For that reason, researchers highlight the urgent need for approaches to safeguard DL-based PV models. In light of the preceding details, Li et al. [177] proposed VeinGuard to defend deep neural network-based vein classifiers from adversarial attacks. It incorporates a local transformer-based GAN (LTGAN) and a purifier. The LTGAN models the unperturbed image distribution using conditional position embedding and local depth-wise convolution in Swin Transformer blocks. The purifier removes perturbations by identifying the nearest sample to the given perturbed image. It comprises a pre-trained generator and a trainable residual network, fine-tuned during testing for vein recognition. LTGAN outperforms SOTA methods under black-box hop-skip-jump-attack (HSJA).

6.2.2. DL-based hashing

Hashing methods offer impressive efficiency in data storage, retrieval speed, and enhanced security, which are vital for internet-of-things (IoT) services. Zhong et al. [178] put forth an end-to-end CNN-based hashing network specifically designed for PV

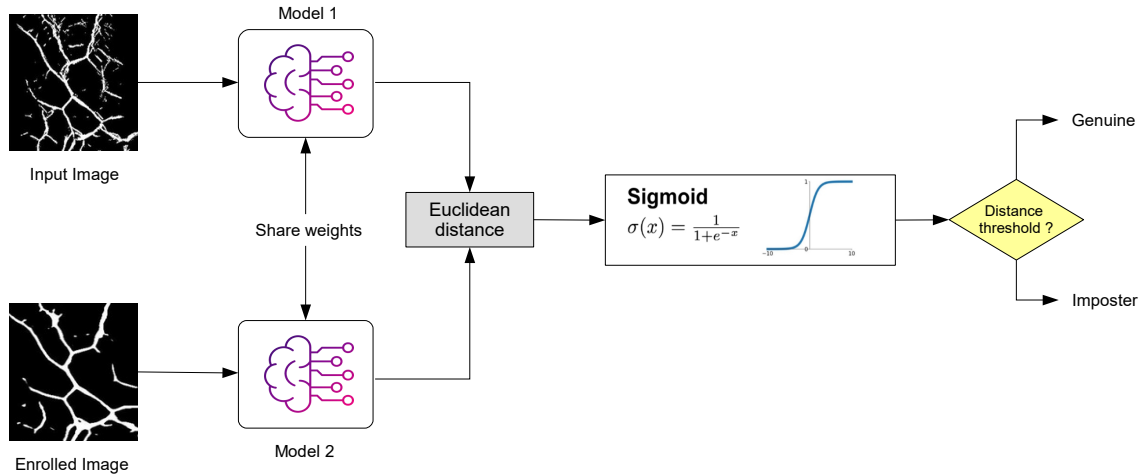


Figure 18: A standard Siamese neural network architecture used in vein biometric systems involves training two identical subnetworks simultaneously, fine-tuning them on two datasets to compare input pairs. It uses Euclidean distance to measure similarity and a sigmoid function to output the likelihood of the inputs being similar.

recognition. They employ a hashing code, generated using *tanh* and *sign* functions, to encode image features into a binary code of consistent length. Through comparing the Hamming distances between the binary codes of various PV images, the proposed method can discern whether they share the same category. In [179], hash codes representing palm print and PV are derived through a deep hashing network. A spatial transformer network is employed to mitigate issues related to rotation and displacement. The methodology incorporates both image-level fusion and score-level fusion techniques. However, the inability to perform cross-modality matching limits the extent of performance enhancement in this study. The work proposed by Dong et al. [180] introduces PalmCohashNet, a biometric hashing network designed for IoT applications, which combines palm print and PV data. PalmCohashNet consists of two separate hashing subnetworks, one for each palm modality, trained together to produce shared hash codes (co-hash codes) for each modality. This approach is depicted in Figure 19, a method widely adopted across all DL-based PV implementations that utilize hashing techniques. A novel cross-modality hashing (CMH) loss function is developed to ensure that co-hash codes from the same individual across PV and palm print modalities are both adjacent and consistent. Simultaneously, it pulls these co-hash codes towards a predetermined identity-specific hash centroid shared by both modalities. This enables the generation of two palm-based co-hash codes for each individual, suitable for deployment due to their compact form for storage and quick matching, making them IoT compliant. PalmCohashNet can be deployed in many operation modes: single-modality matching (e.g., print versus print or vein versus vein), multimodality matching using both print and vein data, and cross-modality matching (print versus vein), depending on the specific requirements of the IoT service. Empirical results on four publicly available palm databases demonstrate that the proposed method consistently outperforms existing SOTA techniques.

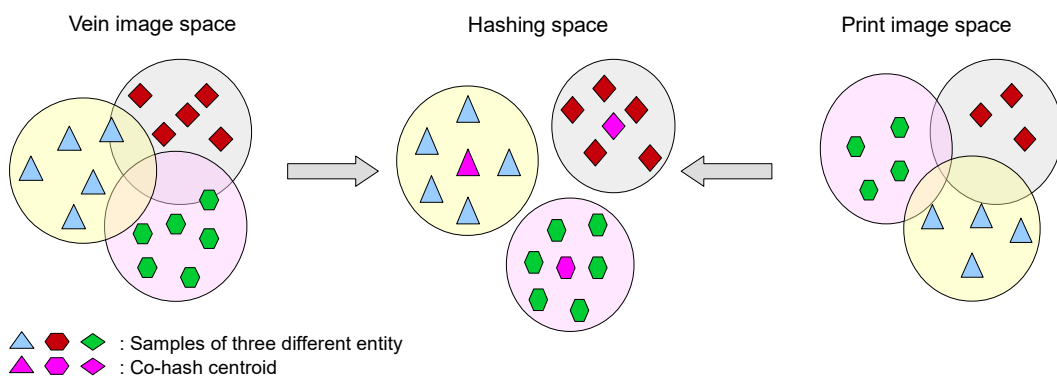


Figure 19: Principle of mapping PV and palm print samples to their respective co-hash centroids linked with each identity. This ensures that the hashing space is maximally utilized, as these co-hash centroids are mutually orthogonal.

6.2.3. DTL-based methods

The authors in [181] presents a PV recognition system utilizing CNNs. Six CNN models were constructed and evaluated for biometric identification using palm images. Four models were adapted from existing architectures through DTL, namely, AlexNet, VGG-16, ResNet-50, and SqueezeNet, while two new architectures were proposed. Experimental comparisons were conducted on identification accuracy and training convergence using the PUT PV database. Various image quality enhancement methods were explored to improve accuracy, which include modifying contrast and normalizing, applying Gaussian smoothing, utilizing CLAHE, and employing coarse vein segmentation based on the Hessian matrix. The ResNet-50 pre-trained model yielded the

highest performance. Cross-modality serves as a form of DTL, transductive DTL, leveraging information from two distinct domains to enhance the accuracy of one of them [3, 182]. Li et al. in [183], the accuracy reaches impressive levels through the fusion of multi-modal information, incorporating both palmprint and PV ROIs into the proposed FNet network. The final descriptor E in FNet is produced via cross-modal DTL, resulting in robust anti-falsification capabilities. Likewise, Wang et al. [184] introduce a framework for both palm print and palmar vein recognition. They conduct feature-level image fusion after extracting features, using wavelet transform, from palm print and palmar vein images at various wavelengths. Their experiment yields a more practical fusion scheme. Building on these fusion results, they suggest enhancing CNN models for identity recognition using multispectral palm print and palmar vein images. The SPP layer addresses the challenge of fixed input image sizes in CNNs, with the ResNet18 architecture demonstrating superior performance in terms of both accuracy and recognition time compared to other methods examined. Similarly, [185] explores the utilization of DL in PV recognition for personal identity authentication. Various CNN architectures are examined and contrasted, with particular focus on the ZFNet architecture, which is fine-tuned using optimal parameters. A comparative analysis is conducted with other existing CNN models like LeNet, AlexNet, and ResNet, revealing ZFNet's superior performance, followed closely by ResNet. Moving on, the study [186] presents a novel approach to PV recognition through DTL, exploring the use of two synthetic databases to pre-train DL models. The research evaluates the performance of these models on real databases. Two end-to-end CNN architectures, based on fine-tuned SingleNet and Resnet32, are implemented for feature learning. Results from experiments on prominent public datasets indicate the efficacy of utilizing synthetic PV images for DTL, exceeding previous SOTA outcomes.

Wu et al. [187] have created a wavelet denoising ResNet scheme, WD Resnet, comprising two components: the wavelet denoising model and the pre-trained ResNet18 model. The fine-tuned model is designed to eliminate noise arising from skin scattering and optical blurring in PV images. Leveraging residual learning technology, it amplifies low-frequency features to integrate them into the DL framework, thus reinforcing the significance of handcrafted features within the network. Meanwhile, the ResNet18 model tackles challenges such as rotation, positional shifts, and scaling variations by selectively enhancing classification features while diminishing less pertinent ones. Marattukalam et al. [188] introduce a design employing a Siamese neural network framework for PV identification in few-shot scenarios. The suggested model utilizes images from both left and right palms for two users, comprising two sub-networks that share user weights to distinguish individuals, as depicted on Figure 18. The effectiveness of this architecture was evaluated on the PolyU multispectral PV database, which has a constrained number of samples.

The work presented in [189] explores the utilization of hand vein patterns for biometric recognition, specifically investigating differences in vein patterns between genders and how these variances affect verification performance. The study assesses the possibility of recognizing male and female individuals based on their hand vein patterns. Transfer DL approach is adopted to analyze hand vein features, taking into account gender-specific characteristics. Specifically, a modified Densenet-161 architecture is applied for processing hand vein patterns. This CNN architecture is fine-tuned to analyze vein patterns and extract relevant features for gender recognition and biometric verification tasks. Results show that gender-specific models can significantly enhance recognition rates. The research conducted by Babalola et al. [190] focuses on enhancing hand vein recognition through the integration of various color spaces within DL frameworks. The authors examined five distinct color spaces (RGB, XYZ, LAB, YUV, HSV) and identify, each time, the most impactful channels for recognizing patterns in PV images. By integrating these color spaces within CNN models such as AlexNet, VGG-19, and ResNet-50, the proposed architecture is able to achieve good accuracy for different datasets. The research demonstrates the effectiveness of considering color space in improving the performance of PV recognition.

6.3. DHV-based methods

DHV recognition is a biometric authentication method that utilizes the unique vein patterns on the back of the hand for identification purposes. This method involves capturing an image of the dorsal hand using infrared or near-infrared light. Subsequently, advanced algorithms analyze the vein characteristics, including their structure, color, distribution, and geometry. DHV recognition is particularly advantageous over other biometric methods such as FV and PV due to the larger surface area of the dorsal hand, which provides more detailed and distinct vein patterns. This enhances the accuracy and reliability of the system.

The robustness of DHV biometrics is further increased as the dorsal hand is less susceptible to wear, tear, or dirt. This method offers several benefits: high accuracy, non-invasiveness, and the difficulty of replicating vein patterns, making it less prone to fraud compared to external features like fingerprints. Additionally, DHV recognition does not require physical contact, which is ideal for applications requiring high levels of hygiene and minimal user interaction, such as secure access control, time attendance systems, and identity verification. Despite its numerous advantages, DHV biometrics also faces challenges such as higher cost and potential privacy concerns. To facilitate a clearer understanding of the existing approaches, Table 10 summarizes the proposed schemes for DL and DTL-based DHV recognition, and highlighting their respective performance.

6.3.1. DL-based methods

The DL-based methods in DHV identification focus on leveraging DL architectures, primarily CNN, to automatically extract and learn features from raw vein images. These methods enhance the accuracy and robustness of DHV identification by capturing complex patterns that are difficult to detect with traditional feature extraction techniques. The primary advantage of DL-based approaches is their ability to model intricate relationships within the data, leading to higher identification accuracy and better scalability with larger datasets. CNNs are widely used for DHV recognition due to their ability to accurately extract and learn features from complex hand patterns and textures. For example, the paper in [194] presents an unsupervised DL method for hand vein recognition. The proposed system involves preprocessing mechanisms, DL models based on CNN, and an alternative approach based on RBM to enhance feature recognition and reduce recognition time. CNN architectures, specifically designed for image recognition tasks, are well-suited for vein recognition applications. The suggested method starts by guessing vein patterns for

Table 9

Summary of proposed works in DL-based PV recognition. In cases where multiple scenarios are examined, only the top-performing outcome is mentioned.

Ref.	Year	DL approach	DTL	Data augmentation	Dataset	Results
[80]	2021	CNN	Fine-tuning	–	CASIA	Acc= 99.4%, EER= 0.0683%
[169]	2021	CNN	–	–	CASIA, PUT	EER= 0.0556%, 0%
[181]	2019	ResNet-50	Fine-tuning	Random rotation	PUT	Acc= 99.83%
[184]	2021	CNN	DA	–	Self-built dataset	EER= 0.38%; Time= 715 ms
[170]	2023	CNN	–	–	PolyU, Tongji	EER= 0.28%, 1.07%
[171]	2021	GAN+CNN	–	Multi-direction GAN	CASIA, PUT	Acc= 98%, 98.82%
[172]	2023	GCNLE+Attention	–	–	PolyU, VERA	Acc= 99.82%, 98.27%
[174]	2019	Encoder-decoder + Triplet Siamese	Fine-tuning	Image augmentor tool	CASIA, IITI, PolyU	EER= 3.71%, 0.93%, 0.66%; CIR= 85.16%, 97.47%, 98.78%
[178]	2018	CNN	–	–	PolyU	EER= 0.0222%
[185]	2021	CNN	–	–	MS-PolyU	Acc= 94.65%
[177]	2023	LST+GAN	Fine-tuning	Local Transformer-based GAN	PolyU, Tongji, MMCBNU6000	Acc= 93.6%, 88.7%, 96.2%
[186]	2023	ResNet-32, SingleNet	Fine-tuning	ROI samples augmentation	CASIA, PolyU	Acc= 99.20%, 100% Acc= 98.42%, 100%
[187]	2021	WD ResNet	DA	Randomly rotate, and flip the image horizontally or vertically	Tongji	Acc= 99.70%, EER= 0.41%
[191]	2019	AlexNet	DA	–	PUT	CIR= 93.92%
[192]	2020	DenseNet-161	DA	–	PolyU	CIR= 99.69%
[193]	2021	MobileNet v3 EfficientNet	DA	–	PolyU	CIR= 100% (For both models)
[175]	2019	DBN	–	–	CASIA, PolyU	EER= 0.33, 0.015

Abbreviation: Local swin Transformer (LST)

biometric identification. Next, DL models like Inception and ResNet50 can automatically pull out distinguishing features from preprocessed vein images, making it easier to find DHVs. Benaouda et al. in [195] introduce a methodology for DHV recognition leveraging CNN. To start the process, the ROI is taken from images of the DHVs. Next, CLAHE is used to prepare the images. Subsequently, a database is constructed. Finally, the identification task is performed via CNN. Hyperparameter optimization refines the experimental results, leading to a high DHV recognition rate. Moving on, the research paper [196] investigates the use of CNNs for hand-dorsa vein detection to improve performance using a database expansion technique that relies on PCA reconstruction. The paper aims to overcome the constraints of DL in vein detection caused by a lack of sufficient dataset samples. It proposes a new image-generating method employing double PCA. The PCA reconstruction method makes the hand-dorsa vein database better by combining features that are similar. This makes the dataset more representative and varied for training CNN models. By expanding the database and enhancing feature representation, the approach attains a high identification rate of 99.61% on datasets of different scales. The PCA reconstruction approach significantly improves the performance of CNN, surpassing other current methods and proving the usefulness of DL in biometric identification. Moving forward, in [197], the proposed research integrates partition local binary patterns (PLBP) with CNN through three schemes (Serial Fusion, Decision Fusio, and Feature Fusion). This combination of traditional PLBP features and CNNs has proven to be effective in DHV recognition. The PLBP feature extraction process involves scaling vein images, dividing them into non-overlapping regions, and extracting features from each sub-image. For the NCUT data set, the fusion process, with specific weights assigned, achieved an SOTA recognition rate. Wan et al. [198] introduces a method for DHV recognition using CNN-based DL approaches. The research involves training CNN models like AlexNet, Reference-CaffeNet, VGG-16, and VGG-19. Before training the CNN models for DHV recognition, several preprocessing techniques were applied to the images. These techniques involve extracting the ROI from DHV images, enhancing the contrast of the images using the CLAHE algorithm, and applying a Gaussian smoothing filter to reduce noise and enhance the quality of the CNN models. Based on the experimental results, the size of the dataset has a significant impact on the recognition rate for DHV recognition. Kuzu et al. [199] look into how similar hand vein patterns are between people using a modified Densenet-161 architecture for biometric recognition. This research employs a DL-based method to analyze vein patterns in different areas of the hands. It builds upon prior studies by considering palm- and dorsal-vein patterns in addition to FV. For training, the network architecture includes a Custom Embedder and an Additive Angular Margin Penalty. Experiments are conducted on various vein databases, including the SDUMLA, PolyU-P, Bosphorus, and R3VEIN datasets. The results indicate that the vein patterns of one hand of a subject show higher similarity with the corresponding traits of the other hand of the same subject. Overall, the authors illustrate how their study contributes to improving the biometric recognition systems' accuracy by understanding the similarities within hand vein patterns. Another recent study, [200], addresses the challenge of accurately extracting ROI from non-contact DHV images in complex backgrounds. It proposed

an improved U-Net model to solve the problem. It proposes an improved U-Net model with a residual module to enhance feature information extraction and help to avoid gradient disappearance and explosion, thereby solving network degradation issues. It also employs the Jensen-Shannon divergence loss function to improve feature map distribution. And finally, it implemented Soft-Argmax for keypoint detection, making it suitable for practical deployment on low-resource platforms.

The research in [201] investigates the verification of human identity through the analysis of biometric DHV images by utilizing a methodology that incorporates DL and GANs (DL-GAN). An approach involving multiple steps is implemented for the selection of features and the preprocessing of images. The DL-GAN demonstrates an efficient capability in recognizing individuals based on DHV images, thereby improving the process of authentication. The use of deep GANs outperforms traditional techniques such as local binary patterns (LBP), local phase quantization (LPQ), Gabor filter, and scale-invariant feature transform (SIFT) in the realm of DHV recognition, highlighting the superior performance of this method in biometric authentication.

6.3.2. DTL-based methods

Building on the strengths of DL-based methods, DTL-based methods in DHV identification aim to further enhance performance by adapting pre-trained DL models to the specific task of DHV recognition. By utilizing models initially trained on large, related datasets, these methods improve performance in DHV identification, particularly in scenarios with limited DHV-specific data. The key advantages of DTL-based approaches include reduced training time, improved accuracy with smaller datasets, and flexibility in adapting to various DHV identification tasks. One of the earliest studies to investigate the application of DL and DTL in DHV was conducted by [202]. In this work, the authors evaluated and compared four different CNN architectures: Caffe AlexNet, Caffe Reference Net, VGG-16 Net, and GoogLeNet. These models are built using a large-scale dataset named ImageNet to extract features and identify DHV patterns. The study shows that deep features are better than traditional methods at representing and recognizing DHV patterns. This leads to a lot more accuracy on the NCUT database. The authors also stress the importance of fine-tuning deep models for this specific task, which leads to promising outcomes for biometric identification systems. Indeed, the fine-tuning process is crucial in DL models for DHV recognition as it enables the models to adjust to the unique attributes of DHV patterns. This adaptation enhances the models' ability to differentiate individuals based on their vein images. Another work rely on pre-trained model suggested in [203], introduces a technique to improve the accuracy of DHV recognition by employing multi-bit planes and the SqueezeNet network. By exploiting the intrinsic relationships among bit planes within images, the proposed algorithm achieves higher recognition rates when compared to conventional methods such as PCA and LBP. The incorporation of the SqueezeNet network additionally improves performance by enabling automatic feature extraction and keeping the model size efficient. The SqueezeNet network is essential in the DHV recognition method for its efficient feature extraction and compact model size. In fact, the squeeze layer condenses the input channels, reducing computational complexity, while the expand layer helps capture detailed features. Therefore, this specific architectural design of the SqueezeNet network enables effective feature extraction while maintaining a lightweight design, making it suitable for small sample sizes and preventing overfitting in the recognition process. The work [204] also employed a pretrained model for DHV recognition, it combines ResNet and histograms of oriented gradients (HOG) features to improve DHV recognition and overcome the limitations of small-scale DHV datasets. The fusion method involves adding HOG features and shallow semantic information (obtained by convolution) to the residual structure of ResNet for classification. This gets around the problem of DL algorithms having small sample sizes. Additionally, the fusion approach integrates the PLBP algorithm for comparison and feature fusion. Experimental results indicate that the proposed feature fusion method outperforms traditional methods like PLBP and HOG alone, emphasizing the effectiveness of the fusion approach.

In [205], Tian and their colleagues suggested a YOLO Nano-Vein model for finding veins on the back of the hand. They wanted it to be more accurate and find veins faster than older models like YOLO Nano and YOLOv3. The authors optimize the proposed model (YOLO Nano-Vein) for embedded systems. It achieves its improvements through architectural modifications, including reducing of unnecessary modules, adjusting output scales, and the addition of an atrous SPP module. These modifications improve the efficiency of vein detection while simplifying the network architecture. Comparative analysis with other models like faster recurrent CNN (RCNN), YOLOv3, and YOLO Nano confirms the effectiveness of these modifications.

6.4. Multi-modal vein-based

Biometrics has emerged as a vital form of identification as they carry rich personal identifying data. However, the shortcomings of single-modal biometric identification technology in terms of recognition accuracy is now becoming more obvious. To address this, multi-modal biometric recognition technology combines multiple complementary biometric modalities, therefore extending the range of biometric identification and enhancing accuracy and security. The growing interest in multimodal biometric systems originates from their ability to provide a more secure and precise authentication solution compared to unimodal systems. Even with this potential, performance improvement may sometimes be challenging since current biometric fusion techniques aren't robust enough to handle the correlations and redundancies of several variables at once. Several DL-based multi-modal vein recognition systems have been proposed in the literature. Table 11 provides an overview of these schemes.

In order to address the mono-mode biometric challenges, the authors [207] proposed a biometric system that combines both palmprint and DHV modalities. The proposed method is primarily based on the use of CNN DL architecture to extract features, particularly the pre-trained function PCANet for evaluating performance in a fusion scheme. The fusion techniques, both at the feature level and score level, have the objective of enhancing the accuracy of the biometric system. In particular, feature-level fusion is used to merge various features from different biometrics. On the other hand, score-level fusion enables the combination of the corresponding scores obtained from different biometric modalities. Moreover, the study [208] discusses a multi-modal biometric system using DL principles. The research aims to enhance the precision of biometric identification by integrating several

Table 10

Summary of proposed works in DL-based DHV recognition. In cases where multiple scenarios are examined, only the top-performing outcome is mentioned.

Ref.	Year	DL approach	DTL	Data augmentation	Dataset	Results
[194]	2023	CNN+RBM	–	Resizing, flipping, rotating, cropping, padding	Badawi, DHVI	Acc= 99.76%, 99.5%
[195]	2022	CNN	–	–	Self-built dataset	Acc= 99%
[202]	2016	CNN	Fine-tuning	–	NCUT	Acc= 99.31%
[196]	2018	CNN	–	Double PCA	NCUT	Acc= 99.61%
[197]	2021	CNN	–	Double PCA	NCUT	Acc= 99.95%
[198]	2017	CNN	Fine-tuning	–	Self-built dataset	Acc= 99.7%
[205]	2022	CNN (YOLO)	DA	–	Self-built dataset	Precision= 93.61%
[203]	2018	SqueezeNet	Feature fusion	–	Self-built dataset	Acc= 99%
[200]	2023	CNN (U-Net)	–	horizontal and vertical flipping, brightness random adjustments	Self-built dataset	Acc= 98.6%
[201]	2021	DL-GAN	–	GAN	Jilin Univ, 11K	Acc= 98.36%, 96.43%; EER= 2.47%, 3.55%
[199]	2022	Modified Densenet-161	–	–	Bosphorus	EER= 2.33%
[204]	2022	ResNet+HOG	Feature fusion	Fusion of many datasets	SDUST, FYO, NCUT	Acc= 93.27%, 95.36%, 93.40%
[206]	2018	VGG-16	Selective feature fusion	–	Self-built dataset	EER= 0.068%

biometric modalities, including palm print, DHV, wrist vein (WV), and PV. The research emphasizes the significance of multi-modal biometric technologies in improving security and authentication procedures. Furthermore, it highlights the need to use DL techniques and optimization methodologies to improve the efficiency of biometric systems. The proposed approach consists of three primary stages: preprocessing, feature extraction, and recognition based on DL. Preprocessing methods, such as median filtering and ROI selection, are used to improve the quality of biometric images. Preprocessed images are used to extract features, and a deep convolution neural network (DCNN) architecture is used to identify if the image belongs to an impostor or a legitimate user. An ensemble classifier is constructed of NN1 (trained using characteristics taken from the WV, dorsal vein, and palm print) and NN2 (trained using PV). The findings are combined using the score-level fusion technique. Next, the combined results are utilized as input for the DCNN. The DCNN is used for distinguishing between imposters and real individuals. An optimization model called butterfly combined Tunicate swarm optimization, named BTSOA, is used to adjust the weights of DCNN in order to enhance detection accuracy. Besides, the research [209] introduces a robust multimodal biometrics identification system that uses DL to combine FV and finger knuckle print data for enhanced security. The study presents two multimodal architectures, each including different fusion levels (feature-level fusion and score level fusion (weighted product, weighted sum, or Bayesian rule)), using CNN architectures such as AlexNet, VGG16, and ResNet50. In the proposed system, the fully connected layer computes a fusion of new characteristics derived from FV and finger knuckle print. The ResNet50 network demonstrates superior accuracy in unimodal identification systems for FV and finger knuckle prints. Moreover, when comparing unimodal and multimodal techniques, the ResNet50-Softmax model combined with weighted sum fusion strategy achieves the highest recognition accuracy. The study used open databases, specifically the FV SDULMA-HMT and the PolyU FKP databases, to test how well and accurately the suggested recognition algorithms worked. Moving on, Deshmukh et al. [210] aim to illustrate how DL and CCA may improve biometric recognition accuracy. The authors present two frameworks for multimodal biometric systems: Deep Multiset CCA and Deep CCA. These frameworks use DL approaches to acquire knowledge of the complex transformations of biometric modalities, resulting in the creation of highly correlated feature sets. These two frameworks outperform traditional fusion methods by enhancing feature fusion, minimizing irrelevant information, and enhancing recognition performance. Tests on the SDUMLA-HMT dataset show that the suggested frameworks get low EER for both two-modal and three-modal biometrics (FV, iris, and face).

The work in [211] introduces a multi-biometric cancellable system (MBCS) that uses DL models to combine fingerprint, FV, and iris biometrics, resulting in high quantitative results. The proposed work makes two primary contributions: developing a multi-exposure deep fusion module to create a combined representation of several biometric modalities; and implementing a deep dream module to construct a cancellable template from the fused biometric images. A comprehensive assessment showed favorable results. The authentication procedure of the MBCS requires just a few sequential stages, making it very efficient for practical application. The research shows how successful the suggested MBCS is by comparing it positively with SOTA techniques. Later, MBCS has been employed in [212] as an efficient solution for cybersecurity-based applications. It is based on DL and bio-hashing. The proposed system uses cascading-style transfer processes on different modalities, like fingerprint, FV, and face images, and then applies a fusion method. This process has the advantage of facilitating the generation of cancellable templates. The system functions are the registration of input biometrics, the extraction of features, the fusion, the reconstruction, style transfer, and the authentication procedure. The overall work is validated on a dataset that includes fingerprint, FV, and face images. The overall performance is

assessed by visual and statistical analysis, which shows good results in terms of AUC and encryption quality evaluation criteria such as SSIM.

The study [213] introduces a novel multimodal biometric authentication system that integrates electrocardiogram (ECG) and FV modalities using deep fusion methods. The system consists of many steps. First, each biometric characteristic is pre-processed to ensure consistency. Next, a CNN model extracts deep features for analysis. Finally, feature-level fusion and score-level fusion approaches are used to integrate the extracted features. The authentication procedure involves using a k-nearest neighbors (KNN) classifier on specifically chosen deep features. The system performs better than existing multimodal techniques and unimodal systems, as shown by extensive testing on many datasets. Huang et al. [214] introduces a novel end-to-end multimodal finger recognition system that addresses limitations in existing biometric fusion methods. It proposes a finger asymmetric backbone network to efficiently extract discriminative features from fingerprint and FV images. A new attention-based encoder fusion network, so called AEF-Net, is also introduced to combine fingerprint and FV features and get rid of unnecessary ones, with a focus on how the different types of features affect each other. The proposed method is evaluated on three multimodal finger databases, demonstrating improved recognition performance compared to SOTA methods. By incorporating attention mechanisms and AE-based training, the system aims to enhance feature fusion effectiveness and achieve better recognition accuracy and speed. The paper also highlights the importance of considering feature fusion effectiveness in biometric recognition methods. Likewise, The study [215] presents an accurate multimodal biometric identification and recognition system that integrates the face and FV modalities. Deep CNNs, inspired by AlexNet, are used to extract features from both facial and FV modalities. These features are then fused at the score level. The combination of facial and FV modalities leads to improved performance measures, including higher accuracy and lower equal mistake rates. This technique successfully addressed the issue of interclass dependencies, enabling accurate identification outcomes for input samples that are cross-paired. The experimental findings demonstrate a significant increase in accuracy for both identification and recognition tasks in comparison with existing systems.

The authors, in [73], present a multimodal vein database, known as FYO, which includes biometric data from the PV, dorsal vein, and WV. The article emphasizes the usefulness of multimodal systems in attack defense, as well as the strict security requirements of vein biometrics. The objective is to improve research on multimodal authentication systems. Hand-crafted feature extractors such as binarized statistical image features (BSIF), Gabor filter, and HOG are used, in addition to a suggested CNN architecture for vein detection. The CNN architecture suggested, which incorporates decision-level integration of biometric features, outperformed hand-crafted techniques and showed greater performance in vein identification. The research conducts a comparison between FYO and other databases, demonstrating the effectiveness of integrating different biometric features for improved security. Wange et al. [216] address gender and identity detection using hand vein data. Indeed, optimizing a task-specific DNN model from VGG-face offers numerous benefits. Utilizing a face database to enhance hand vein detection entails using acquired information, identifying relevant features, and fine-tuning a DL model to improve its generalization ability. This approach aims to use the advantages of face databases and DL methods to improve the precision and effectiveness of gender and identity identification by employing hand vein data. Initially, the model uses DTL to benefit from the knowledge acquired during a large-scale face recognition task, which may improve its performance for the current task. In addition, DNN models are very proficient in extracting specific information from hand vein images, which is essential for achieving correct identification. Furthermore, fine-tuning enhances the model's ability to optimize, particularly for gender and identity identification using hand vein data, resulting in improved performance in comparison to conventional models. The experiments include two main databases, with an emphasis on the face and hand vein. The PolyU NIR-face is one. The lab-made hand-dorsa vein database is another. Similarly, Yang et al. [217] introduce an approach for identifying multimodal biometrics (face and FV images) using stacked extreme learning machines (ELMs) and CCA techniques. At first, it employs ELMs to learn the hidden-layer representation. Then, the CCA transforms the representation into a feature space, which then reproduces the multimodal image features. Next, the obtained features serve as input for a supervised classifier. The obtained results indicate that the proposed approach outperforms some existing approaches when evaluated on hybrid datasets that merge face and FV images. They also demonstrate the effectiveness of multimodal biometric fusion as an alternative way to enhance biometric performance. Moving on, the paper [218] introduces a multi-biometrics algorithm that combines palmprint and DHV images. Deep hashing network (DHN) and biometric graph matching are investigated for recognition. In addition, different fusion strategies are used to combine palmprint and DHV images. DHN is used to encode images into 128-bit codes, which are then used for similarity comparison purposes. Thus, the authors show that the fusion of palmprint and DHV recognition at different levels (pixel, feature, score, decision) can significantly improve accuracy. The proposed scheme also enhances the score level for multi-modal fusion by incorporating SVM for authentication. Consequently, the proposed method demonstrates superior performance in fusion recognition compared to unimodal biometrics.

The suggested work in [219] introduces a multimodal-based DL framework for biometrics identification. Its main objective is to combine three different features from the iris, facial, and finger modalities in order to improve overall identity recognition accuracy. Two fusion methods are used in this paper to combine the data from the different biometric traits, feature-level and score-level fusions. Feature-level fusion involves combining the extracted features from each biometric trait before classification. The score-level fusion involves a combination of similarity scores obtained from individual trait classifiers throughout the recognition process. These strategies seek to use the advantages of each biometric feature to enhance the final performance. This work evaluates the performance of both unimodal and multimodal models on the SDUMLA-HMT dataset in terms of feature extraction and classification. The obtained results show that a multimodal strategy outperforms an unimodal one, resulting in higher accuracy. Additionally, the authors suggest exploring other recognition features and fusion methods as further research directions to improve the performance. In [220], the authors developed a dual-branch-Net method to carefully identify both the inner knuckle print (IKP) and FV. To address the challenges of feature representation and multimodal fusion, they suggested a framework based on CNN, DTL, and the triplet loss function. In order to address the problem of a limited training set, the augmentation technique is applied

Table 11

Summary of proposed works in DL-based multi-modal hand vein recognition. In cases where multiple scenarios are examined, only the top-performing outcome is mentioned.

Ref.	Year	Fused modalities					DL approach	DTL	Data augmentation	Dataset	Results
		FV	PV	DHV	WV	Other					
[73]	2020	X	✓	✓	✓	X	CNN	–	–	FYO	Acc= 100%
[207]	2022	X	X	✓	X	✓	CNN+PCANet	–	–	IITD palmprint, Bosphorus	Acc= 98.86%, EER= 0.93%
[209]	2020	✓	X	X	X	✓	AlexNet, VGG16, ResNet50	Fine-tuning	Translation and cropping	FV, FKP	Acc= 98.84%, 99.89%; EER= 0.0142%, 0.005%
[210]	2022	✓	X	X	X	✓	DL	–	–	SDUMLA-HMT	Acc= 99.98%; EER= 0.7177%
[211]	2021	✓	X	X	X	✓	CNN	–	–	Created, CASIA	NPCR= 99.158%; PSNR= 24.523 dB; SSIM= 0.079.
[213]	2021	✓	X	X	X	✓	CNN	–	–	VeinPolyU, MWMHIT and ECG-ID	EER= 0.12%
[214]	2022	✓	X	X	X	✓	CNN	–	Rotation and translation	HDPR-310, FVC-HKP, CAS-FVU	f1= 99%, 99.3%, 99.4%
[215]	2022	✓	X	X	X	✓	CNN	–	Translation, rotation and illumination	FV-USM, SDUMLA	Acc= 99.85%, 94.87%
[216]	2018	X	X	✓	X	✓	DNN+LDM	Task-driven fine-tuning	Each sample is increased to 100	PolyU NIR-face, created HDV	Acc= 91.6%
[219]	2020	✓	X	X	X	✓	VGG-16	Fine-tuning	Rotation, zooming, shearing, width shifting, and height shifting	SDUMLA-HMT	Acc= 99.39%
[220]	2022	✓	X	X	X	✓	CNN	DA	Translation, clipping, and conversion	PolyU-DB	EER= 0.422%
[221]	2021	X	✓	X	X	✓	DCTNet	–	–	PolyU	GAR= 100%

to increase the dataset size. Experiments validate the effectiveness of the proposed fusion technique compared to other approaches.

7. Research challenges and future directions

The field of vein biometrics, particularly with the integration of DL techniques, holds immense potential for enhancing security and authentication methods. However, several challenges are not sufficiently considered, which often appear in real world application scenarios. Meanwhile, future research directions should focus on developing robust solutions to these challenges while exploring new methodologies and technologies to further advance vein biometrics.

7.1. Research challenges

Biometric hand vein recognition, like any technology, it faces several challenges. Here are some key challenges associated with DL and DTL-based biometric hand vein recognition:

7.1.1. Data acquisition and characteristics of existing datasets

Acquiring high-quality vein images presents several challenges that significantly impact the performance of vein biometric systems. Variations in lighting conditions can lead to inconsistent image quality, making it difficult to extract reliable vein patterns. For instance, inadequate or excessive lighting can obscure vein details or introduce shadows that distort the vein structure. Additionally, differences in skin tone among individuals can affect the visibility and contrast of the veins, complicating the image acquisition process. The presence of hair, scars, or other skin imperfections can further obscure vein patterns, leading to incomplete or noisy images that are challenging for feature extraction and subsequent recognition tasks.

Current image preprocessing methods can improve the recognition performance of vein biometric systems, but selecting the appropriate model to enhance image quality remains challenging. DL techniques have the potential to significantly enhance image quality by learning complex patterns and corrections that traditional methods might miss. Despite this potential, DL methods have been cautiously applied in this context, primarily focusing on FV [86–93]. More research is needed to fully harness their capabilities for all types of hand veins. Introducing more powerful DL-based methods in image preprocessing could address these inconsistencies and artifacts, improving the performance and reliability of vein biometric systems.

The field of hand vein biometrics faces a significant challenge due to the lack of large, publicly accessible datasets. Existing vein biometric datasets are often limited in size and suffer from class imbalance, which constrains the development and evaluation of robust DL models. The efficacy of DL-based methods, which have shown promising performance in vein biometrics, is contingent on the availability of extensive training data. Moreover, most current FV databases are collected using a single capture device. This uniformity fails to account for the variability introduced by different capture devices, leading to evaluations of image preprocessing and feature extraction methods that do not accurately reflect real-world conditions.

7.1.2. *Variability in vein patterns and environment*

Variability in vein patterns presents a significant challenge for vein biometric systems. Factors such as age, health conditions, and physical activities can cause substantial intra-class variations, making it difficult to consistently recognize an individual's vein patterns. As people age, changes in blood vessel structure and skin elasticity can alter the appearance of veins. Health conditions, such as vascular diseases or diabetes, can also impact vein patterns by causing blockages or changes in blood flow. Physical activities, particularly those involving extensive use of the hands or arms, can temporarily or permanently change the visibility and shape of veins. These variations complicate the feature extraction and matching processes, necessitating the development of more robust algorithms that can account for and adapt to these changes to ensure accurate and reliable vein recognition.

Current hand vein biometric systems are often designed under controlled conditions, neglecting the wide-ranging variations encountered in practical use. Factors like temperature changes, skin stretching, and fatigue can degrade accuracy. Furthermore, for DHV recognition, challenges such as tattoos on the dorsal hand, characteristics of elderly hands, and hands with long hair remain understudied despite their impact on real-world performance [19]. Applying DTL to hand vein biometrics can be challenging due to the lack of pre-trained models specific to this domain, necessitating the adaptation of models trained on different tasks.

7.1.3. *Multi modal biometric hand vein recognition system*

Multi-modal biometric vein recognition systems face several challenges that stem from integrating multiple sources of biometric data. Firstly, integrating data from different modalities, such as vein patterns, finger geometry, and palm prints, requires careful consideration. Determining the optimal fusion strategy (score-level, feature-level, etc.) for each modality combination demands thorough research and evaluation. Also, variations in image quality across modalities necessitate robust pre-processing and noise handling techniques to ensure reliable fusion. Secondly, the limited availability of datasets containing multiple modalities for training and testing poses a significant hurdle for algorithm development and validation. Thirdly, The computational complexity of multimodal systems can be a bottleneck, demanding careful optimization of algorithms and hardware resources to achieve efficient processing [72, 222]. Ensuring that the system can process data quickly without compromising accuracy is essential for user acceptance and practical deployment. Finally, multimodal systems may require users to perform multiple actions, potentially impacting user experience and acceptance. Addressing privacy concerns and ensuring user-friendly interactions are crucial for widespread adoption [72]. Simplifying the user interaction process while maintaining high security and accuracy is a key challenge for developers.

7.1.4. *Biometric template protection and aging consideraion*

Several traditional BTP schemes have been developed to enhance privacy. However, these schemes can negatively impact recognition performance. DL approaches have been proposed to mitigate this issue, but their potential has not been fully explored. To date, only a few studies have focused on this area, primarily relying on FV data [166–168]. More research is needed to extend these DL-based protection methods to other types of hand veins.

Aging significantly affects vein patterns, posing a challenge for biometric vein recognition systems. Changes in skin elasticity, collagen, and blood vessels over time can alter vein patterns, impacting the accuracy of long-term recognition technologies. Capturing these changes accurately is essential for maintaining system performance. However, current datasets, often limited to relatively short intervals (up to 106 days as shown in Table 3), fail to fully capture the gradual aging process. This hinders a comprehensive study of aging effects on hand vein biometric systems. DL offers a promising solution by extracting features from vein images, potentially enabling robust and accurate recognition despite aging-related variations.

7.1.5. *PAD systems*

Despite the promising results demonstrated by DL-based PAD approaches in the limited studies on FV biometrics, numerous challenges persist. The primary challenge is the limited availability of evaluation data that includes both genuine and forged samples. Only three publicly accessible PAD datasets for FV exist: SCUT-SFVD [63], ISPR [64], and VERA Finger Vein [65, 66]. Additionally, the interaction between hand vein recognition and PAD within the overall system requires further investigation. Although most PAD systems can independently verify the authenticity of a hand vein sample, understanding their impact on the entire recognition system is crucial, as PAD systems can increase the FNMR of hand vein recognition systems due to potential failures [21].

7.1.6. *Multi view vein recognition*

Most existing databases and algorithms predominantly focus on single-view vein recognition. This method projects a 3D network topology onto a 2D plane, resulting in inevitable 3D feature loss and topological ambiguity in the images. Additionally, single-view methods are sensitive to finger rotation, translation, and hand position in practical applications, which can lead to performance degradation. Currently, there are few dedicated studies and public databases on multi-view vein recognition [58, 156]. More research and development of multi-view databases and algorithms are needed to overcome these limitations and enhance recognition accuracy and robustness.

7.1.7. *Accelerating DL techniques for hand vein biometrics*

DL models have shown impressive performance in hand vein recognition, but their computational demands, especially during training and for complex architectures, pose a significant challenge for real-time performance and deployment on resource-constrained devices. Achieving efficient and fast hand vein recognition requires careful consideration of hardware limitations and algorithmic optimizations.

Current DL models often rely heavily on powerful GPUs, both for training and achieving acceptable inference speeds. While specialized hardware like field programmable gate array (FPGA) offer potential advantages in terms of efficiency, their deployment for hand vein biometrics necessitates further research and development [99, 223]. Furthermore, deploying complex DL models on devices with limited memory, processing power, and battery life, such as mobile devices or embedded systems, presents a major hurdle [224].

Several model optimization techniques can help mitigate these challenges. Model compression techniques like pruning [225], quantization [226], and low-rank factorization [227] can significantly reduce model parameters and operations, leading to smaller models and faster inference. Knowledge distillation, where a smaller "student" model learns to mimic the behavior of a larger pre-trained "teacher" model, can also reduce computational complexity while maintaining performance [228]. Additionally, employing lightweight CNN architectures specifically designed for efficient computation, can enhance performance on resource-constrained platforms [62, 104–108, 115, 149, 151].

Parallel and distributed computing offer further avenues for acceleration. Utilizing multi-node and multi-core architectures, GPU clusters, or cloud computing platforms can significantly speed up both training and inference [229]. However, effectively leveraging these technologies for hand vein biometrics necessitates addressing challenges related to data partitioning, communication overhead, and resource management [230]. Researchers are encouraged to investigate the capabilities of real-time DL-based hand vein recognition by implementing their techniques on embedded platforms like FPGA, and by assessing real-time metrics such as inference time, latency, resource utilization, and algorithmic complexity. These assessments offer critical insights for users and developers, aiding in the selection of the optimal DL for particular hardware configurations and specific types of hand veins.

7.2. Perspectives

Considering the challenges faced by hand vein biometrics, from our humble perspective, the following lines of investigation can be considered by the research community:

7.2.1. *Creating synthetic large datasets*

Collecting large-scale real-world training data for hand vein recognition has proven challenging due to noise and irregular variations during acquisition. One promising future direction is the creation of synthetic large datasets for hand vein biometrics. Developing realistic and diverse synthetic datasets can address the limitations of existing datasets, which are often small and lack the variability needed for robust training and testing. Advanced generative models, such as GAN, can generate synthetic vein patterns that mimic real-world variations in skin tone, age, health conditions, and environmental factors. These synthetic datasets can provide a valuable resource for training DL models, enabling researchers to explore new algorithms and approaches without the constraints of limited real-world data. Additionally, synthetic datasets can facilitate the study of the aging problem by simulating longitudinal changes in vein patterns over extended periods, thus offering a comprehensive platform for testing the robustness and adaptability of biometric recognition systems. The review paper of Salazar-Jurado et al. [18] discusses the challenges, insights, and future perspectives in generating synthetic PV images, highlighting the potential benefits and ongoing advancements in this field.

7.2.2. *3D hand vein recognition*

3D hand vein biometric systems offer enhanced accuracy and security by capturing the depth and spatial characteristics of vein patterns, providing more detailed biometric data than traditional 2D imaging. Current vein verification systems typically use a monocular camera to acquire a single-view 2D image, which limits vein pattern information and causes inconsistencies due to positional variations. These limitations adversely affect system performance, particularly in contact-free modes, where pitch and roll movements create significant variability in the samples. This concern remains a challenge despite some efforts to address it in recent years [58, 156, 231, 232]. Future research should focus on designing software and hardware platforms to capture a comprehensive view of vein patterns, developing methods for 3D reconstruction to construct a complete 3D hand vein image or point cloud [233], advancing 3D feature extraction and matching strategies, and creating diverse 3D datasets.

7.2.3. *Gender and aging recognition based hand vein*

Exploring gender recognition using hand vein patterns presents a novel and promising direction in biometric research. Hand vein patterns, influenced by physiological and anatomical differences between genders, can potentially serve as distinctive biometric traits for gender classification. Advanced ML techniques, particularly DL models, can be employed to extract and analyze features from hand vein images, enabling accurate gender prediction. This approach can enhance the robustness and security of biometric systems by adding an additional layer of verification. This problem has been preliminarily studied [189, 234–238]. However, significant challenges remain, such as the need for large, diverse datasets that capture gender-specific variations in hand vein patterns. Addressing these challenges requires developing sophisticated algorithms capable of handling intra-class variability and ensuring high recognition accuracy. Thus, in the future, more effort should be invested in promoting the research of this problem, focusing on creating comprehensive datasets, refining feature extraction methods, and optimizing classification algorithms to fully realize the potential of gender recognition based on hand vein patterns. DTL can be used to transfer knowledge learned from a source domain (e.g., a dataset of younger individuals) to a target domain (e.g., a dataset of older individuals). This helps in extracting relevant features from vein patterns that are less affected by aging. Besides, fine-tuning pre-trained models on datasets that include both younger and older individuals can help adapt the model to recognize vein patterns across different age groups more effectively.

7.2.4. *FL in hand vein recognition*

FL offers a promising approach to enhancing hand vein recognition systems while preserving user privacy. Unlike traditional methods that collect all data centrally, FL trains models locally on individual devices, sharing only model updates. This decentralized method improves data security and privacy by keeping sensitive vein patterns on users' devices. Additionally, it can leverage the diversity of vein patterns from various devices, enhancing model robustness.

FL has been preliminarily studied in recent hand vein recognition research [96, 97, 164]. However, several challenges remain, such as ensuring consistent model updates across devices with different resources and network conditions, and developing robust aggregation methods for diverse, non-independent and identically distributed (non-IID) data sources. Future research should focus on optimizing FL algorithms, enhancing communication efficiency, and managing the variability in hand vein data across devices. Addressing these challenges will help create more secure and effective biometric recognition technologies.

7.2.5. *DRL and GNN in hand vein recognition*

The perspective of using DRL in hand vein recognition offers intriguing possibilities. DRL can optimize biometric systems by enabling adaptive learning based on feedback from the environment [91]. For instance, DRL algorithms could dynamically adjust feature extraction parameters or model hyperparameters to improve recognition accuracy over time. DRL could also enhance system robustness by optimizing decision-making processes in challenging conditions such as varying illumination or hand posture. However, applying DRL to biometric recognition involves challenges like defining appropriate reward functions and ensuring data privacy and security. Future research may focus on developing DRL frameworks that integrate seamlessly with hand vein recognition systems, optimizing performance while addressing ethical and technical considerations.

Employing GNNs for hand vein modularization offers promising opportunities in biometric classification. GNNs can model intricate relationships between vein patterns as graphs, enhancing feature extraction and classification accuracy. DRL can further optimize GNNs by guiding node and edge updates to refine graph representations based on classification feedback. DRL enables GNNs to dynamically adjust to varying vein patterns, improving adaptability and robustness. This synergy allows for more effective integration of complex spatial and temporal dependencies in hand vein biometrics, paving the way for advanced biometric authentication systems with enhanced accuracy and resilience to environmental variations.

7.2.6. *DL-Based integrity assurance for hand vein images*

Hand vein image datasets benefit from DL-based steganalysis to detect alterations, ensuring data integrity [22]. DL models can effectively analyze subtle changes in vein patterns caused by steganography or watermarking techniques [239], verifying authenticity and preventing unauthorized modifications. Watermarking adds embedded data to images, ensuring traceability, while steganography hides imperceptible data within dataset samples without detection [240]. DL enhances these techniques by robustly identifying alterations in hand vein patterns, crucial for maintaining the reliability and security of biometric data in applications requiring stringent integrity checks, such as healthcare and secure access systems. Further research is necessary to enhance the capabilities of DL in accurately detecting and mitigating sophisticated forms of image tampering in hand vein biometrics.

7.2.7. *IoT authentication and biometrics*

Although the co-hash code proposed for PV is poised for use as an authenticator in IoT services due to its stable, compact, and straightforward nature, it can also serve as an intermediate representation for BTP schemes, as suggested in references [241, 242]. This opens avenues for privacy-enhanced IoT authentication systems with rigorous requirements such as non-invertibility, unlinkability, and revocability. Another significant downstream IoT application of PalmCohashNet is in biometric cryptosystems, where biometrics and cryptography are integrated for purposes like BTP, safeguarding secret keys, and key generation, as outlined in reference.

It is important to note that PalmCohashNet is also applicable in large-scale biometric identification, indexing, and retrieval tasks commonly encountered in IoT-related applications. These applications necessitate that entities (biometric templates) are identified, indexed, or retrieved in a compact and simple format, such as binary representation. Our experiments demonstrate that PalmCohashNet achieves SOTA top-1 identification accuracy on various benchmark datasets, indicating its significant potential for such applications. Although PalmCohashNet utilizes a lightweight CNN, specifically MobileNetV2, as its backbone, a more efficient lightweight CNN backbone, like MPSNet [173], could be integrated to meet the requirements of IoT devices.

7.2.8. *Transformers and LLM for hand vein biometric*

Looking ahead, Transformers and large language models (LLMs) offer promising avenues for advancing hand vein biometric recognition beyond traditional attention mechanisms. Future research might explore novel transformer architectures tailored to capture intricate vein patterns effectively. This could involve designing Transformer variants that integrate convolutional or recurrent layers optimized for processing spatial and temporal features in 3D vein data. LLMs, known for their ability to learn complex patterns from vast datasets, could enhance feature representation and extraction in hand vein recognition. By pre-training LLMs on diverse biometric data, they could learn discriminative features across various demographics and conditions, improving robustness and generalization. Additionally, fine-tuning LLMs on specific vein recognition tasks could enhance their ability to extract relevant features from vein images, potentially outperforming traditional feature extraction methods. These advancements hold potential for developing more accurate, adaptable, and secure hand vein biometric systems, applicable in healthcare, security, and other fields requiring precise and reliable identification methods. Specifically, LLMs such as GPT, BERT, and others [243], can be fine-tuned on hand vein datasets to extract discriminative features. Feasibility lies in training a specialized BiometricChat LLM, tailored for

vein recognition, by pre-training on a diverse set of vein images to capture complex patterns. This would require careful dataset curation, algorithm optimization for biometric tasks, and addressing privacy concerns in biometric data usage.

8. Conclusion

In conclusion, hand vein biometrics, including FV, PV, DHV, and multi-modal-based recognition, have emerged as a highly secure, accurate, and non-intrusive method for identity verification. The distinctiveness and complexity of vein patterns within the hand provide a robust basis for biometric identification, offering significant advantages over other modalities. Hand vein recognition is contactless, which enhances user convenience and hygiene, and the internal location of veins makes them less susceptible to damage or tampering, thereby improving the overall security and reliability of biometric systems.

This comprehensive review has delved into the latest advancements in DL techniques applied to hand vein biometrics. It has covered essential fundamentals of hand vein biometrics and summarized publicly available datasets, providing a valuable resource for researchers in the field. Additionally, the review has discussed SOTA evaluation metrics for finger, palm, and dorsal vein recognition, highlighting the best performance achieved and identifying optimal methods and effective transfer learning approaches.

The review also addressed several research challenges, such as the need for more extensive and diverse datasets, the development of more sophisticated preprocessing techniques, and the refinement of DL models to improve accuracy and efficiency. By outlining future directions and perspectives, this review encourages researchers to build upon existing methods and propose innovative techniques that further enhance the capabilities of hand vein biometrics.

In light of these findings, it is clear that hand vein biometrics hold significant promise for the future of secure and efficient identity verification. The ongoing advancements in DL and related technologies are expected to drive further improvements in the performance and reliability of these systems. As researchers continue to address current challenges and explore new possibilities, hand vein biometrics are poised to play a critical role in the evolution of biometric authentication, offering a highly effective solution for a wide range of applications.

CRedit authorship contribution statement

Mustapha Hemis: Conceptualization; Methodology; Resources; Investigation; Writing original draft; Writing, review, and editing. **Hanza Kheddar:** Conceptualization; Methodology; Data Curation; Resources; Investigation; Visualization; Writing original draft; Writing, review, and editing. **Sami Bourouis:** Conceptualization; Methodology; Data Curation; Resources; Investigation; Visualization; Writing original draft; Writing, review, and editing. **Nasir Saleem:** Conceptualization; Methodology; Data Curation; Resources; Investigation; Visualization; Writing original draft; Writing, review, and editing.

Declaration of competing interest

The authors declare that they have no known competing financial interests or personal relationships that could have appeared to influence the work reported in this paper.

Data availability

No data was used for the research described in the article.

References

1. J. Al-Sarairih, M. R. AlJa'afreh, Keystroke and swipe biometrics fusion to enhance smartphones authentication, *Computers & Security* 125 (2023) 103022.
2. A. Parashar, A. Parashar, A. F. Abate, R. S. Shekhawat, I. Rida, Real-time gait biometrics for surveillance applications: A review, *Image and Vision Computing* (2023) 104784.
3. H. Kheddar, Y. Himeur, S. Al-Maadeed, A. Amira, F. Bensaali, Deep transfer learning for automatic speech recognition: Towards better generalization, *Knowledge-Based Systems* 277 (2023) 110851.
4. H. Kheddar, M. Hemis, Y. Himeur, Automatic speech recognition using advanced deep learning approaches: A survey, *Information Fusion* (2024) 102422.
5. B. Hou, H. Zhang, R. Yan, Finger-vein biometric recognition: A review, *IEEE Transactions on Instrumentation and Measurement* 71 (2022) 1–26.
6. N. Miura, A. Nagasaka, T. Miyatake, Feature extraction of finger-vein patterns based on repeated line tracking and its application to personal identification, *Machine vision and applications* 15 (2004) 194–203.
7. J. Kosmala, K. Saeed, Human identification by vascular patterns, in: *Biometrics and Kansei Engineering*, Springer, 2012, pp. 67–87.
8. K. Syazana-Itqan, A. Syafeeza, N. Saad, N. A. Hamid, W. Saad, A review of finger-vein biometrics identification approaches, *Indian J. Sci. Technol* 9 (2016) 1–9.
9. J. Wang, G. Wang, Quality-specific hand vein recognition system, *IEEE Transactions on Information Forensics and Security* 12 (11) (2017) 2599–2610.
10. C. Kauba, A. Uhl, Sensor ageing impact on finger-vein recognition, in: *2015 International Conference on Biometrics (ICB)*, IEEE, 2015, pp. 113–120.
11. B. Prommegger, C. Kauba, A. Uhl, Longitudinal finger rotation in finger-vein recognition, in: *2018 International Conference of the Biometrics Special Interest Group (BIOSIG)*, IEEE, 2018, pp. 1–8.
12. G. Jaswal, A. Kaul, R. Nath, Knuckle print biometrics and fusion schemes—overview, challenges, and solutions, *ACM Computing Surveys (CSUR)* 49 (2) (2016) 1–46.
13. K. Shaheed, H. Liu, G. Yang, I. Qureshi, J. Gou, Y. Yin, A systematic review of finger vein recognition techniques, *Information* 9 (9) (2018) 213.
14. A. H. Mohsin, A. Zaidan, B. Zaidan, O. Albahri, S. A. B. Ariffin, A. Alemran, O. Enaizan, A. H. Shareef, A. N. Jasim, N. Jalood, et al., Finger vein biometrics: taxonomy analysis, open challenges, future directions, and recommended solution for decentralised network architectures, *Ieee Access* 8 (2020) 9821–9845.
15. G. K. Sidiropoulos, P. Kiratsa, P. Chatzipetrou, G. A. Papakostas, Feature extraction for finger-vein-based identity recognition, *Journal of Imaging* 7 (5) (2021) 89.

16. K. Shaheed, A. Mao, I. Qureshi, M. Kumar, S. Hussain, X. Zhang, Recent advancements in finger vein recognition technology: methodology, challenges and opportunities, *Information Fusion* 79 (2022) 84–109.
17. W. Wu, S. J. Elliott, S. Lin, S. Sun, Y. Tang, Review of palm vein recognition, *IET Biometrics* 9 (1) (2020) 1–10.
18. E. H. Salazar-Jurado, R. Hernández-García, K. Vilches-Ponce, R. J. Barrientos, M. Mora, G. Jaswal, Towards the generation of synthetic images of palm vein patterns: A review, *Information Fusion* 89 (2023) 66–90.
19. W. Jia, W. Xia, B. Zhang, Y. Zhao, L. Fei, W. Kang, D. Huang, G. Guo, A survey on dorsal hand vein biometrics, *Pattern Recognition* 120 (2021) 108122.
20. K. Shaheed, A. Mao, I. Qureshi, M. Kumar, Q. Abbas, I. Ullah, X. Zhang, A systematic review on physiological-based biometric recognition systems: current and future trends, *Archives of Computational Methods in Engineering* (2021) 1–44.
21. K. Shaheed, P. Szczuko, M. Kumar, I. Qureshi, Q. Abbas, I. Ullah, Deep learning techniques for biometric security: A systematic review of presentation attack detection systems, *Engineering Applications of Artificial Intelligence* 129 (2024) 107569.
22. H. Kheddar, M. Hemis, Y. Himeur, D. Megías, A. Amira, Deep learning for steganalysis of diverse data types: A review of methods, taxonomy, challenges and future directions, *Neurocomputing* (2024) 127528.
23. Y. Himeur, S. Al-Maadeed, H. Kheddar, N. Al-Maadeed, K. Abualsaud, A. Mohamed, T. Khattab, Video surveillance using deep transfer learning and deep domain adaptation: Towards better generalization, *Engineering Applications of Artificial Intelligence* 119 (2023) 105698.
24. A. Vaswani, N. Shazeer, N. Parmar, J. Uszkoreit, L. Jones, A. N. Gomez, Ł. Kaiser, I. Polosukhin, Attention is all you need, *Advances in neural information processing systems* 30 (2017).
25. N. Djeflal, H. Kheddar, D. Addou, A. C. Mazari, Y. Himeur, Automatic speech recognition with BERT and CTC transformers: A review, in: *2023 2nd International Conference on Electronics, Energy and Measurement (IC2EM)*, Vol. 1, IEEE, 2023, pp. 1–8.
26. S. Crisan, I. G. Târnovan, T. Crisan, A hand vein structure simulation platform for algorithm testing and biometric identification, in: *16th IMEKO TC4 Symposium*, Florence, Italy, 2008.
27. Etsy, Superficial veins of the hand & cutaneous nerves of the upper limb on the reverse side of the page from grant's human anatomy atlas pss 3898, accessed: 2024-07-14.
URL https://www.etsy.com/fi-en/listing/674537177/superficial-veins-of-the-hand-cutaneous?show_sold_out_detail=1&ref=nla_listing_details
28. H. Kolivand, S. Asadianfam, K. A. Akintoye, M. S. Rahim, Finger vein recognition techniques: a comprehensive review, *Multimedia Tools and Applications* 82 (22) (2023) 33541–33575.
29. L. Wang, G. Leedham, S.-Y. Cho, Infrared imaging of hand vein patterns for biometric purposes, *IET computer vision* 1 (3) (2007) 113–122.
30. D. Zhang, Z. Guo, Y. Gong, D. Zhang, Z. Guo, Y. Gong, Dorsal hand recognition, *Multispectral Biometrics: Systems and Applications* (2016) 165–186.
31. K. Chen, D. Zhang, Band selection for improvement of dorsal hand recognition, in: *2011 International Conference on Hand-Based Biometrics*, IEEE, 2011, pp. 1–4.
32. M. Waluś, K. Bernacki, J. Konopacki, Impact of nir wavelength lighting in image acquisition on finger vein biometric system effectiveness, *Opto-Electronics Review* 25 (4) (2017) 263–268.
33. C. Kauba, A. Uhl, Shedding light on the veins-reflected light or transillumination in hand-vein recognition, in: *2018 International Conference on Biometrics (ICB)*, IEEE, 2018, pp. 283–290.
34. Y. Wang, W. Xie, X. Yu, L.-K. Shark, An automatic physical access control system based on hand vein biometric identification, *IEEE Transactions on Consumer Electronics* 61 (3) (2015) 320–327.
35. Q. Zhu, Z. Zhang, N. Liu, H. Sun, Near infrared hand vein image acquisition and roi extraction algorithm, *Optik* 126 (24) (2015) 5682–5687.
36. S. Joardar, A. Chatterjee, A. Rakshit, Real-time nir imaging of palm dorsal subcutaneous vein pattern based biometrics: An src based approach, *IEEE Instrumentation & Measurement Magazine* 19 (2) (2016) 13–19.
37. A. Kumar, Y. Zhou, Human identification using finger images, *IEEE Transactions on image processing* 21 (4) (2011) 2228–2244.
38. B. T. Ton, R. N. Veldhuis, A high quality finger vascular pattern dataset collected using a custom designed capturing device, in: *2013 International conference on biometrics (ICB)*, IEEE, 2013, pp. 1–5.
39. S. Bazrafkan, T. Nedelcu, C. Costache, P. Corcoran, Finger vein biometric: Smartphone footprint prototype with vein map extraction using computational imaging techniques, in: *2016 IEEE International Conference on Consumer Electronics (ICCE)*, IEEE, 2016, pp. 512–513.
40. R. Ramachandra, K. B. Raja, S. K. Venkatesh, C. Busch, Design and development of low-cost sensor to capture ventral and dorsal finger vein for biometric authentication, *IEEE Sensors Journal* 19 (15) (2019) 6102–6111.
41. L. Wang, G. Leedham, D. S.-Y. Cho, Minutiae feature analysis for infrared hand vein pattern biometrics, *Pattern recognition* 41 (3) (2008) 920–929.
42. D. Huang, Y. Tang, Y. Wang, L. Chen, Y. Wang, Hand-dorsa vein recognition by matching local features of multisource keypoints, *IEEE transactions on cybernetics* 45 (9) (2014) 1823–1837.
43. H. Qin, Z. Chen, X. He, Finger-vein image quality evaluation based on the representation of grayscale and binary image, *Multimedia Tools and Applications* 77 (2018) 2505–2527.
44. C.-H. Hsia, New verification strategy for finger-vein recognition system, *IEEE Sensors Journal* 18 (2) (2017) 790–797.
45. V. Niño-Celis, R. A. Huerta-Santis, E. H. Salazar-Jurado, R. Hernández-García, Palm vein image quality assessment through natural scene and texture statistics, in: *2023 42nd IEEE International Conference of the Chilean Computer Science Society (SCCC)*, IEEE, 2023, pp. 1–7.
46. E. C. Lee, K. R. Park, Restoration method of skin scattering blurred vein image for finger vein recognition, *Electronics Letters* 45 (21) (2009) 1.
47. E. C. Lee, K. R. Park, Image restoration of skin scattering and optical blurring for finger vein recognition, *Optics and Lasers in Engineering* 49 (7) (2011) 816–828.
48. J. Yang, B. Zhang, Y. Shi, Scattering removal for finger-vein image restoration, *Sensors* 12 (3) (2012) 3627–3640.
49. J. Yang, Y. Shi, Towards finger-vein image restoration and enhancement for finger-vein recognition, *Information Sciences* 268 (2014) 33–52.
50. J. Yang, Y. Shi, Finger-vein roi localization and vein ridge enhancement, *Pattern Recognition Letters* 33 (12) (2012) 1569–1579.
51. R. S. Al-Khafaji, M. S. Al-Tamimi, Vein biometric recognition methods and systems: A review, *Advances in Science and Technology. Research Journal* 16 (1) (2022) 36–46.
52. P. E. Kilgore, S. Weisong, J. Cao, Z. Yu, X. Mingyang, Palm vein-based low-cost mobile identification system for a wide age range, *uS Patent App. 15/293,798* (Apr. 20 2017).
53. E. Salazar, R. Hernández-García, R. J. Barrientos, K. Vilches, M. Mora, A. Vásquez, Automatic generation of synthetic palm vein images: a nature-based approach (2021).
54. M. S. M. Asaari, S. A. Suandi, B. A. Rosdi, Fusion of band limited phase only correlation and width centroid contour distance for finger based biometrics, *Expert Systems with Applications* 41 (7) (2014) 3367–3382.
55. Y. Lu, S. J. Xie, S. Yoon, Z. Wang, D. S. Park, An available database for the research of finger vein recognition, in: *2013 6th International congress on image and signal processing (CISP)*, Vol. 1, IEEE, 2013, pp. 410–415.
56. Y. Yin, L. Liu, X. Sun, Sdumla-hmt: A multimodal biometric database, in: *Biometric Recognition: 6th Chinese Conference, CCBP 2011*, Beijing, China, December 3–4, 2011. *Proceedings* 6, Springer, 2011, pp. 260–268.
57. W. Yang, X. Huang, F. Zhou, Q. Liao, Comparative competitive coding for personal identification by using finger vein and finger dorsal texture fusion, *Information sciences* 268 (2014) 20–32.

58. P. Zhao, Y. Song, S. Wang, J.-H. Xue, S. Zhao, Q. Liao, W. Yang, Vpcformer: A transformer-based multi-view finger vein recognition model and a new benchmark, *Pattern Recognition* 148 (2024) 110170.
59. L. Lin, H. Liu, W. Zhang, F. Liu, Z. Lai, Finger vein verification using intrinsic and extrinsic features, in: 2021 IEEE International Joint Conference on Biometrics (IJCB), IEEE, 2021, pp. 1–7.
60. H. Ren, L. Sun, J. Guo, C. Han, A dataset and benchmark for multimodal biometric recognition based on fingerprint and finger vein, *IEEE Transactions on Information Forensics and Security* 17 (2022) 2030–2043.
61. C. Kauba, B. Prommegger, A. Uhl, Focussing the beam—a new laser illumination based data set providing insights to finger-vein recognition, in: 2018 IEEE 9th International Conference on Biometrics Theory, Applications and Systems (BTAS), IEEE, 2018, pp. 1–9.
62. S. Tang, S. Zhou, W. Kang, Q. Wu, F. Deng, Finger vein verification using a siamese cnn, *IET biometrics* 8 (5) (2019) 306–315.
63. X. Qiu, W. Kang, S. Tian, W. Jia, Z. Huang, Finger vein presentation attack detection using total variation decomposition, *IEEE Transactions on Information Forensics and Security* 13 (2) (2018) 465–477.
64. D. T. Nguyen, Y. H. Park, K. Y. Shin, S. Y. Kwon, H. C. Lee, K. R. Park, Fake finger-vein image detection based on fourier and wavelet transforms, *Digital Signal Processing* 23 (5) (2013) 1401–1413.
65. P. Tome, R. Raghavendra, C. Busch, S. Tirunagari, N. Poh, B. Shekar, D. Gragnaniello, C. Sansone, L. Verdoliva, S. Marcel, The 1st competition on counter measures to finger vein spoofing attacks, in: 2015 international conference on biometrics (ICB), IEEE, 2015, pp. 513–518.
66. P. Tome, M. Vanoni, S. Marcel, On the vulnerability of finger vein recognition to spoofing, in: 2014 international conference of the biometrics special interest group (BIOSIG), IEEE, 2014, pp. 1–10.
67. Y. Hao, Z. Sun, T. Tan, C. Ren, Multispectral palm image fusion for accurate contact-free palmprint recognition, in: 2008 15th IEEE International Conference on Image Processing, IEEE, 2008, pp. 281–284.
68. P. Tome, S. Marcel, Palm vein database and experimental framework for reproducible research, in: 2015 international conference of the biometrics special interest group (BIOSIG), IEEE, 2015, pp. 1–7.
69. R. Kabacinski, M. Kowalski, Vein pattern database and benchmark results, *Electronics Letters* 47 (20) (2011) 1.
70. D. Zhang, Z. Guo, G. Lu, L. Zhang, W. Zuo, An online system of multispectral palmprint verification, *IEEE transactions on instrumentation and measurement* 59 (2) (2009) 480–490.
71. L. Zhang, Z. Cheng, Y. Shen, D. Wang, Palmprint and palmvein recognition based on dcnn and a new large-scale contactless palmvein dataset, *Symmetry* 10 (4) (2018) 78.
72. S. Bhilare, G. Jaswal, V. Kanhangad, A. Nigam, Single-sensor hand-vein multimodal biometric recognition using multiscale deep pyramidal approach, *Machine Vision and Applications* 29 (8) (2018) 1269–1286.
73. Ö. Toygar, F. O. Babalola, Y. Bitirim, FYO: A novel multimodal vein database with palmar, dorsal and wrist biometrics, *IEEE Access* 8 (2020) 82461–82470.
74. Y. Wang, H. Wang, Gradient based image segmentation for vein pattern, in: 2009 fourth international conference on computer sciences and convergence information technology, IEEE, 2009, pp. 1614–1618.
75. A. Yuksel, L. Akarun, B. Sankur, Hand vein biometry based on geometry and appearance methods, *IET computer vision* 5 (6) (2011) 398–406.
76. A. M. Badawi, et al., Hand vein biometric verification prototype: A testing performance and patterns similarity., *IPCV* 14 (3) (2006) 9.
77. F. Liu, S. Jiang, B. Kang, T. Hou, A recognition system for partially occluded dorsal hand vein using improved biometric graph matching, *IEEE Access* 8 (2020) 74525–74534.
78. F. Wilches-Bernal, B. Núñez-Álvares, P. Vizcaya, A database of dorsal hand vein images, *arXiv preprint arXiv:2012.05383* (2020).
79. Y. Habchi, Y. Himeur, H. Kheddar, A. Boukabou, S. Atalla, A. Chouchane, A. Ouamane, W. Mansoor, AI in thyroid cancer diagnosis: Techniques, trends, and future directions, *Systems* 11 (10) (2023) 519.
80. M. I. Obayya, M. El-Ghandour, F. Alrowais, Contactless palm vein authentication using deep learning with Bayesian optimization, *IEEE access* 9 (2020) 1940–1957.
81. H. Qin, M. A. El-Yacoubi, Finger-vein quality assessment by representation learning from binary images, in: *Neural Information Processing: 22nd International Conference, ICONIP 2015, Istanbul, Turkey, November 9–12, 2015, Proceedings, Part I 22*, Springer, 2015, pp. 421–431.
82. H. Qin, M. A. El-Yacoubi, Deep representation for finger-vein image-quality assessment, *IEEE Transactions on Circuits and Systems for Video Technology* 28 (8) (2017) 1677–1693.
83. J. Zeng, Y. Chen, C. Qin, Finger-vein image quality assessment based on light-cnn, in: 2018 14th IEEE International Conference on Signal Processing (ICSP), IEEE, 2018, pp. 768–773.
84. H. Ren, L. Sun, J. Guo, C. Han, Y. Cao, A high compatibility finger vein image quality assessment system based on deep learning, *Expert Systems with Applications* 196 (2022) 116603.
85. X.-j. Guo, D. Li, H.-g. Zhang, J.-f. Yang, Image restoration of finger-vein networks based on encoder-decoder model, *Optoelectronics Letters* 15 (6) (2019) 463–467.
86. V. Bros, K. Kotwal, S. Marcel, Vein enhancement with deep auto-encoders to improve finger vein recognition, in: 2021 International Conference of the Biometrics Special Interest Group (BIOSIG), IEEE, 2021, pp. 1–5.
87. J. Choi, K. J. Noh, S. W. Cho, S. H. Nam, M. Owais, K. R. Park, Modified conditional generative adversarial network-based optical blur restoration for finger-vein recognition, *IEEE Access* 8 (2020) 16281–16301.
88. S. Yang, H. Qin, X. Liu, J. Wang, Finger-vein pattern restoration with generative adversarial network, *IEEE Access* 8 (2020) 141080–141089.
89. H. Jiang, L. Shen, H. Wang, Y. Yao, G. Zhao, Finger vein image inpainting using neighbor binary-wasserstein generative adversarial networks (nb-wgan), *Applied Intelligence* (2022) 1–12.
90. J. S. Hong, S. G. Kim, J. S. Kim, K. R. Park, Deep learning-based restoration of multi-degraded finger-vein image by non-uniform illumination and noise, *Engineering Applications of Artificial Intelligence* 133 (2024) 108036.
91. R. Gao, H. Lu, A. Al-Azzawi, Y. Li, C. Zhao, DRL-FVRestore: An Adaptive Selection and Restoration Method for Finger Vein Images Based on Deep Reinforcement, *Applied Sciences* 13 (2) (2023) 699.
92. L. Lei, F. Xi, S. Chen, Finger-vein image enhancement based on pulse coupled neural network, *IEEE Access* 7 (2019) 57226–57237.
93. S. Du, J. Yang, H. Zhang, B. Zhang, Z. Su, Fvsr-net: An end-to-end finger vein image scattering removal network, *Multimedia Tools and Applications* 80 (2021) 10705–10722.
94. H. Qin, M. A. El-Yacoubi, Deep representation-based feature extraction and recovering for finger-vein verification, *IEEE Transactions on Information Forensics and Security* 12 (8) (2017) 1816–1829.
95. R. Das, E. Picciucco, E. Maiorana, P. Campisi, Convolutional neural network for finger-vein-based biometric identification, *IEEE Transactions on Information Forensics and Security* 14 (2) (2018) 360–373.
96. F.-Z. Lian, J.-D. Huang, J.-X. Liu, G. Chen, J.-H. Zhao, W.-X. Kang, Fedfv: A personalized federated learning framework for finger vein authentication, *Machine Intelligence Research* 20 (5) (2023) 683–696.
97. H. Mu, J. Guo, C. Han, L. Sun, PAFedFV: Personalized and Asynchronous Federated Learning for Finger Vein Recognition, *arXiv preprint arXiv:2404.13237* (2024).
98. Y. Zhang, W. Li, L. Zhang, X. Ning, L. Sun, Y. Lu, Adaptive learning gabor filter for finger-vein recognition, *IEEE access* 7 (2019) 159821–159830.

99. R. C.-H. Chang, C.-Y. Wang, Y.-H. Li, C.-D. Chiu, Design of low-complexity convolutional neural network accelerator for finger vein identification system, *Sensors* 23 (4) (2023) 2184.
100. C. Liu, H. Qin, Q. Song, H. Yan, F. Luo, A deep ensemble learning method for single finger-vein identification, *Frontiers in Neurorobotics* 16 (2023) 1065099.
101. H. Huang, S. Liu, H. Zheng, L. Ni, Y. Zhang, W. Li, Deepvein: Novel finger vein verification methods based on deep convolutional neural networks, in: 2017 IEEE international conference on identity, security and behavior analysis (ISBA), IEEE, 2017, pp. 1–8.
102. J. Liu, Z. Chen, K. Zhao, M. Wang, Z. Hu, X. Wei, Y. Zhu, Y. Yu, Z. Feng, H. Kim, et al., Finger vein recognition using a shallow convolutional neural network, in: *Biometric Recognition: 15th Chinese Conference, CCBR 2021, Shanghai, China, September 10–12, 2021, Proceedings 15*, Springer, 2021, pp. 195–202.
103. I. Boucherit, M. O. Zmirli, H. Hentabli, B. A. Rosdi, Finger vein identification using deeply-fused convolutional neural network, *Journal of King Saud University-Computer and Information Sciences* 34 (3) (2022) 646–656.
104. Y. Fang, Q. Wu, W. Kang, A novel finger vein verification system based on two-stream convolutional network learning, *Neurocomputing* 290 (2018) 100–107.
105. C. Xie, A. Kumar, Finger vein identification using convolutional neural network and supervised discrete hashing, *Pattern Recognition Letters* 119 (2019) 148–156, deep Learning for Pattern Recognition.
106. J. Shen, N. Liu, C. Xu, H. Sun, Y. Xiao, D. Li, Y. Zhang, Finger vein recognition algorithm based on lightweight deep convolutional neural network, *IEEE Transactions on Instrumentation and Measurement* 71 (2021) 1–13.
107. D. Zhao, H. Ma, Z. Yang, J. Li, W. Tian, Finger vein recognition based on lightweight cnn combining center loss and dynamic regularization, *Infrared Physics & Technology* 105 (2020) 103221.
108. Z. Zhang, Z. Zhou, X. Yang, H. Meng, G. Wu, Convolutional neural network based on multi-directional local coding for finger vein recognition, *Information Sciences* 623 (2023) 633–647.
109. Y. Wang, H. Lu, X. Qin, J. Guo, Residual gabor convolutional network and fv-mix exponential level data augmentation strategy for finger vein recognition, *Expert Systems with Applications* 223 (2023) 119874.
110. S. Li, H. Zhang, J. Yang, Finger vein recognition based on local graph structural coding and CNN, in: *Tenth International Conference on Graphics and Image Processing (ICGIP 2018)*, Vol. 11069, SPIE, 2019, pp. 1007–1014.
111. G. Wang, C. Sun, A. Sowmya, Multi-weighted co-occurrence descriptor encoding for vein recognition, *IEEE Transactions on Information Forensics and Security* 15 (2019) 375–390.
112. W. Liu, H. Lu, Y. Li, Y. Wang, Y. Dang, An improved finger vein recognition model with a residual attention mechanism, in: *Biometric Recognition: 15th Chinese Conference, CCBR 2021, Shanghai, China, September 10–12, 2021, Proceedings 15*, Springer, 2021, pp. 231–239.
113. D. M. Sulaiman, A. M. Abdulazeez, D. A. Zebari, D. Q. Zeebaree, S. A. Mostafa, S. S. Sadiq, An Attention-Based Deep Regional Learning Model for Enhanced Finger Vein Identification, *Traitement du Signal* 39 (6) (2022) 1991.
114. J. Huang, M. Tu, W. Yang, W. Kang, Joint attention network for finger vein authentication, *IEEE Transactions on Instrumentation and Measurement* 70 (2021) 1–11.
115. Z. Zhang, M. Wang, Convolutional neural network with convolutional block attention module for finger vein recognition, *arXiv preprint arXiv:2202.06673* (2022).
116. W. Liu, H. Lu, Y. Wang, Y. Li, Z. Qu, Y. Li, Mmran: A novel model for finger vein recognition based on a residual attention mechanism: Mmran: A novel finger vein recognition model, *Applied Intelligence* 53 (3) (2023) 3273–3290.
117. Y. Huang, H. Ma, M. Wang, Axially-enhanced local attention network for finger vein recognition, *IEEE Transactions on Instrumentation and Measurement* (2023).
118. J. Huang, A. Zheng, M. S. Shakeel, W. Yang, W. Kang, FVFSNet: Frequency-spatial coupling network for finger vein authentication, *IEEE Transactions on Information Forensics and Security* 18 (2023) 1322–1334.
119. H. Lu, Y. Li, C. Zhao, W. Liu, Y. Li, N. Ma, A novel finger-vein recognition approach based on vision transformer, in: *International Conference on Frontiers of Electronics, Information and Computation Technologies*, 2021, pp. 1–6.
120. J. Huang, W. Luo, W. Yang, A. Zheng, F. Lian, W. Kang, FVT: Finger vein transformer for authentication, *IEEE Transactions on Instrumentation and Measurement* 71 (2022) 1–13.
121. X. Li, B.-B. Zhang, Fv-vit: Vision transformer for finger vein recognition, *IEEE Access* (2023).
122. Z. Lu, R. Wu, J. Zhang, Finger-vein feature extraction method based on vision transformer, *Journal of Electronic Imaging* 31 (4) (2022) 043010–043010.
123. C. Chen, Z. Wu, P. Li, J. Zhang, Y. Wang, H. Li, A finger vein recognition algorithm using feature block fusion and depth neural network, in: *Computational Intelligence and Intelligent Systems: 7th International Symposium, ISICA 2015, Guangzhou, China, November 21–22, 2015, Revised Selected Papers 7*, Springer, 2016, pp. 572–583.
124. B. Hou, R. Yan, Convolutional autoencoder model for finger-vein verification, *IEEE Transactions on Instrumentation and Measurement* 69 (5) (2019) 2067–2074.
125. E. Jalilian, A. Uhl, Finger-vein recognition using deep fully convolutional neural semantic segmentation networks: The impact of training data, in: 2018 IEEE international workshop on information forensics and security (WIFS), IEEE, 2018, pp. 1–8.
126. B. Hou, R. Yan, Convolutional auto-encoder based deep feature learning for finger-vein verification, in: 2018 IEEE international symposium on medical measurements and applications (MeMeA), IEEE, 2018, pp. 1–5.
127. H. Qin, P. Wang, Finger-vein verification based on LSTM recurrent neural networks, *Applied Sciences* 9 (8) (2019) 1687.
128. J. Zhang, Z. Lu, M. Li, H. Wu, GAN-based image augmentation for finger-vein biometric recognition, *IEEE Access* 7 (2019) 183118–183132.
129. B. Hou, R. Yan, Triplet-classifier gan for finger-vein verification, *IEEE Transactions on instrumentation and measurement* 71 (2022) 1–12.
130. Y. Li, H. Lu, Y. Wang, R. Gao, C. Zhao, ViT-Cap: a novel vision transformer-based capsule network model for finger vein recognition, *Applied Sciences* 12 (20) (2022) 10364.
131. N. M. Kamaruddin, B. A. Rosdi, A new filter generation method in PCANet for finger vein recognition, *IEEE Access* 7 (2019) 132966–132978.
132. W. Yang, C. Hui, Z. Chen, J.-H. Xue, Q. Liao, Fv-gan: Finger vein representation using generative adversarial networks, *IEEE Transactions on Information Forensics and Security* 14 (9) (2019) 2512–2524.
133. D. Muthusamy, P. Rakkimuthu, Steepest deep bipolar cascade correlation for finger-vein verification, *Applied Intelligence* 52 (4) (2022) 3825–3845.
134. D. Muthusamy, P. Rakkimuthu, Trilateral Filterative Hermitian feature transformed deep perceptive fuzzy neural network for finger vein verification, *Expert Systems with Applications* 196 (2022) 116678.
135. Y. Song, P. Zhao, W. Yang, Q. Liao, J. Zhou, Eifnet: An explicit and implicit feature fusion network for finger vein verification, *IEEE Transactions on Circuits and Systems for Video Technology* 33 (5) (2022) 2520–2532.
136. H. Zhang, M. Cisse, Y. N. Dauphin, D. Lopez-Paz, mixup: Beyond empirical risk minimization, *arXiv preprint arXiv:1710.09412* (2017).
137. Z. C. Wan, L. Chen, T. Wang, G. C. Wan, An Optimization Algorithm to Improve the Accuracy of Finger Vein Recognition, *IEEE Access* 10 (2022) 127440–127449.
138. H. Qin, C. Fan, S. Deng, Y. Li, M. A. El-Yacoubi, G. Zhou, AG-NAS: An Attention GRU-based Neural Architecture Search for Finger-Vein Recognition, *IEEE Transactions on Information Forensics and Security* (2023).
139. Z. Huang, C. Guo, Towards Cross-Dataset Finger Vein Recognition with Single-Source Data, *IEEE Transactions on Instrumentation and Measurement* (2024).
140. Z. Zhang, G. Chen, W. Zhang, H. Wang, Finger Vein Recognition Based on ResNet with Self-Attention, *IEEE Access* (2023).

141. X. Ma, X. Luo, Finger vein recognition method based on ant colony optimization and improved efficientnetv2, *Mathematical Biosciences and Engineering* 20 (6) (2023) 11081–11100.
142. J. M. Song, W. Kim, K. R. Park, Finger-vein recognition based on deep densenet using composite image, *Ieee Access* 7 (2019) 66845–66863.
143. Z. Tao, H. Wang, Y. Hu, Y. Han, S. Lin, Y. Liu, Dglfv: Deep generalized label algorithm for finger-vein recognition, *IEEE Access* 9 (2021) 78594–78606.
144. N. C. Tran, J.-H. Wang, T. H. Vu, T.-C. Tai, J.-C. Wang, Anti-aliasing convolution neural network of finger vein recognition for virtual reality (vr) human–robot equipment of metaverse, *The Journal of Supercomputing* 79 (3) (2023) 2767–2782.
145. S. V. Deshmukh, N. S. Zulpe, An optimized deep learning based depthwise separable MobileNetV3 approach for automatic finger vein recognition system, *Multimedia Tools and Applications* (2024) 1–29.
146. T. Chai, J. Li, S. Prasad, Q. Lu, Z. Zhang, Shape-driven lightweight CNN for finger-vein biometrics, *Journal of Information Security and Applications* 67 (2022) 103211.
147. C.-H. Hsia, Z.-H. Yang, H.-J. Wang, K.-K. Lai, A new enhancement edge detection of finger-vein identification for carputer system, *Applied Sciences* 12 (19) (2022) 10127.
148. B. Hou, R. Yan, Arcvein-arccosine center loss for finger vein verification, *IEEE Transactions on Instrumentation and Measurement* 70 (2021) 1–11.
149. T. Chai, J. Li, Y. Wang, G. Sun, C. Guo, Z. Zhang, Vascular enhancement analysis in lightweight deep feature space, *Neural Processing Letters* 55 (3) (2023) 2305–2320.
150. H. Hu, W. Kang, Y. Lu, Y. Fang, H. Liu, J. Zhao, F. Deng, FV-Net: learning a finger-vein feature representation based on a CNN, in: 2018 24th international conference on pattern recognition (ICPR), IEEE, 2018, pp. 3489–3494.
151. H. Zheng, Y. Hu, B. Liu, G. Chen, A. C. Kot, A new efficient finger-vein verification based on lightweight neural network using multiple schemes, in: *Artificial Neural Networks and Machine Learning–ICANN 2020: 29th International Conference on Artificial Neural Networks, Bratislava, Slovakia, September 15–18, 2020, Proceedings, Part I 29*, Springer, 2020, pp. 748–758.
152. W.-F. Ou, L.-M. Po, C. Zhou, Y. A. U. Rehman, P.-F. Xian, Y.-J. Zhang, Fusion loss and inter-class data augmentation for deep finger vein feature learning, *Expert Systems with Applications* 171 (2021) 114584.
153. H. G. Hong, M. B. Lee, K. R. Park, Convolutional neural network-based finger-vein recognition using NIR image sensors, *Sensors* 17 (6) (2017) 1297.
154. Y. Lu, S. Xie, S. Wu, Exploring competitive features using deep convolutional neural network for finger vein recognition, *IEEE access* 7 (2019) 35113–35123.
155. K. Shaheed, A. Mao, I. Qureshi, M. Kumar, S. Hussain, I. Ullah, X. Zhang, DS-CNN: A pre-trained Xception model based on depth-wise separable convolutional neural network for finger vein recognition, *Expert Systems with Applications* 191 (2022) 116288.
156. H. Qin, R. Hu, M. A. El-Yacoubi, Y. Li, X. Gao, Local attention transformer-based full-view finger-vein identification, *IEEE Transactions on Circuits and Systems for Video Technology* (2022).
157. X. Li, J. Feng, J. Cai, G. Lin, FV-MViT: Mobile Vision Transformer for Finger Vein Recognition, *Sensors* 24 (4) (2024) 1331.
158. Z. Huang, C. Guo, Robust finger vein recognition based on deep CNN with spatial attention and bias field correction, *International Journal on Artificial Intelligence Tools* 30 (01) (2021) 2140005.
159. D. T. Nguyen, H. S. Yoon, T. D. Pham, K. R. Park, Spoof detection for finger-vein recognition system using NIR camera, *Sensors* 17 (10) (2017) 2261.
160. X. Qiu, S. Tian, W. Kang, W. Jia, Q. Wu, Finger vein presentation attack detection using convolutional neural networks, in: *Biometric Recognition: 12th Chinese Conference, CCBP 2017, Shenzhen, China, October 28–29, 2017, Proceedings 12*, Springer, 2017, pp. 296–305.
161. R. Raghavendra, S. Venkatesh, K. B. Raja, C. Busch, Transferable deep convolutional neural network features for fingervein presentation attack detection, in: 2017 5th International Workshop on Biometrics and Forensics (IWBF), IEEE, 2017, pp. 1–5.
162. S. G. Kim, J. Choi, J. S. Hong, K. R. Park, Spoof detection based on score fusion using ensemble networks robust against adversarial attacks of fake finger-vein images, *Journal of King Saud University-Computer and Information Sciences* 34 (10) (2022) 9343–9362.
163. K. Shaheed, A. Mao, I. Qureshi, Q. Abbas, M. Kumar, X. Zhang, Finger-vein presentation attack detection using depthwise separable convolution neural network, *Expert Systems with Applications* 198 (2022) 116786.
164. H. Mu, J. Guo, X. Liu, C. Han, L. Sun, Federated finger vein presentation attack detection for various clients, *IET Computer Vision* (2024).
165. W. Yang, W. Luo, W. Kang, Z. Huang, Q. Wu, Fvras-net: An embedded finger-vein recognition and antispooing system using a unified cnn, *IEEE Transactions on Instrumentation and Measurement* 69 (11) (2020) 8690–8701.
166. W. Yang, S. Wang, J. Hu, G. Zheng, J. Yang, C. Valli, Securing deep learning based edge finger vein biometrics with binary decision diagram, *IEEE Transactions on Industrial Informatics* 15 (7) (2019) 4244–4253.
167. Y. Liu, J. Ling, Z. Liu, J. Shen, C. Gao, Finger vein secure biometric template generation based on deep learning, *Soft Computing* 22 (2018) 2257–2265.
168. H. O. Shahreza, S. Marcel, Deep auto-encoding and biohashing for secure finger vein recognition, in: *ICASSP 2021–2021 IEEE International Conference on Acoustics, Speech and Signal Processing (ICASSP)*, IEEE, 2021, pp. 2585–2589.
169. Y.-Y. Chen, C.-H. Hsia, P.-H. Chen, Contactless multispectral palm-vein recognition with lightweight convolutional neural network, *IEEE Access* 9 (2021) 149796–149806.
170. Y. Ma, H. Huang, D. Luo, S. Zhang, W. Kang, D. Xie, Focal contrastive learning for palm vein authentication, *IEEE Transactions on Instrumentation and Measurement* (2023).
171. H. Qin, M. A. El-Yacoubi, Y. Li, C. Liu, Multi-scale and multi-direction GAN for CNN-based single palm-vein identification, *IEEE Transactions on Information Forensics and Security* 16 (2021) 2652–2666.
172. H. Qin, C. Gong, Y. Li, X. Gao, M. A. El-Yacoubi, Label enhancement-based multiscale transformer for palm-vein recognition, *IEEE Transactions on Instrumentation and Measurement* 72 (2023) 1–17.
173. S.-J. Horng, D.-T. Vu, T.-V. Nguyen, W. Zhou, C.-T. Lin, Recognizing palm vein in smartphones using RGB images, *IEEE Transactions on Industrial Informatics* 18 (9) (2021) 5992–6002.
174. D. Thapar, G. Jaswal, A. Nigam, V. Kanhangad, Pvsnet: Palm vein authentication siamese network trained using triplet loss and adaptive hard mining by learning enforced domain specific features, in: 2019 IEEE 5th international conference on identity, security, and behavior analysis (ISBA), IEEE, 2019, pp. 1–8.
175. H. Qin, M. A. El Yacoubi, J. Lin, B. Liu, An iterative deep neural network for hand-vein verification, *IEEE Access* 7 (2019) 34823–34837.
176. X. Ma, Y. Niu, L. Gu, Y. Wang, Y. Zhao, J. Bailey, F. Lu, Understanding adversarial attacks on deep learning based medical image analysis systems, *Pattern Recognition* 110 (2021) 107332.
177. Y. Li, S. Ruan, H. Qin, S. Deng, M. A. El-Yacoubi, Transformer based defense gan against palm-vein adversarial attacks, *IEEE Transactions on Information Forensics and Security* 18 (2023) 1509–1523.
178. D. Zhong, S. Liu, W. Wang, X. Du, Palm vein recognition with deep hashing network, in: *Pattern Recognition and Computer Vision: First Chinese Conference, PRCV 2018, Guangzhou, China, November 23–26, 2018, Proceedings, Part I 1*, Springer, 2018, pp. 38–49.
179. T. Wu, L. Leng, M. K. Khan, F. A. Khan, Palmprint-palmvein fusion recognition based on deep hashing network, *IEEE Access* 9 (2021) 135816–135827.
180. X. Dong, M. K. Khan, L. Leng, A. B. J. Teoh, Co-learning to hash palm biometrics for flexible IoT deployment, *IEEE Internet of Things Journal* 9 (23) (2022) 23786–23794.
181. S. Lefkovits, L. Lefkovits, L. Szilágyi, Applications of different CNN architectures for palm vein identification, in: *Modeling Decisions for Artificial Intelligence: 16th International Conference, MDAI 2019, Milan, Italy, September 4–6, 2019, Proceedings 16*, Springer, 2019, pp. 295–306.

182. H. Kheddar, Y. Himeur, A. I. Awad, Deep transfer learning for intrusion detection in industrial control networks: A comprehensive review, *Journal of Network and Computer Applications* 220 (2023) 103760.
183. Z. Li, X. Liang, D. Fan, J. Li, D. Zhang, BPFNet: a unified framework for bimodal palmprint alignment and fusion, in: *Neural Information Processing: 28th International Conference, ICONIP 2021, Sanur, Bali, Indonesia, December 8–12, 2021, Proceedings, Part VI 28*, Springer, 2021, pp. 28–36.
184. L. Wang, Q. Zhang, Q. Qian, J. Wang, Y. Pan, R. Yang, W. Cheng, Multispectral Palm Print and Palm Vein Acquisition Platform and Recognition Method Based on Convolutional Neural Network, *The Computer Journal* 65 (6) (2022) 1461–1471.
185. S. S. Kaddoun, Y. Aberni, L. Boubchir, M. Raddadi, B. Daachi, Convolutional neural algorithm for palm vein recognition using zfnnet architecture, in: *2021 4th International Conference on Bio-Engineering for Smart Technologies (BioSMART)*, IEEE, 2021, pp. 1–4.
186. R. Hernández-García, E. H. Salazar-Jurado, R. J. Barrientos, F. M. Castro, J. Ramos-Cózar, N. Guil, From synthetic data to real palm vein identification: a fine-tuning approach, in: *2023 IEEE 13th International Conference on Pattern Recognition Systems (ICPRS)*, IEEE, 2023, pp. 1–7.
187. W. Wu, Q. Wang, S. Yu, Q. Luo, S. Lin, Z. Han, Y. Tang, Outside box and contactless palm vein recognition based on a wavelet denoising ResNet, *IEEE Access* 9 (2021) 82471–82484.
188. F. Marattukalam, W. H. Abdulla, A. Swain, N-shot palm vein verification using siamese networks, in: *2021 International Conference of the Biometrics Special Interest Group (BIOSIG)*, IEEE, 2021, pp. 1–5.
189. R. S. Kuzu, E. Maiorana, P. Campisi, Gender-specific characteristics for hand-vein biometric recognition: Analysis and exploitation, *IEEE Access* 11 (2023) 11700–11710.
190. F. O. Babalola, Ö. Toygar, Y. Bitirim, Boosting hand vein recognition performance with the fusion of different color spaces in deep learning architectures, *Signal, Image and Video Processing* 17 (8) (2023) 4375–4383.
191. M. Wulandari, D. Gunawan, et al., On the performance of pretrained cnn aimed at palm vein recognition application, in: *2019 11th International Conference on Information Technology and Electrical Engineering (ICITEE)*, IEEE, 2019, pp. 1–6.
192. R. S. Kuzu, E. Maiorana, P. Campisi, Vein-based biometric verification using densely-connected convolutional autoencoder, *IEEE Signal Processing Letters* 27 (2020) 1869–1873.
193. W. Jia, J. Gao, W. Xia, Y. Zhao, H. Min, J.-T. Lu, A performance evaluation of classic convolutional neural networks for 2D and 3D palmprint and palm vein recognition, *International Journal of Automation and Computing* 18 (1) (2021) 18–44.
194. R. Nour, H. E.-D. Moustafa, E. H. AbdelHay, M. M. Ata, Improved Unsupervised Deep Boltzmann Learning Approach for Accurate Hand Vein Recognition, *IEEE Access* (2024).
195. A. Benaouda, A. H. Mustapha, S. Benziane, A CNN Approach for the Identification of Dorsal Veins of the Hand, in: *International Conference on Artificial Intelligence and its Applications*, Springer, 2021, pp. 574–587.
196. K. Li, G. Zhang, P. Wang, Hand-dorsa vein recognition based on deep learning, in: *2018 International Conference on Security, Pattern Analysis, and Cybernetics (SPAC)*, IEEE, 2018, pp. 203–207.
197. K. Li, Q. Liu, G. Zhang, Fusion of partition local binary patterns and convolutional neural networks for dorsal hand vein recognition, in: *Biometric Recognition: 15th Chinese Conference, CCBR 2021, Shanghai, China, September 10–12, 2021, Proceedings 15*, Springer, 2021, pp. 177–184.
198. H. Wan, L. Chen, H. Song, J. Yang, Dorsal hand vein recognition based on convolutional neural networks, in: *2017 IEEE International Conference on Bioinformatics and Biomedicine (BIBM)*, IEEE, 2017, pp. 1215–1221.
199. R. S. Kuzu, E. Maiorana, P. Campisi, On the intra-subject similarity of hand vein patterns in biometric recognition, *Expert Systems with Applications* 192 (2022) 116305.
200. R. Zhang, X. Zou, X. Deng, Z. Wang, Y. Chen, C. Lin, H. Xing, F. Dai, Fast and Accurate ROI Extraction for Non-Contact Dorsal Hand Vein Detection in Complex Backgrounds Based on Improved U-Net, *Sensors* 23 (10) (2023) 4625.
201. K. M. Alashik, R. Yildirim, Human identity verification from biometric dorsal hand vein images using the DL-GAN method, *IEEE Access* 9 (2021) 74194–74208.
202. X. Li, D. Huang, Y. Wang, Comparative study of deep learning methods on dorsal hand vein recognition, in: *Biometric Recognition: 11th Chinese Conference, CCBR 2016, Chengdu, China, October 14–16, 2016, Proceedings 11*, Springer, 2016, pp. 296–306.
203. H. Li, Y. Wang, X. Jiang, Dorsal Hand Vein Recognition Method Based on Multi-bit Planes Optimization, in: *Biometric Recognition: 13th Chinese Conference, CCBR 2018, Urumqi, China, August 11–12, 2018, Proceedings 13*, Springer, 2018, pp. 3–10.
204. J. Li, K. Li, G. Zhang, J. Wang, K. Li, Y. Yang, Recognition of dorsal hand vein in small-scale sample database based on fusion of resnet and hog feature, *Electronics* 11 (17) (2022) 2698.
205. Y. Tian, D. Zhao, T. Wang, An improved YOLO Nano model for dorsal hand vein detection system, *Medical & Biological Engineering & Computing* 60 (5) (2022) 1225–1237.
206. J. Wang, Z. Pan, G. Wang, M. Li, Y. Li, Spatial pyramid pooling of selective convolutional features for vein recognition, *IEEE Access* 6 (2018) 28563–28572.
207. G. Chaudhary, et al., PCANet based biometric system with fusion of palmprint and dorsal hand vein, *Journal of Intelligent & Fuzzy Systems* 42 (2) (2022) 841–849.
208. M. Bharath, K. Radhakrishna Rao, Optimal Score Level Fusion for Multi-Modal Biometric System with Optimised Deep Ensemble Technique, *Computer Methods in Biomechanics and Biomedical Engineering: Imaging & Visualization* (2023) 1–15.
209. S. Daas, A. Yahi, T. Bakir, M. Sedhane, M. Boughazi, E.-B. Bourennane, Multimodal biometric recognition systems using deep learning based on the finger vein and finger knuckle print fusion, *IET Image Processing* 14 (15) (2020) 3859–3868.
210. S. Deshmukh, A. Abhyankar, S. Kelkar, DCCA and DMCCA framework for multimodal biometric system, *Multimedia Tools and Applications* 81 (17) (2022) 24477–24491.
211. B. A. El-Rahiem, M. Amin, A. Sedik, F. E. A. E. Samie, A. M. Ilyyasu, An efficient multi-biometric cancellable biometric scheme based on deep fusion and deep dream, *Journal of Ambient Intelligence and Humanized Computing* (2021) 1–13.
212. B. Abd El-Rahiem, F. E. Abd El Samie, M. Amin, Efficient cancellable multi-biometric recognition system based on deep learning and bio-hashing, *Applied Intelligence* 53 (2) (2023) 1792–1806.
213. B. A. El-Rahiem, F. E. A. El-Samie, M. Amin, Multimodal biometric authentication based on deep fusion of electrocardiogram (ECG) and finger vein, *Multimedia Systems* 28 (4) (2022) 1325–1337.
214. Y. Huang, H. Ma, M. Wang, Multimodal Finger Recognition Based on Asymmetric Networks With Fused Similarity, *IEEE Access* 11 (2023) 17497–17509.
215. S. Tyagi, B. Chawla, R. Jain, S. Srivastava, Multimodal biometric system using deep learning based on face and finger vein fusion, *Journal of Intelligent & Fuzzy Systems* 42 (2) (2022) 943–955.
216. J. Wang, G. Wang, M. Zhou, Bimodal vein data mining via cross-selected-domain knowledge transfer, *IEEE Transactions on Information Forensics and Security* 13 (3) (2017) 733–744.
217. J. Yang, W. Sun, N. Liu, Y. Chen, Y. Wang, S. Han, A novel multimodal biometrics recognition model based on stacked ELM and CCA methods, *Symmetry* 10 (4) (2018) 96.
218. D. Zhong, H. Shao, X. Du, A hand-based multi-biometrics via deep hashing network and biometric graph matching, *IEEE Transactions on Information Forensics and Security* 14 (12) (2019) 3140–3150.
219. N. Alay, H. H. Al-Baity, Deep learning approach for multimodal biometric recognition system based on fusion of iris, face, and finger vein traits, *Sensors* 20 (19) (2020) 5523.

220. L. Jiang, X. Liu, H. Wang, D. Zhao, Finger Vein and Inner Knuckle Print Recognition Based on Multilevel Feature Fusion Network, *Applied Sciences* 12 (21) (2022) 11182.
221. M. Y. Haouam, A. Meraoumia, L. Laimeche, I. Bendib, S-DCTNet: Security-oriented biometric feature extraction technique: An effective pathway to secure and reliable biometric systems, *Multimedia Tools and Applications* 80 (28-29) (2021) 36059–36091.
222. K. J. Noh, J. Choi, J. S. Hong, K. R. Park, Finger-vein recognition based on densely connected convolutional network using score-level fusion with shape and texture images, *Ieee Access* 8 (2020) 96748–96766.
223. K. Janaki, C. Srinivasan, et al., Fpga-enhanced system-on-chip for finger vein-based biometric system using novel dl model, *Integration* (2024) 102231.
224. W. Roth, G. Schindler, B. Klein, R. Peharz, S. Tschiatsek, H. Fröning, F. Pernkopf, Z. Ghahramani, Resource-efficient neural networks for embedded systems, *arXiv preprint arXiv:2001.03048* (2020).
225. S. Han, J. Pool, J. Tran, W. Dally, Learning both weights and connections for efficient neural network, *Advances in neural information processing systems* 28 (2015).
226. B. Jacob, S. Kligys, B. Chen, M. Zhu, M. Tang, A. Howard, H. Adam, D. Kalenichenko, Quantization and training of neural networks for efficient integer-arithmetic-only inference, in: *Proceedings of the IEEE conference on computer vision and pattern recognition*, 2018, pp. 2704–2713.
227. E. L. Denton, W. Zaremba, J. Bruna, Y. LeCun, R. Fergus, Exploiting linear structure within convolutional networks for efficient evaluation, *Advances in neural information processing systems* 27 (2014).
228. G. Hinton, Distilling the knowledge in a neural network, *arXiv preprint arXiv:1503.02531* (2015).
229. J. Dean, G. Corrado, R. Monga, K. Chen, M. Devin, M. Mao, M. Ranzato, A. Senior, P. Tucker, K. Yang, et al., Large scale distributed deep networks, *Advances in neural information processing systems* 25 (2012).
230. M. Li, D. G. Andersen, J. W. Park, A. J. Smola, A. Ahmed, V. Josifovski, J. Long, E. J. Shekita, B.-Y. Su, Scaling distributed machine learning with the parameter server, in: *11th USENIX Symposium on operating systems design and implementation (OSDI 14)*, 2014, pp. 583–598.
231. M. De Santis, S. Agnelli, D. Nardiello, A. Iula, 3D Ultrasound Palm Vein recognition through the centroid method for biometric purposes, in: *2017 IEEE international ultrasonics symposium (IUS)*, IEEE, 2017, pp. 1–4.
232. W. Jia, W. Xia, Y. Zhao, H. Min, Y.-X. Chen, 2D and 3D palmprint and palm vein recognition based on neural architecture search, *International Journal of Automation and Computing* 18 (3) (2021) 377–409.
233. S. S. Sohail, Y. Himeur, H. Kheddar, A. Amira, F. Fadli, S. Atalla, A. Copiaco, W. Mansoor, Advancing 3d point cloud understanding through deep transfer learning: A comprehensive survey, *Information Fusion* (2024) 102601.
234. W. Damak, R. Boukhris Trabelsi, A. Damak Masmoudi, D. Sellami, A. Nait-Ali, Age and gender classification from finger vein patterns, in: *Intelligent Systems Design and Applications: 16th International Conference on Intelligent Systems Design and Applications (ISDA 2016) held in Porto, Portugal, December 16-18, 2016*, Springer, 2017, pp. 811–820.
235. J. Wang, G. Wang, Z. Pan, Gender attribute mining with hand-dorsa vein image based on unsupervised sparse feature learning, *IEICE Transactions on Information and Systems* 101 (1) (2018) 257–260.
236. D. Sellami, Palm vein age and gender estimation using center symmetric-local binary pattern, in: *International Joint Conference: 12th International Conference on Computational Intelligence in Security for Information Systems (CISIS 2019) and 10th International Conference on European Transnational Education (ICEUTE 2019): Seville, Spain, May 13th-15th, 2019 Proceedings*, Vol. 951, Springer, 2019, p. 114.
237. R. Hernández-García, Z. Feng, R. J. Barrientos, F. M. Castro, J. Ramos-Cózar, N. Guil, Cnn-based model for gender and age classification based on palm vein images, in: *2022 12th International Conference on Pattern Recognition Systems (ICPRS)*, IEEE, 2022, pp. 1–6.
238. W. Damak, R. Boukhris, A. Damak, D. Sellami, Pyramid histograms of oriented gradient for age and gender recognition using finger veins, in: *Fifteenth International Conference on Machine Vision (ICMV 2022)*, Vol. 12701, SPIE, 2023, pp. 192–201.
239. E. Rebahi, M. Hemis, B. Boudraa, Image watermarking technique using convolutional autoencoder, in: *2023 International Conference on Advances in Electronics, Control and Communication Systems (ICAECCS)*, IEEE, 2023, pp. 1–6.
240. H. Kheddar, A. C. Mazari, G. H. Ilk, Speech steganography based on double approximation of LSFs parameters in AMR coding, in: *2022 7th International Conference on Image and Signal Processing and their Applications (ISPA)*, IEEE, 2022, pp. 1–8.
241. S. Ebrahimi, S. Bayat-Sarmadi, Lightweight fuzzy extractor based on LPN for device and biometric authentication in IoT, *IEEE Internet of Things Journal* 8 (13) (2021) 10706–10713.
242. X. Yin, S. Wang, M. Shahzad, J. Hu, An IoT-oriented privacy-preserving fingerprint authentication system, *IEEE Internet of Things Journal* 9 (14) (2021) 11760–11771.
243. H. Kheddar, Transformers and large language models for efficient intrusion detection systems: A comprehensive survey, *arXiv preprint arXiv:2408.07583* (2024).